ISSN 2186-3644 Online ISSN 2186-361X

IRDR

Intractable & Rare Diseases Research

Volume 11, Number 1
February, 2022

IRCA BSSA

IACMHR

www.irdrjournal.com

IRDR
Intractable & Rare Diseases Research

ISSN: 2186-3644
Online ISSN: 2186-361X
CODEN: IRDRA3
Issues/Year: 4
Language: English
Publisher: IACMHR Co., Ltd.

Intractable & Rare Diseases Research is one of a series of peer-reviewed journals of the International Research and Cooperation Association for Bio & Socio-Sciences Advancement (IRCA-BSSA) Group and is published quarterly by the International Advancement Center for Medicine & Health Research Co., Ltd. (IACMHR Co., Ltd.) and supported by the IRCA-BSSA.

Intractable & Rare Diseases Research devotes to publishing the latest and most significant research in intractable and rare diseases. Articles cover all aspects of intractable and rare diseases research such as molecular biology, genetics, clinical diagnosis, prevention and treatment, epidemiology, health economics, health management, medical care system, and social science in order to encourage cooperation and exchange among scientists and clinical researchers.

Intractable & Rare Diseases Research publishes Original Articles, Brief Reports, Reviews, Policy Forum articles, Case Reports, Communications, Editorials, News, and Letters on all aspects of the field of intractable and rare diseases research. All contributions should seek to promote international collaboration.

IRCA-BSSA Group Journals

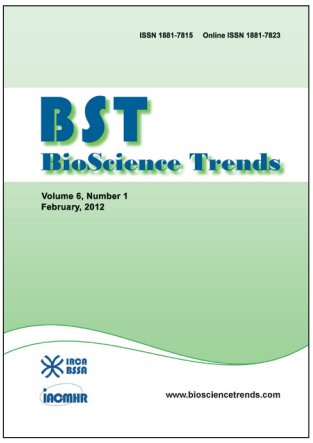

ISSN: 1881-7815
Online ISSN: 1881-7823
CODEN: BTIRCZ
Issues/Year: 6
Language: English
Publisher: IACMHR Co., Ltd.
www.biosciencetrends.com

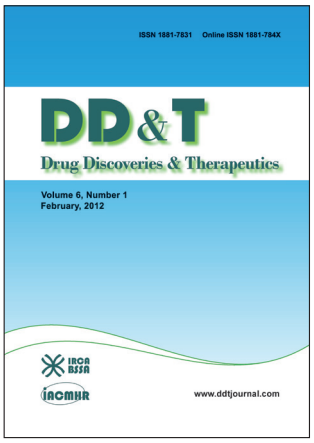

ISSN: 1881-7831
Online ISSN: 1881-784X
CODEN: DDTRBX
Issues/Year: 6
Language: English
Publisher: IACMHR Co., Ltd.
www.ddtjournal.com

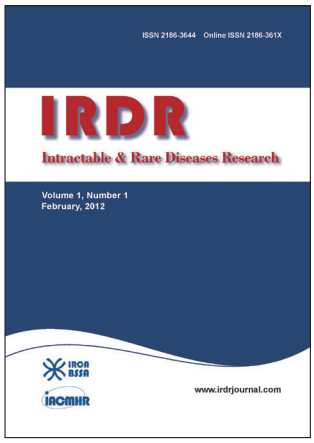

ISSN: 2186-3644
Online ISSN: 2186-361X
CODEN: IRDRA3
Issues/Year: 4
Language: English
Publisher: IACMHR Co., Ltd.
www.irdrjournal.com

Intractable & Rare Diseases Research

Editorial and Head Office

Pearl City Koishikawa 603, 2-4-5 Kasuga, Bunkyo-ku,
Tokyo 112-0003, Japan

E-mail: office@irdrjournal.com
URL: www.irdrjournal.com

Editorial Board

CONTENTS

Volume 11, Number 1, 2022

Original Article

Brief Report

Communication

Letter

Original Article

DOI: 10.5582/irdr.2021.01157

Forearm porphyrin levels evaluated by digital imaging system are increased in patients with systemic sclerosis compared with patients in pre-clinical stage

Kayoko Tabata[1], Chikako Kaminaka[2,*], Misaki Yasutake[1], Ryo Matsumiya[1], Yutaka Inaba[2], Yuki Yamamoto[2], Masatoshi Jinnin[2], Takao Fujii[1]

[1] Department of Rheumatology and Clinical Immunology, Graduate School of Medicine, Wakayama Medical University, Wakayama, Japan;
[2] Department of Dermatology, Graduate School of Medicine, Wakayama Medical University, Wakayama, Japan.

SUMMARY We hypothesized that changes in skin characteristics on the forearm could be useful for early diagnosis of systemic sclerosis (SSc). We used VISIA digital imaging system to investigate this possibility for the first time. Twenty-eight Japanese patients who were diagnosed with typical or very early diagnosis of SSc (VEDOSS) were enrolled in this study, and ten age- and gender-matched patients with other disorders were included as a control group. Eight skin characteristics were analyzed. Our method of evaluating forearm skin characteristics was shown to be reproducible. The scores of WRINKLES, TEXTURE, PORES, and PORPHYRINS were higher in SSc subjects with sclerotic forearm skin (SSc forearm+; 11.004, 5.116, 3.230, and 0.084, respectively) and those without (SSc forearm-: 11.915, 4.898, 2.624, 0.0616, respectively) than in the non-SSc control subjects (10.075, 4.496, 2.459, 0.0223, respectively). Also, the scores of SPOTS, TEXTURE, PORES, UV SPOTS, BROWN SPOTS, and PORPHYRINS were elevated in SSc forearm+ (3.182, 5.116, 3.230, 5.761, 6.704, 0.084, respectively) and SSc forearm- patients (2.391, 4.898, 2.624, 9.835, 5.798, 0.0616, respectively) compared with those with VEDOSS (2.362, 4.738, 2.234, 5.999, 4.898, 0.0169, respectively). We found statistical significance in the difference in score of PORPHYRINS between SSc forearm- and VEDOSS groups ($p = 0.044$), and between SSc forearm+ and VEDOSS groups ($p = 0.012$). Therefore, they can be used to differentiate VEDOSS from early or mild SSc cases, which is sometimes clinically problematic. Our study also suggests that the porphyrin research will lead to a better understanding of SSc pathogenesis.

Keywords forearm, very early diagnosis of SSc (VEDOSS), porphyria cutanea tarda

1. Introduction

Systemic sclerosis (SSc) is characterized by three pathologic features: immunodysfunction/inflammation, vasculopathy, and tissue fibrosis of various organs. Although the exact pathogenesis of SSc remains unknown, tissue fibrosis due to excessive collagen deposition seen in SSc is sometimes irreversible, at least clinically. There is an urgent need to develop new strategies of early diagnosis and careful follow-up. Early diagnosis is often difficult, however, because of the lack of objective typical skin sclerosis in the early stages. For that purpose, the disease concept of very early diagnosis of systemic sclerosis (VEDOSS) was developed, referring to patients with Raynaud's phenomenon but without skin sclerosis. In addition, for early detection, low serum concentration of carbonic anhydrase 9 (CA9) and microRNA-29 in pre-clinical stage SSc may be utilized as early diagnostic markers (*1,2*). Also, we found increased sweating levels on finger pads in SSc patients, and demonstrated its clinical significance for early diagnosis of SSc (*3*).

We hypothesized that changes in skin findings on the forearm could be useful for early diagnosis. Here, we investigate this possibility using a digital imaging system (VISIA) for the first time. VISIA is a facial imaging system by objective computer assessments of eight major skin parameters. As far as we are aware base on search by PubMed using keyword VISIA, systemic sclerosis, and forearm, there has never been any such attempt.

2. Materials and Methods

2.1. Clinical assessment and patient material

Enrolled in this study were 28 female patients who

visited Wakayama Medical University between October 2016 and March 2021.

Twenty-one of these 28 patients met the American College of Rheumatology and the European League Against Rheumatism classification criteria (ACR/EULAR2013) (*4*), while seven did not fulfill the criteria, but were diagnosed as VEDOSS (*5*).

Modified Rodnan total skin thickness score (MRSS), a semi-quantitative skin sclerosis assessment tool, was obtained at the time of skin analysis (*6*). Ten age- and gender-matched patients with other disorders (rheumatoid arthritis: n = 5, polymyalgia rheumatica: n = 3, Sjögren syndrome: n = 1, systemic lupus erythematosus: n = 1) were also included as a control group.

This study was approved by the Wakayama Medical University Institutional Review Board (No.2479), and written informed consent was obtained before patients were entered into this study, in accordance with the Declaration of Helsinki.

2.2. Photography and forearm skin analysis

Photographing and forearm skin analysis were performed by objective computer assessments with digital imaging system (VISIA, Canfield Imaging Systems, Fairfield, NJ).

The system consists of imaging chamber with a 15 million pixel resolution camera, which is connected to computer and quantitative analysis software, and has three kinds of light sources: standard incandescent light, ultraviolet (UV) light, and polarized light.

Eight skin characteristics were evaluated: SPOTS, WRINKLES, TEXTURE, PORES, UV SPOTS, BROWN SPOTS, RED AREAS, and PORPHYRINS. A standard flash light is used to identify SPOTS, WRINKLES, TEXTURE, and PORES, whereas an UV flash-light is used to detect UV SPOTS and PORPHYRINS. A cross-polarized flash light is also used to observe BROWN SPOTS and RED AREAS (*7*).

For example, SPOTS are identified by their color and contrast from the surrounding skin (*8*). The PORPHYRINS scores reflect fluorescence with UV ray. The definition of other parameters was as described previously (*7-12*). Average scores were taken from two independent analyses (left and right forearms).

2.3. Statistical analysis

Statistical analyses were carried out with Kruskal-Wallis test for analysis of more than three groups, and Mann-Whitney tests were used for the comparison of medians between two groups. Correlations were evaluated by Pearson's correlation coefficient. P values < 0.05 were considered to be statistically significant.

3. Results

3.1. Clinical features of patients in this study

Twenty-one female patients with SSc were enrolled in this study. The numbers of SSc patients with or without skin sclerosis of the forearm (SSc forearm+ or SSc forearm-) were n = 6 and 15, respectively. Seven patients with VEDOSS and ten control patients (rheumatoid arthritis: n = 5, polymyalgia rheumatica: n = 3, Sjögren syndrome: n = 1, systemic lupus erythematosus: n = 1) were also included in this study.

Clinical characteristics of patients included in this study are shown in Table 1. The average age of each group was similar (SSc forearm+: 69.8, SSc forearm-: 68.3, VEDOSS: 65.7, and the control: 68.3). The average ACR/EULAR score was higher in SSc forearm+ group than in the other groups: (SSc forearm+: 20.5, SSc forearm-: 12.5, and VEDOSS: 7.1). Consistently, the average MRSS tended to be increased in SSc forearm+ group (SSc forearm+: 11.3, SSc forearm-: 1.8, and VEDOSS: 0). These data thus indicate the credibility of our grouping.

3.2. Comparison of the eight skin characteristics of forearm skin in 4 groups

The eight skin characteristics (SPOTS, WRINKLES, TEXTURE, PORES, UV SPOTS, BROWN SPOTS, RED AREAS, and PORPHYRINS) of forearm skin were analyzed in the four patient groups (SSc forearm+, SSc forearm-, VEDOSS, and the control) by using digital imaging system (VISIA). This is the first report to evaluate forearm skin using VISIA, so we attempted to prove its reproducibility. Each parameter was separately evaluated on the left and right forearms in all subjects, and percentage difference between the two evaluations in each individual was calculated as difference of scores/larger scores × 100 in each patient (Figure 1). The mean percentage differences of each parameter were less than 2-fold, indicating the reproducibility of all parameters by our method, and the mean score of left and right forearms in each patient was evaluated in the following analyses.

The eight parameters were then compared among the four groups. The scores of WRINKLES, TEXTURE, PORES, and PORPHYRINS were higher in SSc forearm+ (WRINKLES; 11.004 ± 4.287, TEXTURE; 5.116 ± 3.254, PORES; 3.230 ± 1.591, PORPHYRINS; 0.084 ± 0.0891) and SSc forearm- groups (WRINKLES; 11.915 ± 2.747, TEXTURE; 4.898 ± 1.864, PORES; 2.624 ± 1.299, PORPHYRINS; 0.0616 ± 0.108) than in control subjects (WRINKLES; 10.075 ± 2.370, TEXTURE; 4.496 ± 2.373, PORES; 2.459 ± 1.590, PORPHYRINS; 0.0223 ± 0.0166) (Table 1). Also, the scores of SPOTS, TEXTURE, PORES, UV SPOTS, BROWN SPOTS, and PORPHYRINS were elevated in patients with SSc forearm+ (SPOTS; 3.182 ± 0.485, TEXTURE; 5.116 ± 3.254, PORES;

Table 1. Clinical characteristics of four groups of patients included in this study

	Age	ACR/EULAR	MRSS	SPOTS	WRINKLES	TEXTURE	PORES	UV SPOTS	BROWN SPOTS	RED AREAS	PORPHYRINS
SSc forearm+	69.8 ± 5.1	20.5 ± 3.3	11.3 ± 6.0	3.182 ± 0.485	11.004 ± 4.287	5.116 ± 3.254	3.230 ± 1.591	5.761 ± 3.421	6.704 ± 1.095	2.083 ± 0.329	0.084 ± 0.0891
SSc forearm-	68.3 ± 7.2	12.5 ± 2.6	1.8 ± 1.3	2.391 ± 1.032	11.915 ± 2.747	4.898 ± 1.864	2.624 ± 1.299	9.835 ± 11.695	5.798 ± 5.700	1.631 ± 0.725	0.0616 ± 0.108
VEDOSS	65.7 ± 11.4	7.1 ± 1.1	0	2.362 ± 1.183	11.034 ± 0.965	4.738 ± 1.360	2.234 ± 1.279	5.999 ± 5.138	4.898 ± 3.030	1.814 ± 0.526	0.0169 ± 0.0188
Control	68.3 ± 5.9	-	-	2.512 ± 1.596	10.075 ± 2.370	4.496 ± 2.373	2.459 ± 1.590	8.616 ± 6.824	6.546 ± 4.097	1.920 ± 0.750	0.0223 ± 0.0166

Patients were divided into four groups: SSc forearm+ (SSc patients with skin sclerosis of the forearm); SSc forearm- (SSc patients without skin sclerosis of the forearm); VEDOSS, (patients with very early diagnosis of systemic sclerosis), and control subjects. ACR/EULAR scores were calculated according to the ACR/EULAR2013 classification criteria of systemic sclerosis. MRSS: modified Rodnan total skin thickness score. Mean value ± standard deviation (SD) of each parameter determined by VISIA is shown.

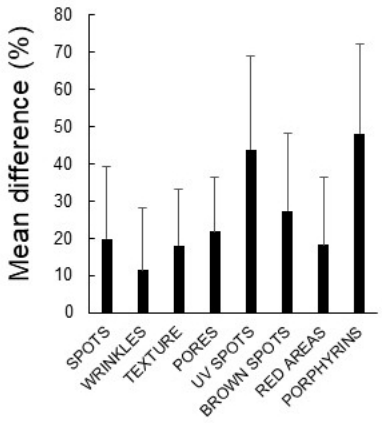

Figure 1. Reproductivity of forearm skin parameters measured by digital imaging system. Eight skin characteristics (SPOTS, WRINKLES, TEXTURE, PORES, UV SPOTS, BROWN SPOTS, RED AREAS, and PORPHYRINS) of forearm skin were analyzed by VISIA in the 38 patients included in this study. Each parameter was separately evaluated on left and right forearms in all subjects to prove its reproducibility, and percentage difference between the two evaluations in each individual was calculated as difference of scores/larger scores × 100 in each patient. The mean percentage differences of each parameter + standard deviation (SD) are shown on the ordinate.

3.230 ± 1.591, UV SPOTS; 5.761 ± 3.421, BROWN SPOTS; 6.704 ± 1.095, PORPHYRINS; 0.084 ± 0.0891) and SSc forearm- (SPOTS; 2.391 ± 1.032, TEXTURE; 4.898 ± 1.864, PORES; 2.624 ± 1.299, UV SPOTS; 9.835 ± 11.695, BROWN SPOTS; 5.798 ± 5.700, PORPHYRINS; 0.0616 ± 0.108) compared with those with VEDOSS (SPOTS; 2.362 ± 1.183, TEXTURE; 4.738 ± 1.360, PORES; 2.234 ± 1.279, UV SPOTS; 5.999 ± 5.138, BROWN SPOTS; 4.898 ± 3.030, PORPHYRINS; 0.0169 ± 0.0188). By Kruskal-Wallis test, out of the eight parameters there were no significant differences except for PORPHYRINS. On the other hand, for example, although telangiectasia is also a common feature of SSc skin, the scores of RED AREAS were not significantly different among the four groups. Furthermore, contrary to our expectation based on the previous analysis of SSc faces (*13*), the scores of WRINKLES, TEXTURE, or PORES were not significantly different.

Mann-Whitney tests showed statistical significance in the score of PORPHYRINS between SSc forearm- and VEDOSS groups ($p = 0.044$) and between SSc forearm+ and VEDOSS groups ($p = 0.012$) (Figure 2). There was no significant difference between the other groups. Increased porphyrins levels may therefore be a specific change to SSc with or without skin sclerosis of the forearm.

3.3. Correlations of PORPHYRINS scores with MRSS or ACR/EULAR 2013 scores in patients with SSc

To confirm the possibility that PORPHYRINS scores can be related to systemic disease activity in patients

with SSc, we next examined the correlation between PORPHYRINS scores and MRSS or ACR/EULAR2013 scores. However, PORPHYRINS did not show correlation with MRSS (R = 0.20, Figure 3A) and ACR/EULAR2013 scores (R = 0.047, Figure 3B). Therefore, although PORPHYRINS scores were increased in SSc forearm skin, we could not prove their direct correlation with systemic disease activity.

4. Discussion

VISIA digital imaging system is commonly used for facial analysis in the field of cosmetic dermatology. There have been several studies on facial skin characteristics in patients with hyperpigmented spots and acne using the system (*14*). We have also performed facial skin analysis of SSc patients using VISIA (*13*). In that report, we found the severity of WRINKLES, TEXTURE, and PORES were significantly lower in patients with SSc than in control subjects. Among them, WRINKLES showed better correlation with MRSS (*8*). However, the usefulness for the early diagnosis could not be evaluated due to the lack of disease controls in the early stage (*e.g.*, VEDOSS).

In the present study, we performed forearm skin analysis using the VISIA system for the first time. The skin condition of fingers and the hand can be affected by ulcers, rings, and bracelets, so we instead focused on the forearm, which is not affected by these factors. The mean percentage differences between two independent measurements of eight parameters were less than 2-fold, indicating the reproducibility of all parameters by our method. Our method can thus be considered as a new option in evaluation of forearm skin characteristics.

Comparison among the four patient groups showed the scores of WRINKLES, TEXTURE, PORES, and PORPHYRINS were higher in SSc forearm+ group and SSc forearm- group than in control subjects. Also, the scores of SPOTS, TEXTURE, PORES, UV SPOTS, BROWN SPOTS, and PORPHYRINS were elevated in patients in the SSc forearm+ group and SSc forearm- group compared with those in the VEDOSS group.

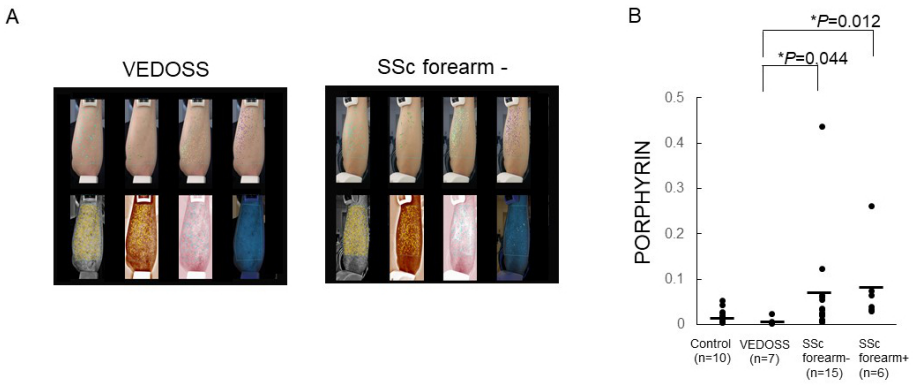

Figure 2. Objective computer assessments of PORPHYRIN levels. (A) A representative photograph showing comparison of a patient with very early diagnosis of systemic sclerosis (VEDOSS) and a SSc patient without skin sclerosis of the forearm (SSc forearm-). Upper row: SPOTS, WRINKLES, TEXTURE, PORES. Lower row: UV SPOTS, BROWN SPOTS, RED AREAS, PORPHIRINS. **(B)** The score of PORPHIRINS in VEDOSS patients (VEDOSS), SSc patients without skin sclerosis of the forearm (SSc forearm-), SSc patients with skin sclerosis of the forearm (SSc forearm+), and in control subjects (Control) are plotted along the ordinate. *P*-values are determined by Mann-Whitney *U*-test.

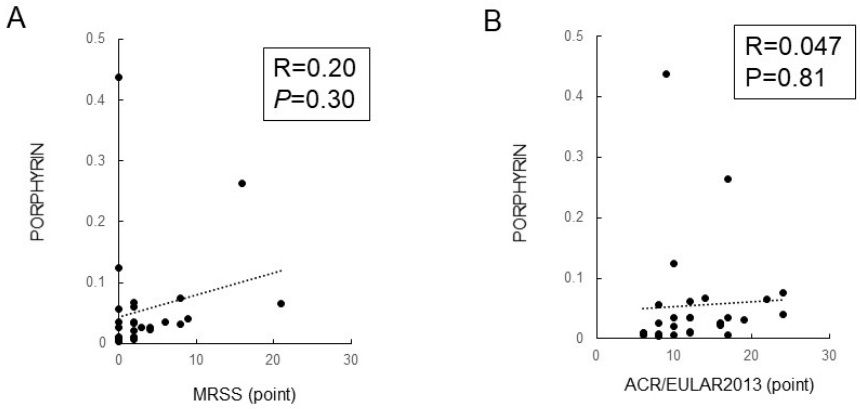

Figure 3. Correlation of PORPHIRINS scores with MRSS or ACR/EULAR2013 score in SSc patients. (A) Correlation of MRSS with PORPHIRINS scores in SSc patients. **(B)** Correlation of ACR/EULAR2013 score with PORPHIRINS scores in SSc patients. Correlations were assessed by Pearson's correlation coefficient.

Additionally, unlike in the previous study focusing on SSc facial analysis, out of the eight parameters there was significant difference in this study among the four groups only in PORPHYRINS scores. There was no correlation of PORPHYRINS scores with MRSS or ACR/EULAR scores, so they may not be useful in evaluation of systemic disease activity. PORPHYRINS scores can be an early diagnostic tool, however, because they can be used to differentiate VEDOSS from early or mild SSc cases in whom skin sclerosis is not yet present in the forearm.

Porphyrins are products that play roles in heme metabolism of liver or bone marrow, and the accumulation of porphyrin in the skin is found in several diseases, especially acnes or porphyria cutanea tarda (PCT). In PCT known to cause SSc-like skin sclerosis, pigmentation, blisters, skin fragility, erosion and scar formation, there is a hypothesis that SSc-like sclerosis results from phototoxicity of porphyrin (*7*). Actually, urine levels of porphyrin precursors (*i.e.*, delta-aminolevulinic acid and porphobilinogen) detected by spectrophotometry are reported to be increased in patients with SSc (*15*). Our results are consistent with these notions. As a possible mechanism of skin sclerosis by porphyrin, uroporphyrin I reportedly induces the production of collagen fibers from normal human cultured fibroblasts (*16-18*), and the increased levels of porphyrin precursors result in an overgrowth of collagen fibers (*15*). In addition, the presence of coproporphyrin in the skin produces oxygen radicals (*19*), which may further cause vasculopathy such as Raynaud's phenomenon and immunodysfuction such as autoantibodies in SSc (*20*). Moreover, a phase III clinical trial of MT-7117, a selective melanocortin 1 receptor agonist dersimelagon, in patients with erythropoietic protoporphyria and X-linked protoporphyria with a history of photosensitivity began in June 2020. Subsequently, a global phase 2 DECODE study of MT-7117 for the treatment of diffuse cutaneous SSc (dcSSc) was also initiated in the United States, Canada and in Europe. Study of porphyrins may therefore lead to the development of novel therapies as well as early diagnosis.

On the other hand, there are some limitations in the present study. First, the data of healthy subjects was not available, because they rarely visit our hospital as a center in the area. Thus, we could not compare the VISIA data of SSc patients with those of healthy controls. Next, we have not directly measured porphyrin levels in skin, blood or urine. Therefore, the actual increase of porphyrins in the patients is not confirmed. This is a pilot study, and the number of patients included is rather low to allow reliable conclusion. To confirm the result, further detailed researches with larger number of samples and confirmation with other experimental methods are necessary in the future.

In summary, the scores of WRINKLES, TEXTURE, PORES, and PORPHYRINS were higher in SSc forearm+ and SSc forearm- groups than in control subjects. Scores of SPOTS, TEXTURE, PORES, UV SPOTS, BROWN SPOTS, and PORPHYRINS were elevated in patients in SSc forearm+ and SSc forearm- groups compared with those in VEDOSS group. We found statistical significance in the score of PORPHYRINS between SSc forearm- and VEDOSS, and between SSc forearm+ and VEDOSS. Therefore, they can be used to differentiate VEDOSS from early or mild SSc cases, which is sometimes clinically problematic. Furthermore, it may have great potential as a new therapeutic tool. Our study also suggests that the porphyrin research will lead to a better understanding of SSc pathogenesis.

Acknowledgements

We acknowledge proofreading and editing by Benjamin Phillis at the Clinical Study Support Center, Wakayama Medical University.

Funding: None.

Conflict of Interest: The authors have no conflicts of interest to disclose.

References

1. Makino K, Jinnin M, Makino T, Kajihara I, Fukushima S, Inoue Y, Ihn H. Serum levels of soluble carbonic anhydrase IX are decreased in patients with diffuse cutaneous systemic sclerosis compared to those with limited cutaneous systemic sclerosis. Biosci Trends. 2014; 8:144-148.
2. Kawashita Y, Jinnin M, Makino T, Kajihara I, Makino K, Honda N, Masuguchi S, Fukushima S, Inoue Y, Ihn H. Circulating miR-29a levels in patients with scleroderma spectrum disorder. J Dermatol Sci. 2011; 61:67-69.
3. Tabata K, Jinnin M, Furukawa K, Tani S, Okuhira H, Mikita N, Fujii T. Finger sweating levels evaluated by video capillaroscopy system are increased in patients with systemic sclerosis compared to preclinical stage patients. Drug Discov Ther. 2021; 14:325-329.
4. van den Hoogen F, Khanna D, Fransen J, *et al.* 2013 classification criteria for systemic sclerosis: an American college of rheumatology/European league against rheumatism collaborative initiative. Ann Rheum Dis. 2013; 72:1747-1755.
5. Matucci-Cerinic M, Allanore Y, Czirják L, *et al.* The challenge of early systemic sclerosis for the EULAR Scleroderma Trial and Research group (EUSTAR) community. It is time to cut the Gordian knot and develop a prevention or rescue strategy. Ann Rheum Dis. 2009; 68:1377-1380.
6. Clements PJ, Lachenbruch PA, Seibold JR, *et al.* Skin thickness score in systemic sclerosis: an assessment of interobserver variability in 3 independent studies. J Rheumatol. 1993; 20:1892-1896.
7. Linming F, Wei H, Anqi L, Yuanyu C, Heng X, Sushmita P, Yiming L, Li L. Comparison of two skin imaging

analysis instruments: The VISIA® from Canfield *vs.* the ANTERA 3D® CS from Miravex. Skin Res Technol. 2018; 24:3-8.
8. Goldsberry A, Hanke CW, Hanke KE. VISIA system: a possible tool in the cosmetic practice. Drugs Dermatol. 2014; 13:1312-1314.
9. Kislevitz M, Lu KB, Wamsley C, Hoopman J, Kenkel J, Akgul Y. Novel use of non-invasive devices and microbiopsies to assess facial skin rejuvenation following laser treatment. Lasers Surg Med. 2020; 52:822-830.
10. Kuo SCH, Huang F, Chi SY, Lin HP, Chien PC, Hsieh CH. Investigate the improvement of facial skin texture with the VISIA system after total thyroidectomy. BMC Surg. 2021; 21:94.
11. Ichibori R, Fujiwara T, Tanigawa T, Kanazawa S, Shingaki K, Torii K, Tomita K, Yano K; Osaka Twin Research Group, Sakai Y, Hosokawa K. Objective assessment of facial skin aging and the associated environmental factors in Japanese monozygotic twins. J Cosmet Dermatol. 2014; 13:158-163.
12. Lee SJ, Seok J, Jeong SY, Park KY, Li K, Seo SJ. Facial pores: Definition, causes, and treatment options. Dermatol Surg. 2016; 42:277-285.
13. Sawamura S, Jinnin M, Kajihara I, Makino K, Aoi J, Ichihara A, Makino T, Fukushima S, Ihn H. Do scleroderma patients look young?: Evaluation by using facial imaging system. Drug Discov Ther. 2017; 11:342-345.
14. Takahashi Y, Fukushima Y, Kondo K, Ichihashi M. Facial skin photo-aging and development of hyperpigmented spots from children to middle-aged Japanese woman. Skin Res Technol. 2017; 23:613-618.
15. Osiecka B J, Ziółkowski P, Gamian E, Nockowski P. The evaluation of porphyrin content in patients with systemic scleroderma: Preliminary study. Dermatologia Kliniczna. 2006; 8:249-251.
16. Grossman ME, Bickers DR, Poh-Fitzpatrick MB, Deleo VA, Harber LC. Porphyria cutanea tarda. Clinical features and laboratory findings in 40 patients. Am J Med. 1979; 67:277-286.
17. Epstein JH, Tuffanelli DL, Epstein WL. Cutaneous changes in the porphyrias. A microscopic study. Arch Dermatol. 1973; 107:689-698.
18. Varigos G, Schiltz JR, Bickers DR. Uroporphyrin I stimulation of collagen biosynthesis in human skin fibroblasts. A unique dark effect of porphyrin. J Clin Invest. 1982; 69:129-135.
19. Ryu A, Arakane K, Koide C, Arai H, Nagano T. Squalene as a target molecule in skin hyperpigmentation caused by singlet oxygen. Biol Pharm Bull. 2009; 32:1504-1509.
20. Herrick AL, Rieley F, Schofield D, Hollis S, Braganza JM, Jayson MI. Micronutrient antioxidant status in patients with primary Raynaud's phenomenon and systemic sclerosis. J Rheumatol. 1994; 21:1477-1483.

Received December 20, 2021; Revised January 31, 2022; Accepted February 4, 2022.

**Address correspondence to:*
Chikako Kaminaka, Department of Dermatology, Wakayama Medical University Graduate School of Medicine, 811-1 Kimiidera, Wakayama 641-0012, Japan.
E-mail: kamikami@wakayama-med.ac.jp

Released online in J-STAGE as advance publication February 10, 2022.

Original Article

DOI: 10.5582/irdr.2021.01162

Pulmonary affection of patients with Pseudoxanthoma elasticum: Long-term development and genotype-phenotype-correlation

Max Jonathan Stumpf[1,§,*], Christian Alexander Schaefer[1,§], Thorsten Mahn[1], Anna Elisabeth Wolf[1], Leonie Biener[1], Doris Hendig[2], Georg Nickenig[1], Nadjib Schahab[1], Carmen Pizarro[1], Dirk Skowasch[1]

[1] Department of Internal Medicine II, Cardiology, Pneumology and Angiology, University Hospital Bonn, Bonn, Germany;
[2] Institute for Laboratory and Transfusion Medicine, Heart and Diabetes Centre North Rhine Westphalia, University Hospital of the Ruhr University Bochum, Bad Oeynhausen, Germany.

SUMMARY Pseudoxanthoma elasticum (PXE) is a rare, heritable disease caused by various, mainly recessively transmitted mutations in the *ABCC6* gene. Due to calcification of soft connective tissue phenotypic hallmarks are progressive loss of vision, alternation of the skin and early onset atherosclerosis. Beside these main features patients also suffer from impaired alveolar diffusion. The present study focused on impaired lung functioning based on a large cohort of patients with PXE, its long-term development, and genotype-phenotype correlation. Retrospectively, 98 patients and 45 controls were enrolled. All patients underwent body plethysmography and carbon monoxide diffusion testing. Of 35 patients three or more body plethysmographic records were available for long-term analysis. For genotype-phenotype analysis *ABCC6* genotypes were grouped as two missense, mixed, or two nonsense mutations. Patients with PXE showed significantly reduced vital capacity ($p < 0.05$), diffusion capacity ($p < 0.01$), and diffusion transfer coefficient ($p < 0.05$). Over a mean period of 38 months diffusion capacity ($p < 0.05$) and diffusion transfer coefficient ($p < 0.01$) dropped significantly whereas lung volumes remained unchanged. Genotype-phenotype correlation revealed no connection between gene variants and lung functioning. In conclusion, PXE is accompanied by progressive reduction of alveolar diffusion indicating progressive alterations of lung tissue. Genotype-phenotype correlation with genotypes sorted as missense and nonsense mutations do not explain impaired lung functioning.

Keywords Pseudoxanthoma elasticum, lung functioning, restrictive lung disease, alveolar diffusion, genotype-phenotype-correlation

1. Introduction

Pseudoxanthoma elasticum (PXE) is a rare, genetic, metabolic disease caused by autosomal recessive mutations of *ABCC6* gene (*1-3*) with an estimated prevalence between 1:25.000 and 1:56.000 (*4-6*). The human ATP-binding cassette family C member 6 (*ABCC6*) gene encodes an ABC transporter protein, which is mainly expressed in liver and kidneys. *ABCC6* deficiency is associated with low plasma pyrophosphate levels (*7*). Pyrophosphate is one main inhibitor of systemic calcification (*8*). Mutations of *ABCC6*, therefore, would result in decreased blood levels of pyrophosphate and, subsequently, systemic calcification. Resulting characteristic PXE phenotype consists of progressive loss of vision (*9,10*), formation of yellowish papules and coalescing plaques in the skin (*1,11*), and early-onset atherosclerosis (*12,13*). Still, the main substrate of *ABCC6*-encoded transporter protein remains unknown and pathology, subsequently, is yet to be illuminated.

Since PXE is a rare disease, current research mostly focuses on these main features of the disease while other less obvious characteristics remain unexplored until now. Nonetheless, they are essential to fully understand PXE and the medical condition of afflicted persons.

One of these less obvious characteristics is the affection of the lung in patients with PXE. The first report of impaired lung functioning in patients with PXE was published by our department in 2016 by Pingel *et al.* (*14*). Herein, the authors reported reduced carbon monoxide (CO) diffusion capacity in a group of 35 patients with PXE, which was interpreted as a preclinical state of interstitial lung disease. This assumption was supported by several postmortem

examinations of patients with PXE: for example, Jackson and Loh (1980) reported one case with a substantial amount of calcified deposits in alveolar septa with fibrous thickening and perivascular fibrosis (*15*). Puvaneswary (1986) observed bilateral radiographical opacities due to pulmonary calcification induced by elastic tissue damage (*16*). Yamamoto *et al.* presented a case of a woman with calcified nodules scattered in alveolar septa (*17*). Lately, Vos *et al.* (2018) found pleural lesions in a patient with PXE (*18*). Recently, our department characterized pathological nailfold capillaries in patients with PXE (*19*). Herein, body plethysmography revealed reduced vital capacity and Tiffeneau Index in patients with PXE compared to a control group. However, no impairment of CO diffusion capacity occurred.

There is a wide interindividual variance of characteristic features in patients with PXE. Therefore, many attempts have been made to describe genotype-phenotype correlations to better predict individual risk of a severe course of the disease (*20-23*). However, this is difficult regarding the variety of pathogenic *ABCC6* mutations (*22-24*) and possible moderating cofactors such as mutations the *ENPP1* and *GGCX* genes (*25,26*). Additionally, often small sample sizes hinder informative value of these studies. Due to the complicacy of reasonable grouping *ABCC6* mutations, classification according to functionality of the translated protein has been established (*22,23*). Therefore, mutations are classified *via* their resulting protein as missense and nonsense mutations or truncating and non-truncating variants, respectively. Recently, Legrand *et al.* (*22*) and Bartstra *et al.* (*23*) showed that patients with nonsense, or truncating variants respectively, were more severely affected from eye lesions and arterial calcification. Genotype-phenotype correlation regarding lung functioning has never been attempted.

This retrospective study intended to clarify the severity of impaired lung functioning by means of a large cohort of patients with PXE. It further aimed for enlightening the development of lung functioning parameters in long-term follow up, and, in a final step, for specific genotype-phenotype-correlations in relation to impaired lung function.

2. Patients and Methods

This study surveyed body plethysmographic data of patients with PXE assessed between August 2014 and December 2020. It was conducted according to the principles of the Declaration of Helsinki for Human research and has been approved by the local ethics committee of the University of Bonn (no. 126/21). Written informed consent has been obtained from all patients and controls. Diagnosis of PXE was confirmed either genetically or by the results of fundoscopy combined with the results of skin biopsy.

2.1. Patients and controls

Inclusion criteria were sufficient information concerning baseline characteristics and conduction of body plethysmography at baseline. If patients showed three or more records of body plethysmography, records of one-year-follow-up as well as the latest record were included to illustrate long-term development of lung functioning parameters.

In total, 103 patients with PXE were surveyed. 5 Patients were excluded due to missing body plethysmographic data. Therefore, 98 patients were included. Of those, 35 patients presented with three or more records of body plethysmography (baseline, FU-1, FU-2) and entered subgroup analysis of long-term development. Of 69 patients *ABCC6* genotype was available.

Body plethysmographic data of 45 patients without PXE were assessed during clinical routine serving as control group. Baseline characteristics are presented in Table 1, no intergroup differences between baseline and control occurred.

2.2. Body plethysmography

All patients and controls underwent body plethysmography and CO-diffusion testing. Examinations were performed by qualified personnel using Body plethismograph Jaeger® respectively Alveo-Diffusionstest Jaeger® in single breath mode according to current guidelines (*27*). All assessed values were recorded as standard value and percentage of predicted value. The latter were calculated by integrated software during body plethysmography referring to reference values provided by the Global Lung Initiative (*28*). Abbreviations corresponding to percentage of predicted values are labeled with "%". The following parameters entered statistical analysis: total lung capacity (TLC, TLC%), vital capacity (VC, VC%), residual volume (RV%), forced expiratory volume (FEV1, FEV1%), Tiffeneau Index (FEV1/FVC), and Hb-adjusted diffusion parameters (DLCO/SB%, DLCO/

Table 1. Baseline characteristics

Variables	PXE Baseline (n = 98)	Control (n = 45)	p
Gender [female] (%)	63 (64.3)	21 (46.7)	0.067
Age [years]	49.6 ± 14.2	54.1 ± 13.8	0.078
BMI [kg/m^2]	27.33 ± 6.02	26.50 ± 4.23	n.s.
Nicotine abuse* (%)	46 (46.9)	26 (57.8)	n.s.
Packyears	5.8 ± 10.5	9.1 ± 20.0	n.s.
Diabetes (%)	3 (3.1)	3 (6.7)	n.s.
Hypertension (%)	38 (38.8)	17 (37.8)	n.s.
Renal dysfunction (%)	0 (0.0)	0 (0.0)	n.s.
Dyslipidemia (%)	36 (36.7)	10 (22.2)	n.s.
COPD (%)	2 (2.0)	3 (6.7)	n.s.
Asthma (%)	0 (0.0)	0 (0.0)	n.s.

*Current and former nicotine abuse. BMI: Body Mass Index, COPD: Chronic obstructive pulmonary disease.

VA%). DLCO/SB (diffusion capacity) describes the amount of CO diffusing from alveoli into the blood in 10 ± 2 seconds. DCLO/VA (diffusion transfer coefficient) describes CO diffusion in relation to alveolar volume. Isolated reduced values of DLCO/SB indicate impaired gas distribution (*e.g.*, emphysema) whereas concomitant reduction of DLCO/VA implicates impaired diffusion (*27*).

Obstructive and restrictive body plethysmographic pattern was defined according to Pellegrino *et al.* (2005). Thereby, an obstructed pattern was assumed in patients with reduced FEV1/FVC (< 70%) and normal VC or, respectively, reduced VC and normal TLC. Restrictive pattern was diagnosed in patients presenting with normal FEV1/FVC and reduced VC and TLC (*29*).

2.3. Genotype-phenotype analysis

All 69 patients with available mutational analysis were included in genotype-phenotype analysis. Patients without or incomplete *ABCC6*-sequencing were excluded as well as those without a detected mutation on the second allele. Grouping of the remaining 58 patients was performed according to Legrand *et al.* (2017) (*22*). Therefore, mutations were sorted by mutation type as missense and nonsense mutations. As a result, included patients were assigned to three groups according to mutation combination of their alleles (missense/missense, missense/nonsense, nonsense/nonsense). Intergroup differences were calculated by means of baseline TLC%, VC%, RV%, FEV1%, and CO-diffusion parameters.

Patients with complete *ABCC6* sequencing and long-term body plethysmography data were analyzed as a subgroup according to the development of diffusion parameters in relation to genotype.

2.4. Statistical analysis

Statistical analysis was performed using IMB® SPSS® Statistics, Version 26. To calculate intergroup differences of nominal and ordinal scaled variables Cramer's V and χ^2-test, respectively, were applied. Continuously scaled parameters were compared *via* independent-sample *t*-test respectively ANOVA for calculating intergroup differences in long-term follow up subgroup analysis. Two-tailed *p*-value was defined significant at 0.05-level. Continuously scaled variables are presented as mean ± standard deviation.

3. Results

No significant differences regarding baseline characteristics occurred (Table 1). Of note, the control group was insignificantly older, reported a higher amount of pack years, and contained more men compared to PXE.

3.1. Body plethysmography at baseline

Results of body plethysmography are presented in Table 2. Four patients presented with restrictive pattern, two showed obstructive body plethysmographic pattern. Patients with PXE showed significantly reduced values of TLC, VC, VC%, and FEV1 compared to control. No differences occurred regarding TLC%, FEV1%, and RV%.

Regarding diffusion parameters both DLCO/SB ($p < 0.01$) and DLCO/VA ($p < 0.05$) were significantly lower in patients with PXE. 40% of patients with PXE showed reduced DLCO/SB% corresponding to a Z-score ≤ -1 (decreased DLCO/SB% ≥ one standard deviation) compared to control ($p < 0.001$).

3.2. Long-term development of body plethysmographic parameters

A total number of 35 patients merged into subgroup analysis for long-term development (Table 3). First

Table 2. Results of body plethysmography

Variables	PXE (*n* = 98)	Control (*n* = 45)	*p*
Restrictive pattern [*n* (%)]	4 (4.1)	2 (4.4)	n.s.
Obstructive pattern [*n* (%)]	2 (2.0)	3 (6.7)	n.s.
TLC [l]	5.86 ± 1.23	6.58 ± 1.40	< 0.01
TLC% [%]	102 ± 14	104 ± 16	n.s.
VC [l]	3.57 ± .84	4.10 ± 1.07	< 0.01
VC% [%]	95 ± 15	101 ± 17	< 0.05
RV% [%]	119 ± 34	121 ± 31	n.s.
FEV1 [l]	3.04 ± .71	3.35 ± .87	< 0.05
FEV1% [%]	99 ± 16	103 ± 14	n.s.
FEV1/FVC [%]	85 ± 10	83 ± 6	n.s.
DLCO/SB% [%]	78 ± 13	85 ± 10	< 0.01
DLCO/VA% [%]	87 ± 13	93 ± 12	< 0.05
DLCO/SB% (Z-score ≤ -1) [*n* (%)]	39 (40.0)	4 (8.9)	< 0.001
DLCO/VA% (Z-score ≤ -1) [*n* (%)]	12 (12.2)	1 (2.2)	0.062

Abbreviations amended with % represent percentage of predicted value; TLC: total lung capacity; VC: vital capacity; RV: residual volume; FEV1: forced expiratory volume; FEV1/FVC: Tiffeneau Index; DLCO/SB: CO-diffusion capacity; DLCO/VA: diffusion transfer coefficient.

Table 3. Long-term development of body plethysmographic parameters

Variables	Baseline (n = 35)	FU-1 (n = 35)	FU-2 (n = 35)	p
Period to baseline [months]		12 ± 4	38 ± 12	
Restrictive pattern [n (%)]	1 (2.9)	2 (5.7)	1 (2.9)	n.s.
Obstructive pattern [n (%)]	0 (0.0)	0 (0.0)	0 (0.0)	n.s.
TLC% [%]	100 ± 12	103 ± 13	108 ± 13	< 0.05
VC% [%]	97 ± 12	98 ± 12	97 ± 12	n.s.
RV% [%]	113 ± 24	119 ± 30	128 ± 27	n.s.
FEV1% [%]	103 ± 15	102 ± 14	99 ± 14	n.s.
FEV1/FVC [%]	87 ± 6	85 ± 6	85 ± 6	n.s.
DLCO/SB% [%]	78 ± 11	77 ± 14	70 ± 10	< 0.05
DLCO/VA% [%]	87 ± 12	86 ± 13	77 ± 12	< 0.01
DLCO/SB% (Z-score ≤ -1) [n (%)]	14 (40)	18 (51)	29 (83)	< 0.001
DLCO/VA% (Z-score ≤ -1) [n (%)]	4 (11)	6 (17)	15 (43)	< 0.01

Abbreviations amended with % represent percentage of predicted value; TLC: total lung capacity; VC: vital capacity; RV: residual volume; FEV1: forced expiratory volume; FEV1/FVC: Tiffeneau Index; DLCO/SB: diffusion capacity; DLCO/VA: diffusion transfer coefficient.

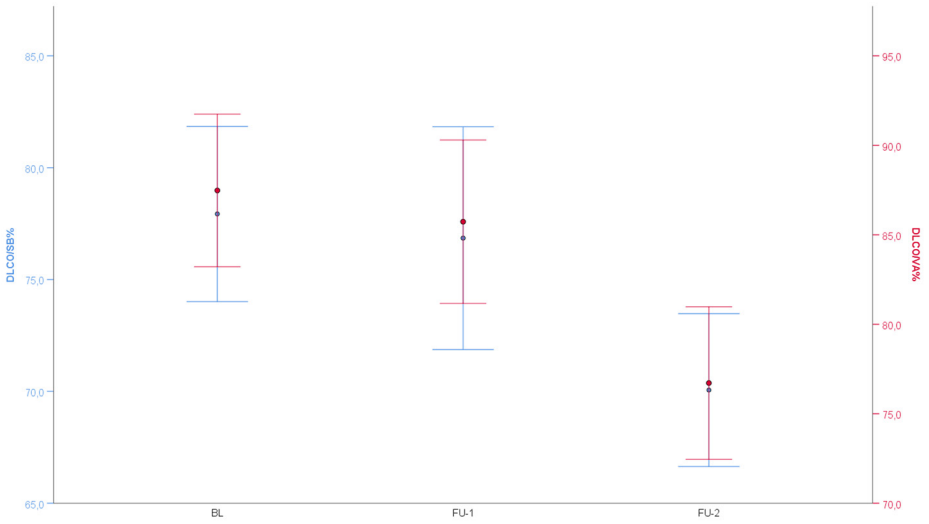

Figure 1. Mean values of diffusion capacity (DLCO/SB%) and diffusion transfer coefficient (DLCO/VA%) at baseline (BL), after 12 months (FU-1), and after 38 months (FU-2).

follow up examination (FU-1) after baseline was conducted after 12 ± 2 months. The second follow up examination (FU-2) was performed after 38 ± 12 months. None of the patients observed in long-term development showed an obstructive ventilatory pattern. Further, no increase of patients with restrictive pattern was observed. No relevant intergroup differences regarding body plethysmography occurred. Diffusion parameters decreased over time (Figure 1). Decrease of DLCO/VA% was even more distinct ($p < 0.01$) compared to DLCO/SB% ($p < 0.05$). Also, the number of patients with relevant reduced DLCO/SB% ($p < 0.001$) and DLCO/VA% ($p < 0.01$) (Z-score ≤ -1) grew significantly.

3.3. Genotype-phenotype-correlation

ABCC6 mutation analysis was available for 69 patients with PXE. Within those, 46 different mutations occurred. Mutations and their incidence are presented in Supplemental Table S1(*http://www.irdrjournal.com/action/getSupplementalData.php?ID=89*). The c.3421C>T (p.Arg1141*) mutation was detected in 49 alleles and, therefore, occurred most frequently by far. Interestingly, in 11 patients with complete *ABCC6* mutation analysis no mutation on the second allele was found. Further, to the best of our knowledge, the seven mutations c.3179C>G (p.Pro1060Arg), c.2399G>A (p.Gly800Arg), c.2230A>C (p.Thr744Pro), c.2090C>T (p.Pro697Leu), c.1589T>C (p.Leu530Pro), c.3679_3770insC, and c.2071-1G>A on *ABCC6* gene have not been reported previously.

No intergroup differences between patients with missense/missense (m/m; n = 11), missense/nonsense (m/n; n = 18), and nonsense/nonsense (n/n, n = 29) occurred (Table 4A). Of those, 25 patients had three or more body plethysmographic records and entered subgroup analysis (Table 4B, Figure 2). The decrease of diffusion parameters seen in long term analysis was mirrored by all three groups (m/m; m/n; n/n).

Although diffusion values were lower in patients with n/n mutation pattern, no level of significance has been reached.

4. Discussion

Clinical data on impaired lung functioning of patients with PXE is scarce. A comprehensive PubMed search using the search item "*Pseudoxanthoma elasticum AND lung*" yielded two results (*14,19*). Therefore, this study is the largest clinical investigation of lung functioning in patients with PXE up to now. It was demonstrated that PXE is frequently accompanied by reduced diffusion parameters. Moreover, patients with PXE presented with significantly reduced TLC, VC, VC% and FEV1. The combination of reduced total lung capacity, vital capacity, and diffusion parameters can be interpreted as restrictive lung disease. This conclusion, however, cannot be drawn unconditionally from present data. That is, on the one hand, due to VC% values within reference and, on the other hand, due to stable or even increasing values of TLC% and VC% in long-term development. Moreover, there was no relevant number of patients with a restrictive ventilatory pattern. With 2% of patients with an obstructive ventilatory pattern in PXE, chronic obstructive pulmonary disease (COPD) is underrepresented in this sample compared to the literature (*30*). This may be due to relatively young age and a low mean number of pack years in this sample. Also, patients with PXE, being aware of their diagnosis, often live a healthy lifestyle.

Therefore, these results mainly indicate an isolated impairment of alveolar diffusion in PXE and, subsequently, confirm the assumptions of Pingel *et al.* (2016) (*14*).

In general, reports of long-term development in patients with PXE are rare. This investigation surveyed body plethysmographic data over a mean period of 38 months. During this time, diffusion parameters dropped significantly whereas mobilizable lung volume remained unchanged. This indicates a progressive impediment of diffusion through the alveolar-capillary membrane. A rationale based on pathology, however, is not easy to find since there still is a lack of knowledge regarding high-resolution CT-Imaging of the lungs and

Table 4A. Diffusion parameters in relation to genotype

Variables	m/m (n = 11)	m/n (n = 18)	n/n (n = 29)	p
TLC% [%]	102 ± 14	102 ± 12	98 ± 13	n.s.
VC% [%]	99 ± 20	98 ± 11	94 ± 15	n.s.
RV% [%]	116 ± 20	117 ± 24	108 ± 27	n.s.
FEV1% [%]	101 ± 25	103 ± 11	102 ± 13	n.s.
DLCO/SB% [%]	76 ± 11	79 ± 8	82 ± 15	n.s.
DLCO/VA% [%]	88 ± 12	88 ± 8	92 ± 15	n.s.

Abbreviations amended with % represent percentage of predicted value; TLC: total lung capacity; VC: vital capacity; RV: residual volume; FEV1: forced expiratory volume; DLCO/SB: CO-diffusion capacity; DLCO/VA: diffusion transfer coefficient; m: missense mutation; n: nonsense mutation.

Table 4B. Long-term development of diffusion parameters in relation to genotype

Variables	m/m (n = 6)	m/n (n = 9)	n/n (n = 10)	p
Baseline				
DLCO/SB% [%]	81 ± 8	77 ± 6	77 ± 13	n.s.
DLCO/VA% [%]	90 ± 9	90 ± 8	85 ± 16	n.s.
FU-1				
Period to baseline [months]			12 ± 4	
DLCO/SB% [%]	77 ± 5	77 ± 10	74 ± 12	n.s.
DLCO/VA% [%]	86 ± 12	88 ± 12	84 ± 14	n.s.
FU-2				
Period to baseline [months]			38 ± 12	
DLCO/SB% [%]	73 ± 9	71 ± 11	68 ± 8	n.s.
DLCO/VA% [%]	80 ± 16	81 ± 16	73 ± 12	n.s.

Abbreviations amended with % represent percentage of predicted value; DLCO/SB: CO-diffusion capacity; DLCO/VA: diffusion transfer coefficient; m: missense mutation; n: nonsense mutation.

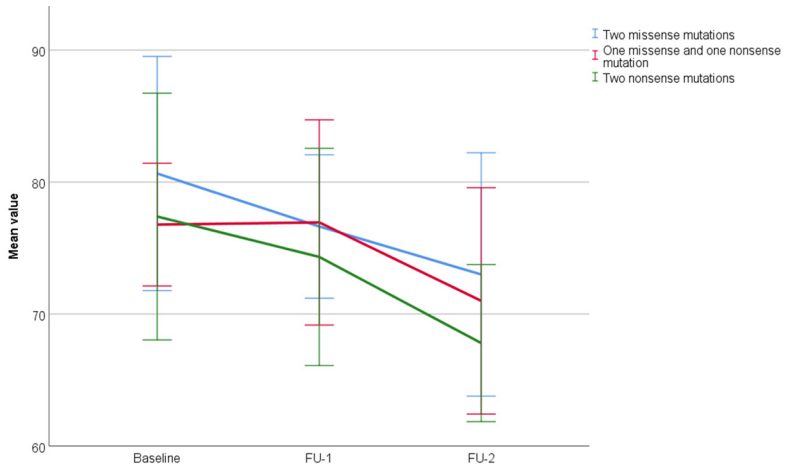

Figure 2. Mean values of diffusion capacity (DLCO/SB%) and diffusion transfer coefficient (DLCO/VA%) at baseline, after 12 months (FU-1), and after 38 months (FU-2) according to mutation type.

histological characteristics of lung tissue. Nonetheless, at least three different explanatory approaches are needed to discuss this context. First, decreasing CO-diffusion capacity can be explained by emphysema. However, emphysema does not explain increasing CO-diffusion transfer coefficient which relates CO diffusion to lung surface participating in gas exchange (*27*). Moreover, chronic pulmonary obstructive disease as representative of pulmonary disease with emphysema is not frequently accompanied by reduction of both, CO-diffusion capacity and coefficient (*31*). Second, impaired diffusion parameters may be due to structural alterations of the alveolar-capillary membrane as indicated by cited case studies (*15-18*). Reduced diffusion parameters would, therefore, be induced by progressive calcification of lung tissue and fragmentation of elastic fibers. This results in thickening of alveolar-capillary membrane and hindered diffusion. Third, impaired gas exchange can be caused by alterations of pulmonary capillaries. Especially, capillary dilatations have been associated with reduced alveolar diffusion (*32*). Since there is no data on morphology of pulmonary capillaries in PXE it remains a matter of speculation weather or not pulmonary capillaries in PXE are altered. However, alterations of nailfold capillaries correlate with capillary alteration in different sites of the body (*33*). Nailfold capillaries in PXE show a highly pathological pattern with ramification, dilatations, and perivascular edema (*19*). If this pattern is mirrored by pulmonary capillaries, this might also explain reduced diffusion parameters as well as unimpaired vital and total lung capacities. Autopsy studies and high-resolution CT-scans are necessary to shed light on pathology of pulmonary involvement in PXE.

According to our clinical experience patients with PXE do not frequently suffer from dyspnea. However, physical fitness is often limited by intermittent claudication due to early onset atherosclerosis and vascular occlusion (*12*) as well as visual impairment (*9*). Therefore, dyspnea may not occur due to a lack of physical activity. Reduced diffusion parameters should be taken into account regarding, for example, medical consultations in questions of physical resilience in patients with PXE.

Genotype-phenotype correlation showed no significant association between impaired diffusion parameters and mutational pattern in patients with PXE. Patients with nonsense mutations on both alleles, however, showed insignificant lower values of DLCO/SB and DLCO/VA in long-term follow up. This would be in line with the finding of Legrand *et al.* and Bartstra *et al.* (*22,23*) who found patients with two *ABCC6* nonsense mutations to present with a more severe PXE phenotype. However, the present study is most likely underpowered to elaborate significant differences in this matter.

Nonetheless, grouping according to missense and nonsense mutations is arbitrary. It cannot be applied on every symptom of PXE. For example, severity of skin alterations neither correlates with truncated proteins nor nonsense mutations (*22,23*). Therefore, phenotypic impairment of diffusion in the lungs may not be explainable by mutation locus on the *ABCC6* gene. Larger cohorts as well as analysis of other PXE causing genes such as *ENPP1* or *GGCX* or genetic co-factors are needed to resolve the open questions of genotype-phenotype correlations in PXE.

This study has several limitations. Although this study included approximately between seven and ten percent of all patients with PXE in Germany, the first and foremost limitation is the sample size which restrains validity of the results. Also, retrospective and single-center study design without the possibility of blinding examining personnel regarding diagnosis of PXE lessens the validity. Larger studies are needed regarding genotype-phenotype correlation including analysis of other PXE causing genetic factors such as *ENPP1* or modifier genes.

5. Conclusions

This study encompasses the largest evaluation of body plethysmographic data in PXE up to now. Patients with PXE presented with significantly reduced vital capacity as well as impaired diffusion capacity and diffusion transfer coefficient. Beyond that, it revealed relevant progression of impaired alveolar diffusion over a mean period of 38 months. This indicates progressive alterations of lung tissue in PXE or pathologies of pulmonary capillaries without influencing mobilizable lung volumes. Well-established grouping of *ABCC6*-mutations according to missense and nonsense mutations did not reveal any association with impaired alveolar diffusion. More research is needed in this matter.

Acknowledgements

The authors would like to thank all medical personnel for their great support, not only regarding this work. Further, we would like to thank the "Selbsthilfegruppe für PXE-Erkrankte Deutschlands e.V." represented by Norbert Bosch and Joachim Pott.

Funding: None.

Conflict of Interest: The authors have no conflicts of interest to disclose.

References

1. Neldner KH. Pseudoxanthoma elasticum. Int J Dermatol. 1988; 27:98-100.
2. Uitto J, Li Q, Jiang Q. Pseudoxanthoma elasticum: molecular genetics and putative pathomechanisms. J

Invest Dermatol. 2010; 130:661-670.
3. Jiang Q, Endo M, Dibra F, Wang K, Uitto J. Pseudoxanthoma elasticum is a metabolic disease. J Invest Dermatol. 2009; 129:348-354.
4. Kranenburg G, Baas AF, de Jong PA, Asselbergs FW, Visseren FLJ, Spiering W; SMART study-group. The prevalence of pseudoxanthoma elasticum: Revised estimations based on genotyping in a high vascular risk cohort. Eur J Med Genet. 2019; 62:90-92.
5. Struk B, Neldner KH, Rao VS, St Jean P, Lindpaintner K. Mapping of both autosomal recessive and dominant variants of pseudoxanthoma elasticum to chromosome 16p13.1. Hum Mol Genet. 1997; 6:1823-1828.
6. Germain DP. Pseudoxanthoma elasticum. Orphanet J Rare Dis. 2017; 12:85.
7. Jansen RS, Küçükosmanoglu A, de Haas M, Sapthu S, Otero JA, Hegman IE, Bergen AA, Gorgels TG, Borst P, van de Wetering K. *ABCC6* prevents ectopic mineralization seen in pseudoxanthoma elasticum by inducing cellular nucleotide release. Proc Natl Acad Sci U S A. 2013; 110:20206-20211.
8. Lomashvili KA, Cobbs S, Hennigar RA, Hardcastle KI, O'Neill WC. Phosphate-induced vascular calcification: role of pyrophosphate and osteopontin. J Am Soc Nephrol. 2004; 15:1392-1401.
9. Gliem M, Müller PL, Birtel J, Hendig D, Holz FG, Charbel Issa P. Frequency, Phenotypic Characteristics and Progression of Atrophy Associated With a Diseased Bruch's Membrane in Pseudoxanthoma Elasticum. Invest Ophthalmol Vis Sci. 2016; 57:3323-3330.
10. Gliem M, Zaeytijd JD, Finger RP, Holz FG, Leroy BP, Charbel Issa P. An update on the ocular phenotype in patients with pseudoxanthoma elasticum. Front Genet. 2013 Apr 4;4:14.
11. Uitto J, Jiang Q, Váradi A, Bercovitch LG, Terry SF. PSEUDOXANTHOMA ELASTICUM: DIAGNOSTIC FEATURES, CLASSIFICATION, AND TREATMENT OPTIONS. Pseudoxanthoma elasticum: diagnostic features, classification, and treatment options. Expert Opin Orphan Drugs. 2014; 2:567-577.
12. Pingel S, Pausewang KS, Passon SG, Blatzheim AK, Gliem M, Charbel Issa P, Hendig D, Horlbeck F, Tuleta I, Nickenig G, Schahab N, Skowasch D, Schaefer CA. Increased vascular occlusion in patients with pseudoxanthoma elasticum. Vasa. 2017; 46:47-52.
13. Kranenburg G, de Jong PA, Mali WP, Attrach M, Visseren FL, Spiering W. Prevalence and severity of arterial calcifications in pseudoxanthoma elasticum (PXE) compared to hospital controls. Novel insights into the vascular phenotype of PXE. Atherosclerosis. 2017 Jan;256:7-14.
14. Pingel S, Passon SG, Pausewang KS, Blatzheim AK, Pizarro C, Tuleta I, Gliem M, Charbel Issa P, Schahab N, Nickenig G, Skowasch D, Schaefer CA. Pseudoxanthoma Elasticum – Also a Lung Disease? The Respiratory Affection of Patients with Pseudoxanthoma Elasticum. PLoS One. 2016; 11:e0162337.
15. Jackson A, Loh CL. Pulmonary calcification and elastic tissue damage in pseudoxanthoma elasticum. Histopathology. 1980; 4:607-611.
16. Puvaneswary M. Pulmonary radiographic changes in pseudoxanthoma elasticum. Australas Radiol. 1986; 30:310-312.
17. Yamamoto N, Hasegawa H, Sakamoto H, Numata H, Fukuda T, Komatsu S, Kido Y. Pseudoxanthoma elasticum with pulmonary calcification. Nihon Kyobu Shikkan Gakkai Zasshi. 1996; 34:716-720. (in Japanese)
18. Vos A, Kranenburg G, de Jong PA, Mali WPTM, Van Hecke W, Bleys RLAW, Isgum I, Vink A, Spiering W. The amount of calcifications in pseudoxanthoma elasticum patients is underestimated in computed tomographic imaging; a post-mortem correlation of histological and computed tomographic findings in two cases. Insights Imaging. 2018; 9:493-498.
19. Stumpf MJ, Mahn T, Steinmetz M, Fimmers R, Pizarro C, Nickenig G, Skowasch D, Schahab N, Schaefer CA. Pseudoxanthoma elasticum – also a microvascular disease. Vasa. 2020; 49:57-62.
20. Le Saux O, Beck K, Sachsinger C, Silvestri C, Treiber C, Göring HH, Johnson EW, De Paepe A, Pope FM, Pasquali-Ronchetti I, Bercovitch L, Marais AS, Viljoen DL, Terry SF, Boyd CD. A spectrum of *ABCC6* mutations is responsible for pseudoxanthoma elasticum. Am J Hum Genet. 2001; 69:749-764.
21. Pfendner EG, Vanakker OM, Terry SF, *et al.* Mutation detection in the *ABCC6* gene and genotype-phenotype analysis in a large international case series affected by pseudoxanthoma elasticum. J Med Genet. 2007; 44:621-628.
22. Legrand A, Cornez L, Samkari W, Mazzella JM, Venisse A, Boccio V, Auribault K, Keren B, Benistan K, Germain DP, Frank M, Jeunemaitre X, Albuisson J. Mutation spectrum in the *ABCC6* gene and genotype-phenotype correlations in a French cohort with pseudoxanthoma elasticum. Genet Med. 2017; 19:909-917.
23. Bartstra JW, Risseeuw S, de Jong PA, *et al.* Genotype-phenotype correlation in pseudoxanthoma elasticum. Atherosclerosis. 2021; 324:18-26.
24. Götting C, Schulz V, Hendig D, Grundt A, Dreier J, Szliska C, Brinkmann T, Kleesiek K. Assessment of a rapid-cycle PCR assay for the identification of the recurrent c.3421C>T mutation in the *ABCC6* gene in pseudoxanthoma elasticum patients. Lab Invest. 2004; 84:122-130.
25. Nitschke Y, Baujat G, Botschen U, *et al.* Generalized arterial calcification of infancy and pseudoxanthoma elasticum can be caused by mutations in either ENPP1 or ABCC6. Am J Hum Genet. 2012; 90:25-39.
26. Hendig D, Knabbe C, Götting C. New insights into the pathogenesis of pseudoxanthoma elasticum and related soft tissue calcification disorders by identifying genetic interactions and modifiers. Front Genet. 2013; 4:114.
27. Graham BL, Brusasco V, Burgos F, Cooper BG, Jensen R, Kendrick A, MacIntyre NR, Thompson BR, Wanger J. 2017 ERS/ATS standards for single-breath carbon monoxide uptake in the lung. Eur Respir J. 2017; 49:1600016.
28. Quanjer PH, Stanojevic S, Cole TJ, Baur X, Hall GL, Culver BH, Enright PL, Hankinson JL, Ip MS, Zheng J, Stocks J; ERS Global Lung Function Initiative. Multi-ethnic reference values for spirometry for the 3-95-yr age range: the global lung function 2012 equations. Eur Respir J. 2012; 40:1324-1343.
29. Pellegrino R, Viegi G, Brusasco V, *et al.* Interpretative strategies for lung function tests. Eur Respir J. 2005; 26:948-968.
30. Burney P, Patel J, Minelli C, *et al.* Prevalence and population attributable risk for chronic airflow obstruction in a large multinational study. Am J Respir

Crit Care Med. 2020; 203:1353-1365.
31. Wagner PD. The physiological basis of pulmonary gas exchange: implications for clinical interpretation of arterial blood gases. Eur Respir J. 2015; 45:227-243.
32. Rodríguez-Roisin R, Krowka MJ. Hepatopulmonary syndrome – a liver-induced lung vascular disorder. N Engl J Med. 2008; 358:2378-2387.
33. Tian J, Xie Y, Li M, Oatts J, Han Y, Yang Y, Shi Y, Sun Y, Sang J, Cao K, Xin C, Siloka L, Wang H, Wang N. The Relationship Between Nailfold Microcirculation and Retinal Microcirculation in Healthy Subjects. Front Physiol. 2020; 11:880.

Received December 28, 2021; Revised February 3, 2022; Accepted February February 9, 2022.

[§]These authors contributed equally to this work.
**Address correspondence to:*
Max Jonathan Stumpf, University Hospital of Bonn, Medical Department II, Cardiology, Pneumology, and Angiology, Venusberg-Campus 1, 53127 Bonn, Germany.
E-mail: max.stumpf@ukbonn.de

Released online in J-STAGE as advance publication February 12, 2022.

Original Article

DOI: 10.5582/irdr.2021.01138

Pan-cancer analysis of osteogenesis imperfecta causing gene *SERPINF1*

Chao Zhang, Wei Yang, Shanshan Zhang, Yongtao Zhang, Pengchao Liu, Xianxian Li, Wei Zhi, Dan Yang, Mian Li, Yanqin Lu*

Key Laboratory for Biotech-Drugs of National Health Commission, Key Laboratory for Rare & Uncommon Diseases of Shandong Province, Biomedical Sciences College & Shandong Medicinal Biotechnology Centre, Shandong First Medical University & Shandong Academy of Medical Sciences, Ji'nan, China.

SUMMARY Osteogenesis imperfecta (OI) type VI causative gene *SERPINF1*, encodes a member of the serpin family that does not display the serine protease inhibitory activity shown by many of the other serpin proteins. The encoded protein (pigment epithelium-derived factor, PEDF) has anti-tumor, anti-angiogenesis, anti-inflammation, nutrition and nerve protection functions, and participates in fat metabolism. In this paper, a series of bioinformatics analyses were conducted based on the regulation of *SERPINF1* in the human. Pan-cancer analysis of *SERPINF1* revealed it to play a role in the prognosis of tumors, especially in KIRC, and that high expression of *SERPINF1* leads to a poor prognosis of the disease, the occurrence of which is largely related to the high expression of *SERPINF1* leading to immune infiltration of cancer associated fibroblasts. Mutation analysis found that *SERPINF1* had eight identical amino acids alterations sites with different in both cancer and OI patients. which hints the possible relationship between genotype and phenotype.

Keywords *SERPINF1*, osteogenesis imperfecta, pan-cancer analysis, cancer

1. Introduction

Osteogenesis imperfecta (OI) type VI disease-causing gene, *SERPINF1*, located on chromosome 17P13.3 encodes for pigment epithelium-derived factor (PEDF), which is expressed actively in adult bone, especially in active bone growth sites (*1,2*). PEDF belongs to the serpin super family, functions in anti-tumor, anti-angiogenesis, anti-inflammation, nutrition and nerve protection, and participates in fat metabolism (*3-6*).

In bone, PEDF can promote the differentiation and mineralization of osteoblasts, facilitate the gene expression of osteoblasts, inhibit the maturation of osteoclasts, and activate the Wnt/β-Catenin signal transduction pathway (*2,7,8*). In osteoblasts, PEDF can hardly be detected in the serum of patients with osteogenesis imperfecta induced by *SERPINF1* mutation (*9*). In tumors, PEDF selectively induces apoptosis of endothelial cells in vessels undergoing remodeling (*4*). PEDF has also been shown to have suppressor-like activity *in vivo* and directly inhibits tumor growth and metastasis, and reduced PEDF levels have also been associated with a worse prognosis in a variety of tumors (*4*).

In this paper, we used the GCBI website to find the related diseases reported by the *SERPINF1* gene in the article. Through the pan-cancer analysis of *SERPINF1* gene, the potential molecular mechanisms of *SERPINF1* in the pathogenesis or clinical prognosis were found in different cancers. We also analyzed the mutation sites of *SERPINF1* in cancer and osteogenesis imperfecta, to find out the potential diseases connection among these diseases.

2. Methods and Materials

2.1. Gene's research status and regulation mechanism

We input *SERPINF1* in the "Gene radar" module of GCBI (Gene Cloud of Biotechnology Information) web (*https://www.gcbi.com.cn*) and found the research status, regulation network and transcription factor prediction for the *SERPINF1* gene.

2.2. Gene expression analysis

The Human Protein Atlas website (*https://www.proteinatlas.org*) was used to get the expression of *SERPINF1* in different human tissues and cell types (*10,11*).

We used the TIMER2 (tumor immune estimation resource, version 2) website (*http://timer.cistrome.org*) to observe the difference in *SERPINF1* expression between tumor and paracancerous tissues (*12*).

For tumors without normal tissue or highly restricted normal tissue [*e.g.*, TCGA-ACC (The Cancer Genome Atlas, Adrenocortical carcinoma), TCGA-BLCA (Bladder urothelial carcinoma), *etc.*], GEPIA2 (Gene Expression Profiling Interactive Analysis, version 2) was used to obtain the block diagram of the expression difference between these tumor tissues and corresponding normal tissues in the GTEX (genotype tissue expression) database, under the settings of *p*-value cutoff = 0.01, $\log_2$FC (folding change) cutoff = 1 and "matching TCGA normal and GTEX data" (*13*). In addition, we obtained the violin diagram of *SERPINF1* expression in different pathological stages of all TCGA tumors through the "pathological stage diagram" module of GEPIA2 (*13*). The log2 [TPM (Transcripts per million) +1] transformed expression data were applied for the box or violin plots (*13*).

2.3. Survival prognosis analysis

We used the "survival map" in the "survival analysis" module of the GEPIA2 website to obtain the OS (overall survival) and DFS (disease-free survival) map data related to *SERPINF1* in all tumors in TCGA (log rank test as hypothesis test). Cutoff-high (50%) and cutoff-low (50%) values was used as expression thresholds to separate high expression and low expression cohorts in survival maps and survival plots (*13*).

2.4. Immune infiltration analysis

We used the "Immune-Gene" module of the TIMER2 web server to explore the association between *SERPINF1* expression and immune infiltration across all TCGA tumors. CD^{8+} T-cells, CD^{4+} T-cells, neutrophils, cancer-associated fibroblasts and endothelial cells were selected and the TIMER, CIBERSORT, CIBERSORT-ABS, QUANTISEQ, XCELL, MCPCOUNTER and EPIC algorithms were applied for immune infiltration estimations. The *P*-values and partial correlation values were obtained *via* the purity-adjusted Spearman's rank correlation test and the data were visualized as a heatmap and a scatter plot (*12*).

2.5. Genetic alteration analysis

CBioPortal website (*https://www.cbioportal.org*) was used to obtain the change frequency, mutation type and CNA (copy number alteration) of *SERPINF1* gene in all TCGA tumors (*14*). We used the OI website (*https://oi.gene.le.ac.uk*) to find the *SERPINF1* mutations that cause osteogenesis imperfecta (*15*).

2.6. *SERPINF1* -related gene enrichment analysis

The experimentally determined PEDF binding proteins were obtained by us using the string (*https://string-db.org*) website, with the following settings: full network, evidence, experiments, low confidence (0.150), no more than 50 interactors in the first outer shell.

GeneMANIA websites (*http://genemania.org*) helped us find possible interacting genes by searching many large and open biological data sets (*16*).

Venn plot was drawn using (*http://bioinformatics.psb.ugent.be/webtools/Venn*) to conduct an intersection analysis to compare PEDF binding protein and interacting gene. In addition, we performed KEGG pathway analysis and go analysis on these two groups of data. First, the data of function annotation diagram was obtained by using the DAVID website (*https://david.ncifcrf.gov*), and the data with $P < 0.05$ was selected; the enriched paths are displayed by using "tidyr" and "ggplot2" R packages. R package "cluster profiler" was used for GO (gene ontology) enrichment analysis. By using the cnetplot function (circular = F, color edge = T, node tag = T), the data of GO analysis can be visualized as cnetplot. R language software [R-4.0.5, 64-bit] (*https://www.r-project.org*) was used in this analysis.

3. Results

PEDF belongs to serpin superfamily and is actively expressed in adult bone. It has been identified as an OI type VI pathogenic gene (*1,2*). In addition, it has anti-angiogenesis anti-tumor and other functions (*3,4*). In this study, we aimed to provide a comprehensive analysis on the association of human *SERPINF1* (NM_ 001329903.2 for mRNA, NP_ 001316832.1 for protein, Figure S1 A, *http://www.irdrjournal.com/action/getSupplementalData.php?ID=88*) with the development of cancer and the connection between cancer and osteogenesis imperfecta. As shown in Figure S1 B, in different species (*e.g.*, Homo sapiens, Mus musculus, Equus caballus), the structure of PEDF is usually composed of serpin (cl38926) domain. Phylogenetic tree data confirmed that the structure of PEDF is highly conserved across the different species, suggesting that PEDF may play an important role in basic biological processes (Figure S2, *http://www.irdrjournal.com/action/getSupplementalData.php?ID=88*).

3.1. Gene's research status and regulation mechanism

By searching the GCBI database, we found literature reports about *SERPINF1* related to 20 human diseases, and the most reported disease is cancer. OI disease related document number ranked 12th (Figure 1A).

The regulatory network of *SERPINF1* contains one targeted miRNA (hsa-miR-335-5p), 97 related lncRNA, a downstream phosphorylation gene (*EPM2AIP1*) and

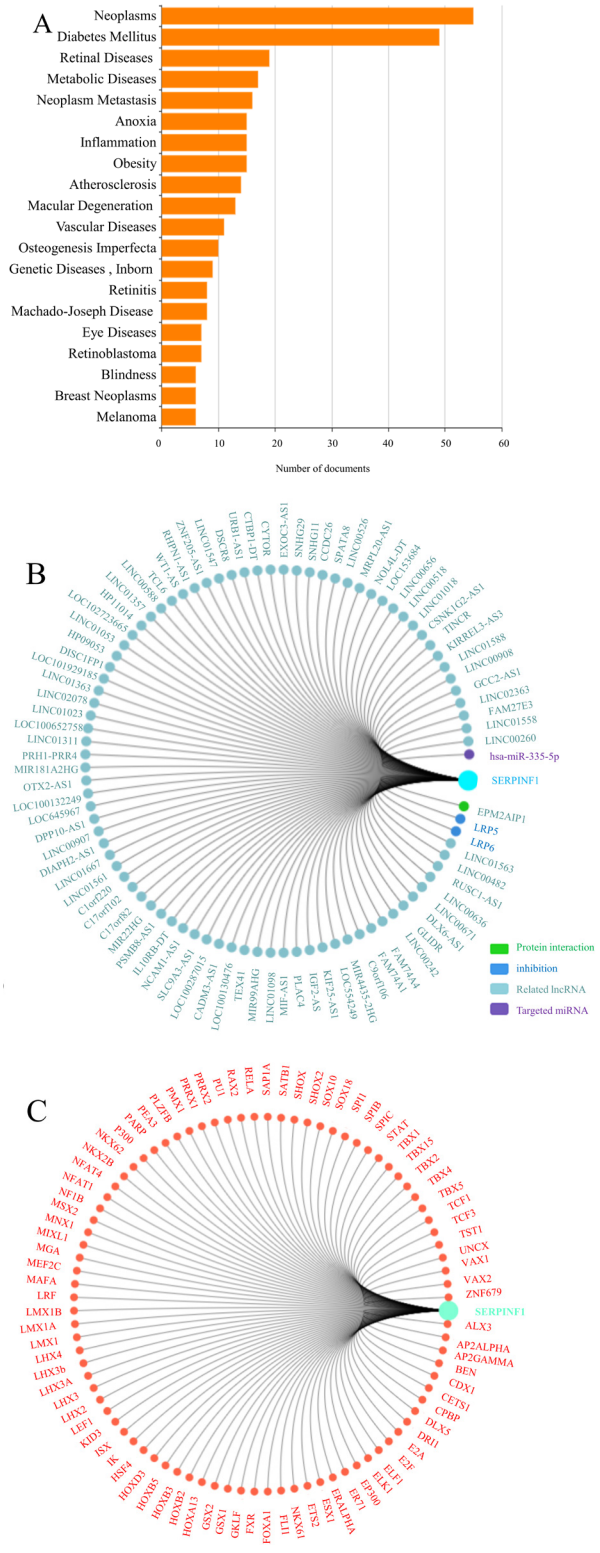

Figure 1. *SERPINF1* research status and regulation mechanism. **(A)** Literature reported about *SERPINF1* in human diseases. **(B)** The regulatory network of *SERPINF1*. **(C)** Transcription factors highly related to *SERPINF1*.

two genes (*LRP5* and *LRP6*) that inhibit *SERPINF1* expression (Figure 1B). Also, there are 87 transcription factors highly associated with *SERPINF1*, which are closely related to the specific expression of *SERPINF1* (Figure 1C)

3.2. Gene expression analysis

We analyzed the expression of *SERPINF1* in different tissues. As shown in Figure S3 (*http://www.irdrjournal.com/action/getSupplementalData.php?ID=88*), *SERPINF1* can be expressed in all detected tissues (all consensus normalized expression values > 0.1). And based on the combination of the HPA (Human protein atlas), GTEx and FANTOM5 (Function annotation of the mammalian genome 5) datasets, *SERPINF1* shows highest expression in the retina, followed by the liver, dendritic cells, and pons and medulla.

We used the TIMER2 website to analyze the expression of *SERPINF1* in different tumor types in the TCGA database. As shown in Figure 2B, the expression level of *SERPINF1* in tumor tissue of BLCA (Bladder Urothelial Carcinoma), BRCA (Breast invasive carcinoma), CHOL (Cholangiocarcinoma), COAD (Colon adenocarcinoma), KICH (Kidney Chromophobe), KIRC (Kidney renal clear cell carcinoma), LUAD (Lung adenocarcinoma), PRAD (Prostate adenocarcinoma), THCA (Thyroid carcinoma), UCEC (Uterine Corpus Endometrial Carcinoma) ($P < 0.001$), CESC (Cervical squamous cell carcinoma and endocervical adenocarcinoma) ($P < 0.01$), GBM (Glioblastoma multiforme), PCPG (Pheochromocytoma and Paraganglioma), and READ (Rectum adenocarcinoma) ($P < 0.05$) is lower than the corresponding control tissues. And the expression of *SERPINF1* in KIRC and LUAD ($P < 0.0001$) is higher than in normal control tissues (Figure 2A).

In cases where tumor and normal tissue data were not available from TCGA, we further evaluated the expression differences of *SERPINF1* between tumor and normal tissues using the GTEX dataset. We found that the expression level of *SERPINF1* in tumor tissue of ACC (Adrenocortical carcinoma), BLCA, BRCA, CESC, CHOL, COAD, KICH, LAML (Acute Myeloid Leukemia), LGG (Brain Lower Grade Glioma), OV (Ovarian serous cystadenocarcinoma), PRAD, READ, TGCT (Testicular Germ Cell Tumors), THCA, UCEC and UCS (Uterine Carcinosarcoma) ($P < 0.01$) is lower than the corresponding control tissues (Figure 2B). And the expression of *SERPINF1* in DLBC (Lymphoid Neoplasm Diffuse Large B-cell Lymphoma), KIRC, PRAD and THYM (Thymoma) ($P < 0.01$) is higher than in normal control tissues (Figure 2C). There was no significant difference in *SERPINF1* expression in other cancers [*e.g.*, LUAD, ESCA (Esophageal carcinoma), GBM, HNSC (Head and Neck squamous cell carcinoma), and KIRP (Kidney renal papillary cell carcinoma)], as shown in Figure S4 (*http://www.irdrjournal.com/action/getSupplementalData.php?ID=88*).

GEPIA2 was used to obtain the expression map of *SERPINF1* at different stages of tumors (Figure S5, *http://www.irdrjournal.com/action/getSupplementalData.php?ID=88*). Among them, the

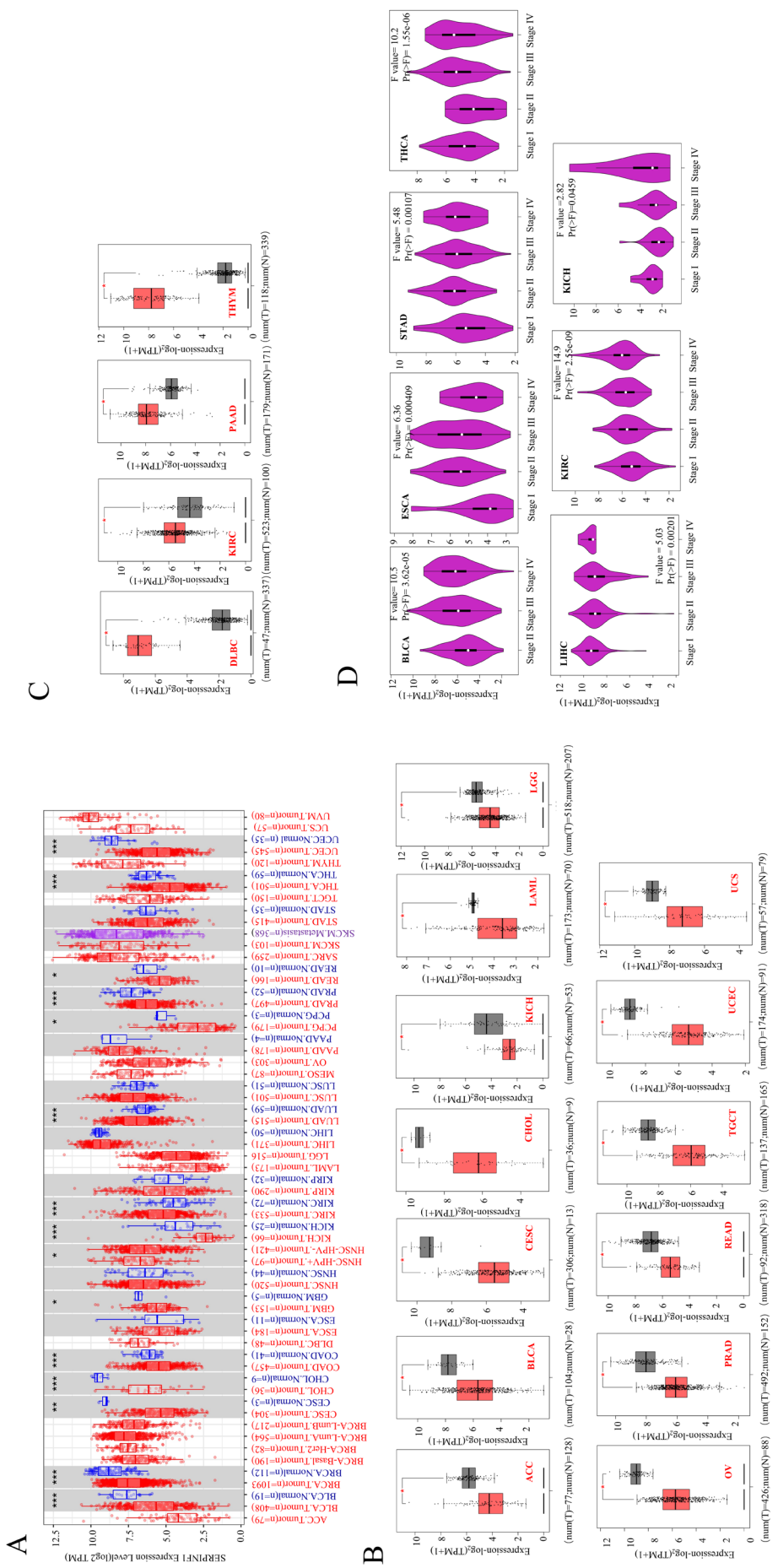

Figure 2. *SERPINF1* expression analysis data. (A) Expression levels of *SERPINF1* in TCGA tumor *vs.* adjacent tissues as visualized by TIMER2. $^{*}P < 0.05$; $^{**}P < 0.01$; $^{***}P < 0.001$. **(B)** *SERPINF1* high expression in tumor tissues by using GEPIA2 website to analyze the expression of *SERPINF1* in different types of cancer (for tumor with no normal tissue or highly restricted normal tissue in TCGA) matched with TCGA normal and GTEx data. **(C)** *SERPINF1* low expression in cancer tissues by using GEPIA2 website to analyze the expression of *SERPINF1* in different types of cancer (for tumor with no normal tissue or highly restricted normal tissue in TCGA) matched with TCGA normal and GTEx data. **(D)** Stage-dependent expression level of *SERPINF1*.

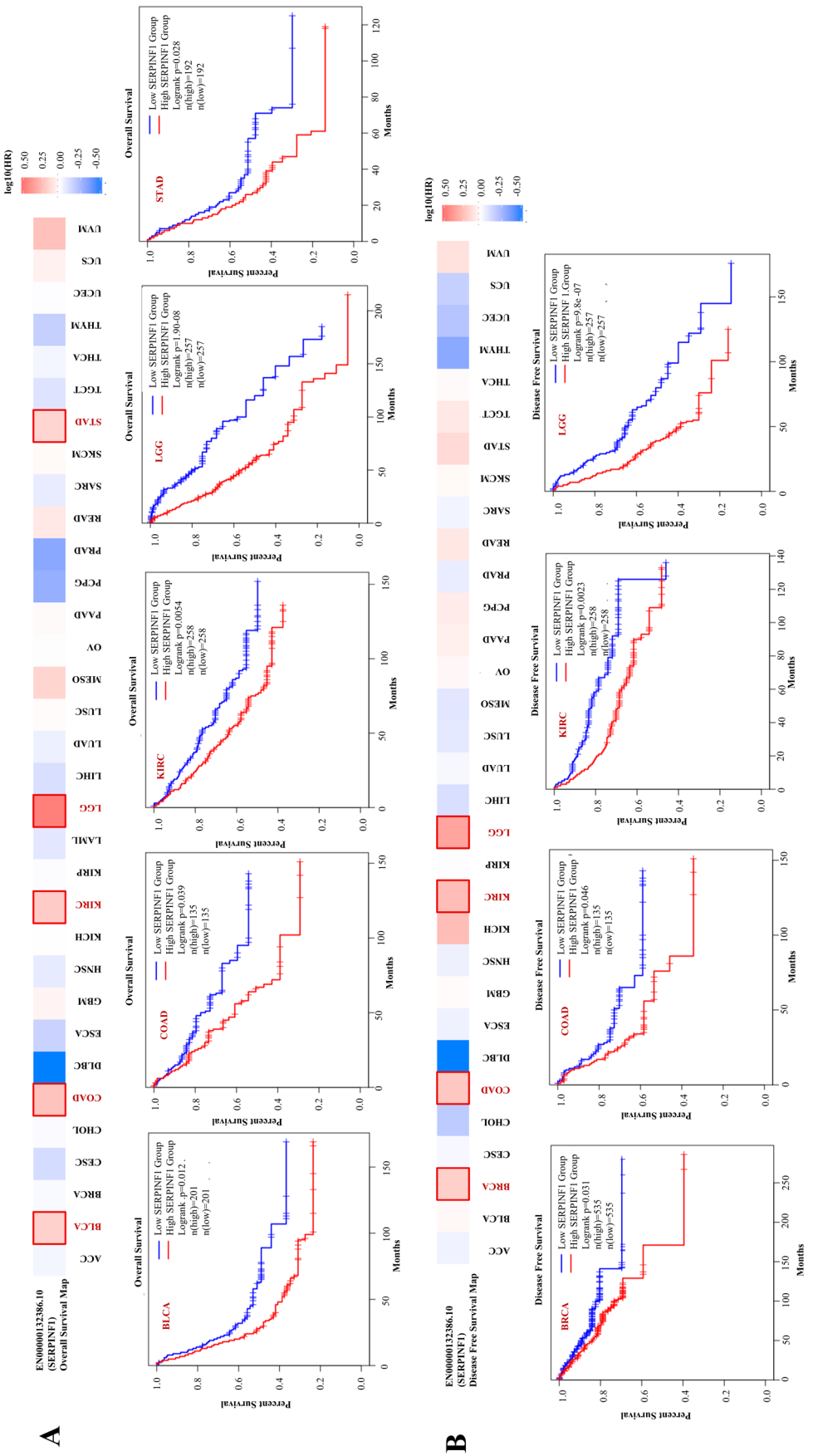

Figure 3. Relationship between *SERPINF1* expression and survival rate in TCGA tumors. **(A)** Relationship between *SERPINF1* gene expression and survival (overall survival). **(B)** Relationship between *SERPINF1* gene expression and survival (disease-free survival).

expression of *SERPINF1* was variable at different stages of ACC, BLCA, CESC, COAD, KICH, LUAD, PAAD, and THCA (Figure 2E, all $P < 0.05$) (Figure 2D).

3.3. Survival analysis data

TCGA and GEO data sets were used to study the correlation between *SERPINF1* expression and prognosis of different tumor patients. As shown in Figure 3A, high expression of *SERPINF1* was associated with poor OS (overall survival) prognosis of BLCA (P = 0.012), COAD (P = 0.039), KIRC (P = 0.0054), LGG (P = 1.9e-8) and STAD (P = 0.028) in TCGA program. Disease-free survival (DFS) analysis data disclosed that a correlation between high *SERPINF1* expression and poor prognosis in TCGA cases of BRCA (P = 9.8e-07), COAD (P = 0.0023), KIRC (P = 0.046) and LGG (P = 0.031) (Figure 3B). It is noteworthy that the high expression of *SERPINF1* leads to a decrease in the OS and DFS survival curves of COAD, KIRC and LGG.

3.4. Immune infiltration analysis data

As an important component of the tumor microenvironment, tumor infiltrating immune cells are closely associated with cancer initiation, progression or metastasis (*17,18*). Cancer associated fibroblasts in tumor microenvironments have been reported to be involved in regulating the function of various tumor infiltrating immune cells and play a key role in tumor adaptation to the host (*19-21*). Here, we used the XCELL, MCPCOUNTER, EPIC and TIDE algorithms to investigate the potential relationship between the level of infiltration of cancer associated fibroblasts and *SERPINF1* gene expression in different TCGA cancer types.

As shown in Figure 4, *SERPINF1* expression in the vast majority of tumors was statistically positively correlated with the value of cancer associated fibroblast infiltration and endothelial cells, but the infiltration ability of CD^{4+} T cells, CD^{8+} T cells, and neutrophils did not correlate with the expression of *SERPINF1*.

It is noteworthy that in KIRC and THCA, the infiltrative capacity of endothelial cells inversely correlated with the expression of *SERPINF1*.

3.5. Genetic alteration analysis data

We observed the genetic alteration status of *SERPINF1* in different tumor samples of the TCGA cohort. As shown in Figure 5A, the highest alteration frequency (> 4%) of *SERPINF1* was present in patients with uterine tumors of the predominant type with "mutations". It is worth noting that the "deep deletion" type of CNA is the predominant type in diffuse large B-cell lymphoma, thymoma, thyroid cancer, acute myeloid leukemia, and pancreatic cancer, whereas "amplified" type CNA are the predominant mutation type in uterine carcinosarcoma, renal clear cell carcinoma, and brain lower grade glioma. The type, location, and number of cases with alterations of *SERPINF1* are further shown in Figure 5A. We found that missense mutations in *SERPINF1* were the predominant type of genetic alteration, with 58 missense mutations, 11 truncating mutations, and one in-frame mutation, with the largest number of duplications (4 times) at the X147_splice/K147K and R99Q loci (Figure 5B, Table S1, *http://www.irdrjournal.com/action/getSupplementalData.php?ID=88*).

From OI database, we found 45 *SERPINF1* mutations reported (Table S2, *http://www.irdrjournal.com/action/getSupplementalData.php?ID=88*) (*15,22*). No common mutation sites were found by comparing the mutation sites of *SERPINF1* in tumors and OI patients. Then, we analyzed whether there were changes in the same amino acids in tumor and OI patients and found eight identical site amino acid with different changes. They are sites 27, 56, 99, 131, 133, 147, 178, and 201, which may lead to different functions of the PEDF and has been associated with tumor prognosis and osteogenesis (Table 1). Significantly, alterations of the amino acids at positions 99 and 147 of *SERPINF1* were the most recurrent in tumors (4 times).

3.6. *SERPINF1*-related gene enrichment analysis date

To further investigate the molecular mechanism of *SERPINF1*, we attempted to screen *SERPINF1* binding proteins and *SERPINF1* expression related genes for a series of pathway enrichment analyses. Based on the string tool, we obtained a total of 31 *SERPINF1* binding proteins that are supported by experimental evidence. The interaction network of these proteins is shown in Figure 6A.

GeneMANIA predicts 20 genes related to *SERPINF1* co-expression, as shown in Figure 6B. GeneMANIA and String web together predicted 48 genes related to the function of *SERPINF1*. Venn plot shows that they have three common members, namely, *EPM2AIP1*, *PNPLA2* and *SERPINA6* (Figure 6C).

We combined the String and GeneMANIA two datasets to perform KEGG and GO enrichment analyses. The KEGG data suggest that "Viral carcinogenesis", "PI3K-Akt signaling pathway" and "cell cycle" might be involved in the effect of *SERPINF1* functions ((Figure 6D). GO enrichment analysis data further show that most of these genes are related to protein metabolism pathways or components and functions of extracellular mechanisms, *e.g.*, extracellular matrix structural constituent, cadherin binding, collagen-containing extracellular matrix, complex of collagen trimers and others. (Figure 6, E-G).

4. Discussion

SERPINF1 is a causative gene for osteogenesis imperfecta, and by searching the GCBI database, we

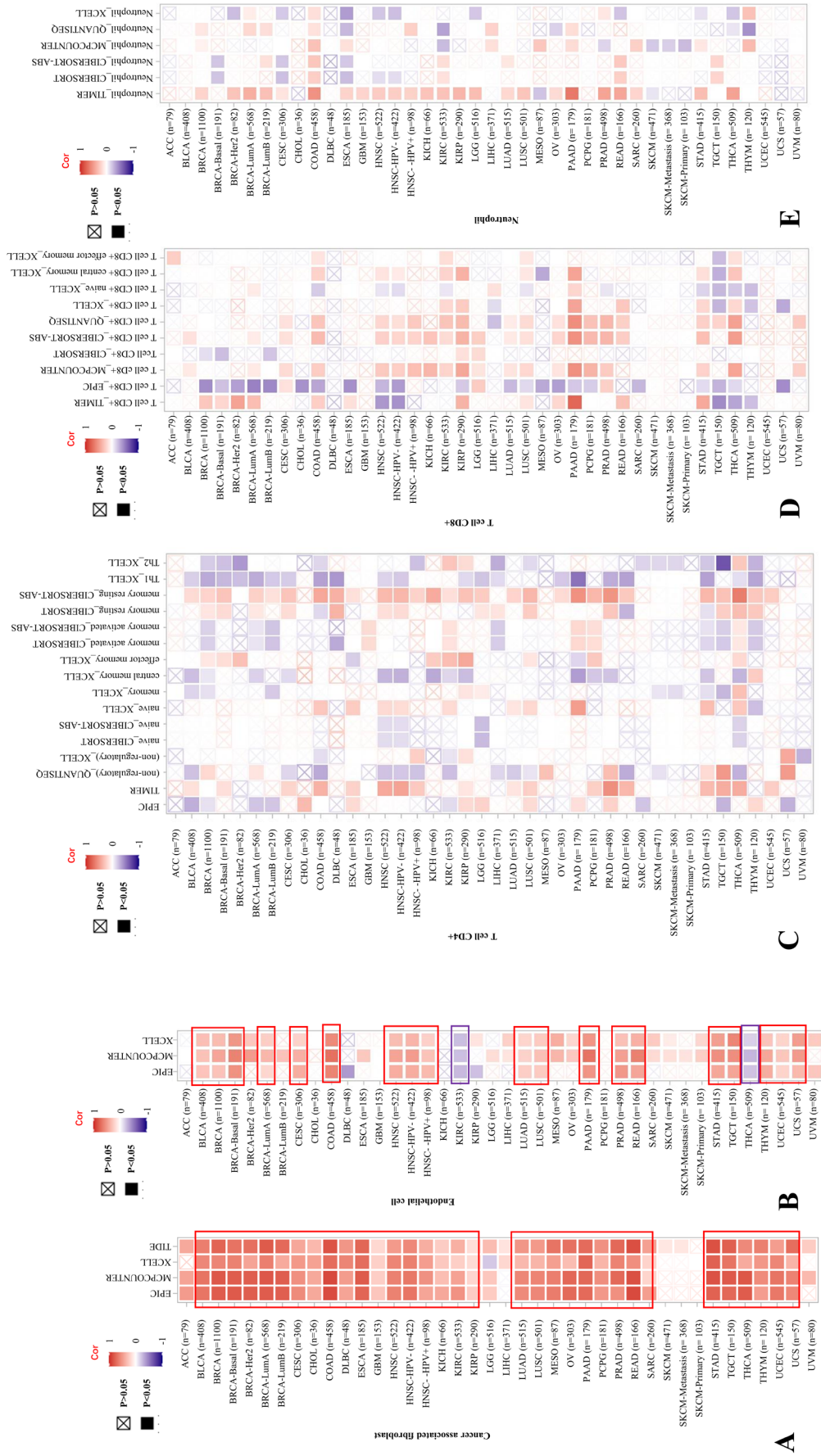

Figure 4. The correlation between *SERPINF1* expression level and infiltration of cancer-associated fibroblasts, endothelial cells, CD^{8+} T cells, CD^{4+} T cells, and neutrophils. (A-E) TIMER, CIBERSORT, CIBERSORT-ABS, TIDE, XCELL, MCPCOUNTER, QUANTISEQ and EPIC algorithms were used for the correlative analysis of the level of cancer-associated fibroblasts, endothelial cells, CD8+ T cells, CD4+ T cells, and neutrophils and the expression levels of the *SERPINF1* gene across all tumors in TCGA. The red color indicates a positive correlation (0–1), while the blue color represents a negative correlation (−1–0). The correlation with *P*-value < 0.05 is considered statistically significant. Statistically insignificant correlation values are marked with crosses.

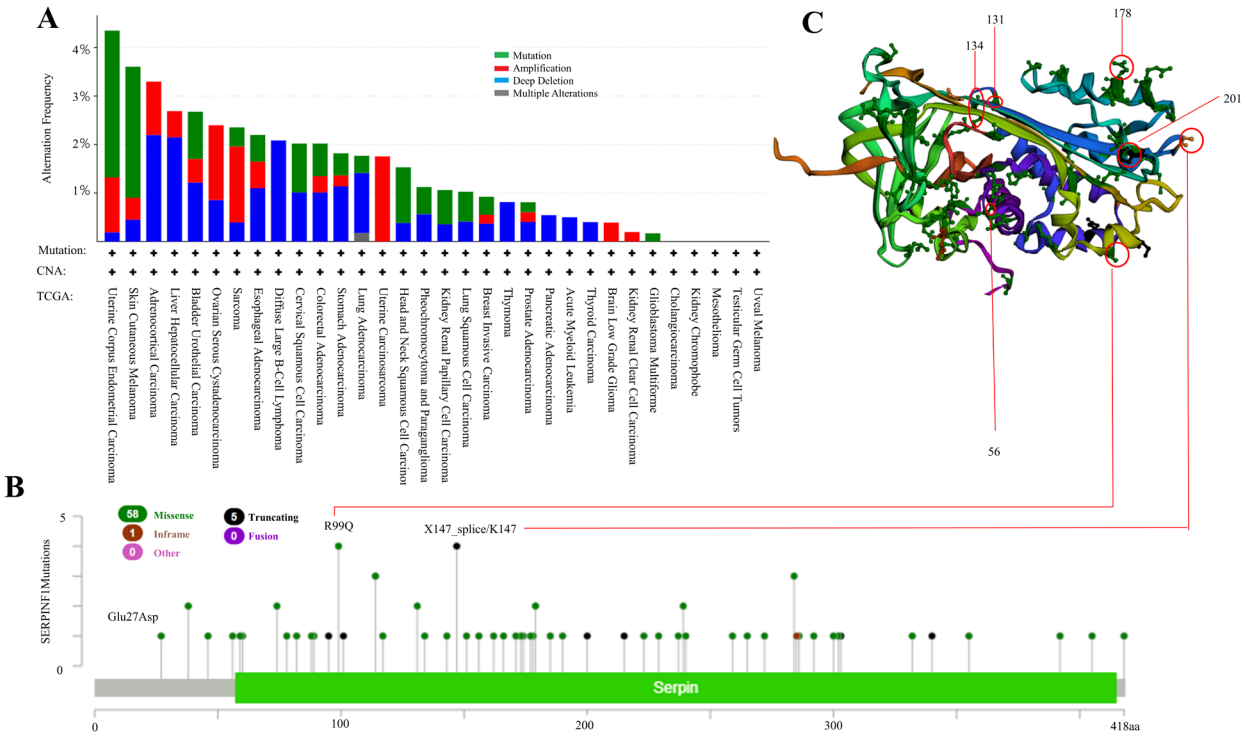

Figure 5. Mutation status of *SERPINF1* in TCGA tumors. (A) The alteration frequency with mutation type. **(B)** Mutation site. **(C)** Mutation site (56, 99, 131, 147, 178, 201) are shown in the 3D structure of *SERPINF1*.

Table 1. PEDF Change at the same sites in Cancer and OI

Cancer	OI
Glu27Asp	Glu27Glyfs*38
Ala56Val	Ala56Gly
Arg99Gln	Arg99*
Ala131Val	Ala131Asp
Gln133Argfs*18	Gln133*
X147_splice	Lys147_Gly215delArg
Gln178His	Gln178*
Asp201Metfs*18	Asp201Asn

found that there are literature reports that *SERPINF1* is associated with 20 human diseases, and the most frequently reported disease is cancer. In our study, homologous genes and phylogenetic tree data confirm the conservatism of PEDF structure in different species, but additional functional gain and functional loss studies are needed to further explore its functions in different cellular environments.

An increasing number of studies focus on the function of *SERPINF1* in diseases including cancer. It remains to be answered whether *SERPINF1* can play a role in the pathogenesis of different tumors through some common molecular mechanisms. Through literature search, we have not retrieved any publications from the overall cancer perspective for *SERPINF1* pan-cancer analysis. Therefore, based on the data of TCGA, CPTAC and GEO database, gene expression and gene change, we detected the *SERPINF1* gene in 33 different tumors. In addition, we compared the mutation sites of cancer with those of osteogenesis imperfecta, and found that there were 8 amino acids at the same sites, at positions 27, 56, 99, 131, 133, 147, 178, and 201. Mutations in the *SERPINF1* gene lead to the development of osteogenesis imperfecta, but whether these mutations are linked to tumorigenesis will require more data and studies to prove.

The results showed that the expression level of *SERPINF1* in tumor tissues of ACC, BLCA, BRCA, CESC, CESC, CHOL, COAD, GBM, KICH, KICH, KIRC, LAML, LGG, LUAD, OV, PCPG, PRAD, READ, TGCT, THCA, UCEC, UCS was lower than that of the corresponding control group, whereas higher expression was observed in DLBC, KIRC, PRAD and THYM.

Differences in *SERPINF1* expression levels in different tumor types may reflect different underlying functions and mechanisms. We further found that for patients with tumors with high expression of *SERPINF1*, such as BLCA, COAD, KIRC, LGG and STAD, overexpression of *SERPINF1* generally predicted poor OS. It is noteworthy that the high expression of *SERPINF1* leads to a decrease in the OS and DFS curves of COAD, KIRC and LGG. These results suggest that *SERPINF1* is a potential biomarker for predicting the prognosis of patients with tumors. Especially in KIRC, we found that *SERPINF1* expression was higher than in the control group ($P < 0.01$), and the high expression of *SERPINF1* was associated with poor prognosis of OS ($P = 0.0054$) and DFS ($P = 0.0023$).

SERPINF1 has been reported to have antitumor

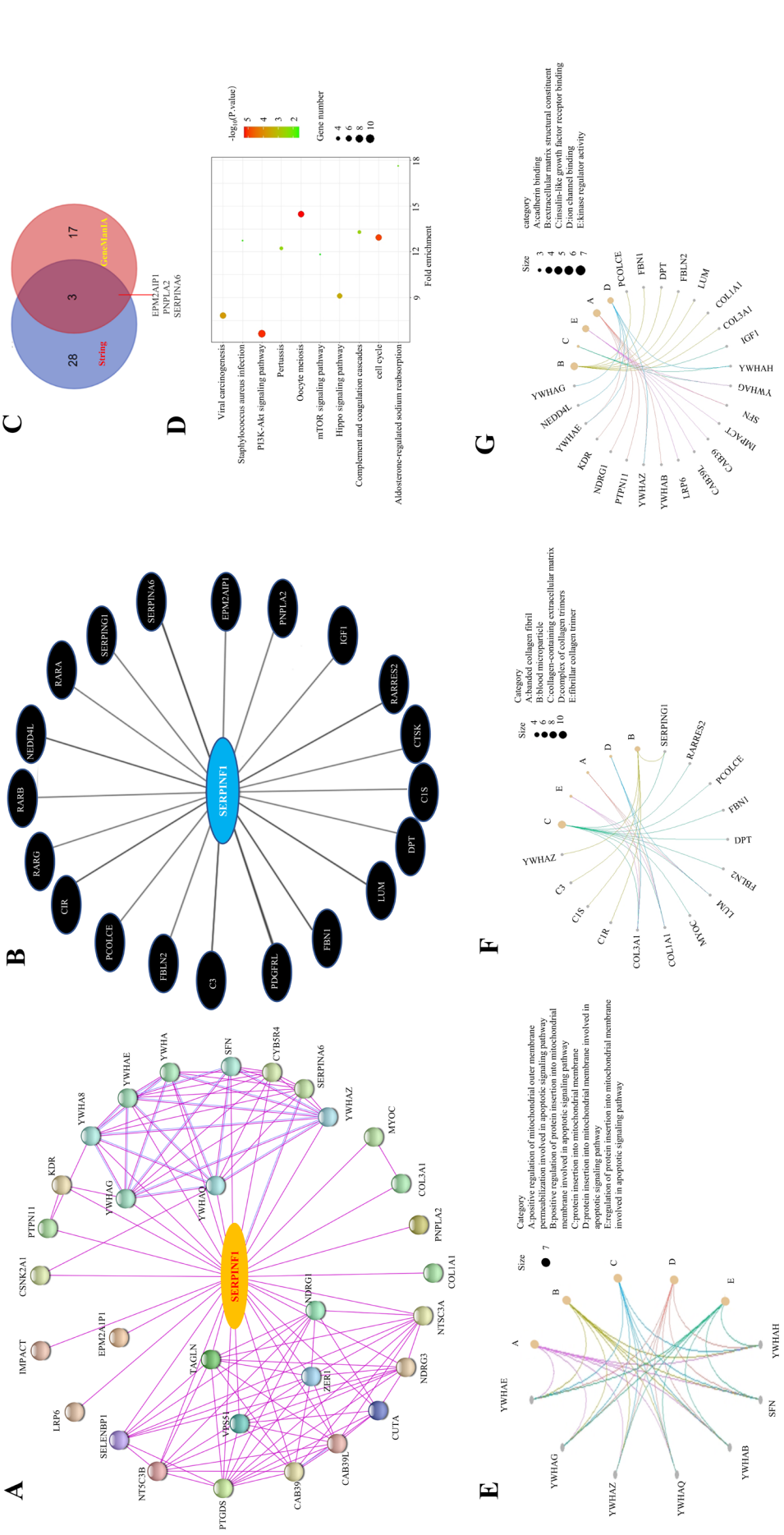

Figure 6. *SERPINF1*-related gene enrichment and pathway analysis. (A) STRING protein network map of experimentally determined PEDF-binding proteins. **(B)** GeneMANIA predicted gene network diagram associated with *SERPINF1* co-expression. **(C)** Venn plot of (A) and (B). **(D)** KEGG pathway analysis based on the *SERPINF1*-binding and co-expression genes. **(E)** GO pathway analysis (Biological Process, BP) based on the *SERPINF1*-binding and co-expression genes. **(F)** GO pathway analysis (Cellular Component, CC) based on the *SERPINF1*-binding and co-expression genes. **(G)** GO pathway analysis (Molecular Function, MF) based on the *SERPINF1*-binding and co-expression genes.

effects (*4*). It is doubtful that high expression of *SERPINF1* leads to poor prognosis in cancer, such as COAD, LGG and KIRC. It has been reported that the tumor microenvironment is related to the occurrence and development of cancer (*18*). Our immune infiltration analysis showed that the high expression of *SERPINF1* was not related to infiltration of immune cells, but positively correlated with the infiltration ability of cancer associated fibroblasts and endothelial cells. Interestingly, in KIRC, high *SERPINF1* expression was inversely correlated with the invasive capacity of endothelial cells, indicating that infiltration of cancer associated fibroblasts is an important factor leading to poor prognosis of KIRC.

In conclusion, from our bioinformatics analysis of *SERPINF1*, we found that there were 8 amino acid changes at the same locus in OI and cancer. But more data and studies are needed to determine their relation to the occurrence of cancer. From our comprehensive pan-cancer analysis of *SERPINF1*, it is helpful to elucidate the role of *SERPINF1* in tumor development from multiple perspectives.

Funding: This work was supported by a grant from the Shandong government (2018WS178) and the Academic Promotion Programme of Shandong First Medical University (LJ001).

Conflict of Interest: The authors have no conflicts of interest to disclose.

References

1. Broadhead ML, Akiyama T, Choong PF, Dass CR. The pathophysiological role of PEDF in bone diseases. Curr Mol Med. 2010; 10:296-301.
2. Becker J, Semler O, Gilissen C, *et al.* Exome sequencing identifies truncating mutations in human *SERPINF1* in autosomal-recessive osteogenesis imperfecta. Am J Hum Genet. 2011; 88:362-371.
3. Mejias M, Coch L, Berzigotti A, Garcia-Pras E, Gallego J, Bosch J, Fernandez M. Antiangiogenic and antifibrogenic activity of pigment epithelium-derived factor (PEDF) in bile duct-ligated portal hypertensive rats. Gut. 2015; 64:657-666.
4. Becerra SP, Notario V. The effects of PEDF on cancer biology: mechanisms of action and therapeutic potential. Nat Rev Cancer. 2013; 13:258-271.
5. Sanchez A, Tripathy D, Yin X, Luo J, Martinez J, Grammas P. Pigment epithelium-derived factor (PEDF) protects cortical neurons *in vitro* from oxidant injury by activation of extracellular signal-regulated kinase (ERK) 1/2 and induction of Bcl-2. Neurosci Res. 2012; 72:1-8.
6. Borg ML, Andrews ZB, Duh EJ, Zechner R, Meikle PJ, Watt MJ. Pigment epithelium-derived factor regulates lipid metabolism *via* adipose triglyceride lipase. Diabetes. 2011; 60:1458-1466.
7. Farber CR, Reich A, Barnes AM, Becerra P, Rauch F, Cabral WA, Bae A, Quinlan A, Glorieux FH, Clemens TL, Marini JC. A novel IFITM5 mutation in severe atypical osteogenesis imperfecta type VI impairs osteoblast production of pigment epithelium-derived factor. J Bone Miner Res. 2014; 29:1402-1411.
8. Glorieux FH, Ward LM, Rauch F, Lalic L, Roughley PJ, Travers R. Osteogenesis imperfecta type VI: a form of brittle bone disease with a mineralization defect. J Bone Miner Res. 2002; 17:30-38.
9. Wang JY, Liu Y, Song LJ, Lv F, Xu XJ, San A, Wang J, Yang HM, Yang ZY, Jiang Y, Wang O, Xia WB, Xing XP, Li M. Novel Mutations in *SERPINF1* Result in Rare Osteogenesis Imperfecta Type VI. Calcif Tissue Int. 2017; 100:55-66.
10. Uhlén M, Fagerberg L, Hallström BM, *et al.* Proteomics. Tissue-based map of the human proteome. Science. 2015; 347:1260419.
11. Thul PJ, Åkesson L, Wiking M, *et al.* A subcellular map of the human proteome. Science. 2017; 356.
12. Li T, Fu J, Zeng Z, Cohen D, Li J, Chen Q, Li B, Liu XS. TIMER2.0 for analysis of tumor-infiltrating immune cells. Nucleic Acids Res. 2020; 48:W509-W514.
13. Tang Z, Li C, Kang B, Gao G, Li C, Zhang Z. GEPIA: a web server for cancer and normal gene expression profiling and interactive analyses. Nucleic Acids Res. 2017; 45:W98-W102.
14. Cerami E, Gao J, Dogrusoz U, *et al.* The cBio cancer genomics portal: an open platform for exploring multidimensional cancer genomics data. Cancer Discov. 2012; 2:401-404.
15. Dalgleish R. The human type I collagen mutation database. Nucleic Acids Res. 1997; 25:181-187.
16. Warde-Farley D, Donaldson SL, Comes O, *et al.* The GeneMANIA prediction server: biological network integration for gene prioritization and predicting gene function. Nucleic Acids Res. 2010; 38:W214-W220.
17. Steven A, Seliger B. The role of immune escape and immune cell infiltration in breast cancer. Breast Care (Basel). 2018; 13:16-21.
18. Fridman WH, Galon J, Dieu-Nosjean MC, Cremer I, Fisson S, Damotte D, Pagès F, Tartour E, Sautès-Fridman C. Immune infiltration in human cancer: prognostic significance and disease control. Curr Top Microbiol Immunol. 2011; 344:1-24.
19. Chen X, Song E. Turning foes to friends: targeting cancer-associated fibroblasts. Nat Rev Drug Discov. 2019; 18:99-115.
20. Kwa MQ, Herum KM, Brakebusch C. Cancer-associated fibroblasts: how do they contribute to metastasis? Clin Exp Metastasis. 2019; 36:71-86.
21. Fearon DT. The carcinoma-associated fibroblast expressing fibroblast activation protein and escape from immune surveillance. Cancer Immunol Res. 2014; 2:187-193.
22. Dalgleish R. The human collagen mutation database 1998. Nucleic Acids Res. 1998; 26:253-255.

Received September 2, 2021; Revised January 23, 2022; Accepted January 31, 2022.

**Address correspondence to:*
Yanqin Lu, Shandong First Medical University & Shandong Academy of Medical Sciences, #6699 Qingdao Road, Ji'nan 250117, China.
E-mail: yqlu@sdfmu.edu.cn (YL)

Released online in J-STAGE as advance publication February 7, 2022.

Brief Report

DOI: 10.5582/irdr.2022.01011

No preferential mode of inheritance for highly constrained genes

Alexandre Fabre[1,2,*], Julien Mancini[3,4]

[1] Aix Marseille Univ, INSERM, MMG, Marseille, France;
[2] APHM, Service de Pédiatrie Multidisciplinaire, Hôpital de La Timone Enfants, Marseille, France;
[3] Aix Marseille Univ, INSERM, IRD, ISSPAM, SESSTIM, Marseille, France;
[4] APHM, BIOSTIC, Hop Timone, Marseille, France.

SUMMARY Genetic constraint metrics such as the gnomAD probability of being loss-of-function (LoF) intolerant (pLI) are used to prioritize candidate genes but the mode of inheritance of highly constrained genes has never specifically been studied. We compared 605 genes with a pLI of 1 (pLI1 group) with a random sample of 635 genes from gnomAD (the random group) in terms of genetic constraint metrics, associations with Mendelian disease, modes of inheritance, and two intragenic constraint scores: the percentage of constraint coding regions (CCR) in the 99th percentile and the gene variation intolerance rank (GeVIR). The proportion of genes associated with a Mendelian disease was 35.9% (217/605) in the pLI1 group and 19.5% (124/635) in the random group ($p < 0.0001$). The modes of inheritance in the random group were autosomal dominant for 35 genes (28.2%), autosomal recessive for 69 (55.6%), mixed for 14 (11.3%) and X-linked for 6 genes (4.8%). The corresponding distribution in the pLI1 group was 150 (69.1%), 26 (12.0%), 14 (6.5%) and 27 (12.4%) ($p < 0.0001$). The percentage of CCRs in the 99th percentile was 0.3 in the random group versus 1.12 in the pLI1 group ($p < 0.0001$). The GeVIR score was 50.9 for the random group versus 15.1 for the pLI1 group ($p < 0.0001$). High genetic constraint does not seem to be associated with a particular mode of inheritance but does seem to be associated with the intragenic constraint scores considered here. Some highly constrained genes are associated with two different modes of inheritance.

Keywords Mendelian inheritance, pLI, gnomAD, ExAC

1. Introduction

The Exome Aggregation Consortium (ExAC) database, created in October 2014, contains exome sequence data from 60 706 individuals and has rapidly become an essential tool in the study of Mendelian diseases (*1*). The ExAC database has allowed levels of genetic constraint to be estimated (*2*) and a popular metric is the probability of loss-of-function (LoF) intolerance (pLI). The pLI ranges from 0 to 1 and genes with a pLI ≥ 0.9 are very likely to be intolerant to loss-of-function variations and are often associated with haploinsufficiency and dominant genetic diseases. Despite some limitations, the pLI has been widely used to prioritize candidate genes (*3*). The successor of the ExAC database, the genome aggregation database (gnomAD) (*4*), contains more than 100,000 human exome and genome sequences along with annotations including the pLI and missense and synonymous Z-scores. Just as for the pLI, higher (more positive) Z-scores indicate greater intolerance to the corresponding type of variation. Other measures of genetic constraint derived from gnomAD data have been proposed to identify candidate genes, including the gene variation intolerance rank (GeVIR) (*5*) and the mapping of constraint coding regions (CCRs) in genes (*6*). While modes of inheritance clearly affect genetic constraints (*4,7*), the Mendelian mode of inheritance of highly constrained genes has never been specifically studied. The aim of this study was therefore to analyze the modes of inheritance of the most constrained genes (with a pLI of 1) in comparison with those of a random selection.

2. Material and Methods

The gnomAD constraint metric by gene table (4) containing 19,704 genes was downloaded from the gnomAD website (*https://gnomad.broadinstitute.org/downloads*, file "pLoF Metrics by Gene TSV") on 15 October 2019. Gene constraint metrics (pLI, missense and synonymous Z-scores) and chromosome location were extracted for the 605 genes with a pLI = 1 (the pLI1 gene group) and a random sample of 650 genes

(the random gene (RG) group). Manual searches were performed for each gene on the Online Mendelian Inheritance in Man (OMIM website, *https://omim.org/*) between 15 October 2019 and 20 May 2020. The data retrieved were the existence of an associated Mendelian disease (non-diseases and multifactorial disorders were not included), and for each disease, the mode of inheritance (autosomal dominant, autosomal recessive, or X-linked). For genes associated with multiple phenotypes, the number of associated Mendelian diseases was also recorded and the mode of inheritance was recorded as mixed if it varied between phenotypes. The number of CCRs in the 99th percentile for each gene was obtained from Abramov *et al*. (*5*) and GeVIRs were obtained from Havrilla *et al*. (*6*).

Continuous variables were expressed as mean (standard deviation). Comparisons were made with t-tests when comparing highly constrained and randomly selected genes. Kruskal-Wallis tests were used when comparing the 4 groups according to the mode of inheritance. Chi-square test was used for comparison of categorical variables. The alpha level was set at 0.05 for all two-tailed tests. The analyses were conducted using IBM SPSS Statistics 27.0 (IBM Inc., New York, USA). Differences in gene ontology terms for biological processes, molecular function and cellular components were analyzed with Panther (*http://pantherdb.org/*) (*8*).

No ethics approval was required under French law as the study only involved data analysis. Database data were used in accordance with the corresponding data use agreements. Tables of raw data (genetic constraint, GeVIR score, Number of CCRs in 99th percentile, Mendelian mode of inheritance) are available upon request.

3. Results and Discussion

One thousand two hundred and forty genes were analyzed, 605 in the pLI1 group and 635 in the RG group (15 of the 650 randomly selected genes were removed because they had a pLI of 1 and were therefore part of the pLI1 group). Their characteristics are compared in Table 1. One hundred and fifty-nine genes were not present in the OMIM database (131 in the RG group and 18 in pLI1 group, $p < 0.0001$) and 342 genes were associated with at least one Mendelian disease (124 in the RG group and 217 in the pLI1 group, $p < 0.0001$). The groups differed significantly in terms of the distribution of modes of inheritance (AD, AR, XL or mixed; $p < 0.0001$), the number of CCRs in the 99th percentile (higher in the pLI1 group, $p < 0.0001$), the GEVIR score (lower for pLI1 genes; $p < 0.0001$) and borderline significantly in terms of the mean number of OMIM phenotypes per disease-associated gene (higher in the pLI1 group, $p = 0.071$; Table 1). The genes in both groups were first associated with a Mendelian disease in 2008 on average (Table 1).

Considering genes with different modes of inheritance separately (Supplemental Table S1, *http://www.irdrjournal.com/action/getSupplementalData.php?ID=90*), the mean missense Z-score and the number of CCRs in the 99th percentile were in each case significantly higher in the pLI1 group than in the RG group, and the mean GEVIR score was significantly lower. The first association with a Mendelian disease occurred significantly later in the pLI group for autosomal recessive diseases.

Within the pLI1 group, the variables significantly associated with the mode of inheritance were the mean GEVIR score and number of CCRs in the 99th percentile (Figure 1 and Table 2; $p < 0.001$ and $p = 0.001$ respectively), while in the RG group, the variables significantly associated with the mode of inheritance were the GEVIR score and the missense Z-score (Table 3; $p < 0.001$ in both cases).

Among highly constrained genes (pLI1 group), those associated with a Mendelian disease did not differ significantly from those not associated with a Mendelian

Table 1. Gene characteristics

Characteristics	Highly constrained genes[a]	Randomly selected genes	*p*
Genes	605	635	
Present in OMIM database	577 (95.4%)	504 (79.4%)	< 0.0001
Associated with Mendelian disease in OMIM database	217 (37.6%)	124 (24.6%)	< 0.0001
Autosomal dominant inheritance	150 (69.1%)	35 (28.2%)	
Autosomal recessive inheritance	26 (12%)	69 (55.6%)	< 0.0001
Mixed inheritance	14 (6.5%)	14 (11.3%)	
X linked inheritance	27 (12.4%)	6 (4.8%)	
OMIM phenotypes per disease-associated gene	1.5 (1.3)	1.3 (0.7)	0.071
Missense Z-Score	3.1 (1.8)	0.7 (1.2)	< 0.0001
Synonymous Z-Score	-0.5 (2.0)	-0.3 (1.4)	0.014
Number of CCRs in 99th percentile	1.1 (2.2)	0.03 (0.29)	< 0.0001
GeVIR score	15.1 (14.4)	50.9 (28.5)	< 0.0001
Year of first molecular association with a Mendelian disease	2008.8 (8.6)	2008.0 (7.8)	0.42
Year of first molecular association with Mendelian disease for all phenotypes	2008.0 (8.7)	2008.1 (7.6)	0.92

Data are reported as frequency (%) or mean (standard deviation). [a]With a probability of loss-of-function intolerance of 1. OMIM, Online Inheritance in Man; GeVIR, gene variation intolerance rank; CCR, constraint coding region.

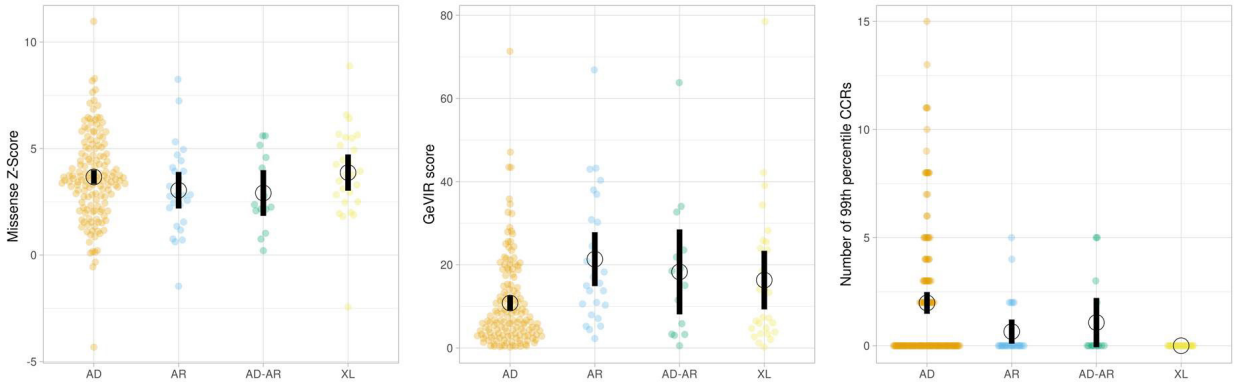

Figure 1. Dot plot distributions of missense Z-scores, GeVIR, number of CCRs in 99th percentile for highly constrained genes (those with a probability of loss-of-function intolerance of 1) for different Mendelian modes of inheritance. Figure prepared with *https://huygens.science.uva.nl/PlotsOfData/*.

Table 2. Comparison of constraint metrics for highly constrained (pLI = 1) genes in terms of their mode of inheritance

Characteristics	Autosomal dominant inheritance	Autosomal recessive inheritance	Mixed inheritance	X linked inheritance	*p*
Genes	150	26	14	27	
Missense Z-Score	3.7 (2.0)	3.0 (2.1)	2.9 (1.8)	3.9 (2.1)	0.15
Synonymous Z-Score	-0.9 (2.4)	-0.2 (1.4)	-0.8 (1.2)	-0.4 (1.3)	0.46
Number of CCRs in 99th percentile	2.0 (3.1)	0.7 (1.4)	1.1 (1.9)	0	< 0.001
GeVIR score	10.8 (10.9)	21.4 (15.8)	18.3 (17.1)	16.3 (17.5)	0.001

Data are reported as mean (standard deviation). pLI, probability of loss-of-function intolerance; GeVIR, gene variation intolerance rank; CCR, constraint coding region.

Table 3. Comparison of constraint metrics for randomly selected genes in terms of their mode of inheritance

Characteristics	Autosomal dominant inheritance	Autosomal recessive inheritance	Mixed inheritance	X linked inheritance	*p*
Genes	35	69	14	6	
Missense Z-Score	1.3 (1.5)	0.3 (1.0)	2.9 (1.8)	1 (0.9)	0.0004
Synonymous Z-Score	-0.6 (1.9)	-0.6 (1.4)	-0.8 (1.2)	-0.7 (1.8)	0.86
Number of CCRs in 99th percentile	0.06 (0.34)	0	1.1 (1.9)	0	0.24
GeVIR score	28.6 (25.1)	52.5 (20.1)	18.3 (17.1)	41.9 (19.6)	< 0.0001

Data are reported as mean (standard deviation). GeVIR, gene variation intolerance rank; CCR, constraint coding region.

disease in terms of gene ontologies. Among pLI1 genes associated with a Mendelian disease, genes with autosomal dominant inheritance were significantly more likely than those with autosomal recessive inheritance to be associated with DNA binding (fold enrichment, FE = 11.2, $p = 0.001$) and significantly less likely to be associated with guanyl-nucleotide exchange (FE = 0.06, $p = 0.004$). None of the other associations between pLI1 gene ontology and mode of inheritance were statistically significant.

Considering genes with different modes of inheritance separately, there were no significant differences in terms of gene ontologies between the pLI1 and RG groups for genes with autosomal dominant or mixed inheritance. Among genes with X linked inheritance, GO:005634 (cellular component, nucleus) was significantly overrepresented (FE = 2.9; $p = 0.048$). Among genes with autosomal recessive inheritance, 11 gene ontologies were significantly overrepresented in the pLI1 group compared with the RG group: five biological process gene ontologies (GO:0001932: regulation of protein phosphorylation, FE = 10.9, $p = 0.022$; GO:0031175: neuron projection development, FE = 8.2, $p = 0.018$; GO:0007010: cytoskeleton organization, FE = 8.2, $p = 0.018$; GO:0035556: intracellular signal transduction, FE = 6.14, $p = 0.048$; GO:0034613: cellular protein localization FE = 6.14, $p = 0.048$), four molecular function gene ontologies (GO:0005096: GTPase activator activity, FE = 19.1, $p = 0.014$; GO:0008092: cytoskeletal protein binding, FE = 16.4, $p = 0.045$; GO:0005198: structural molecule activity, FE = 9.6, $p = 0.042$; GO:0140096: catalytic activity, acting on a protein activity, FE = 7.3, $p = 0.0333$), and two cellular component gene ontologies (GO:0070161: anchoring

junction activity, FE = 21.9, $p = 0.004$; and GO:0005856: cytoskeleton, FE = 4.4, $p = 0.007$).

Although it has been clear from the first articles on ExAC and gnomAD that constrained genes are overrepresented in haploinsufficiency diseases, the Mendelian inheritance of the most constrained genes has never been analyzed in detail. The results of the present study confirm that highly constrained genes are mostly (69.1%) autosomal dominant, whereas randomly selected genes are mostly (55.6%) autosomal recessive. Nevertheless, around one in five highly constrained genes (18.5%) was found to be autosomal recessive, and this mode of inheritance should therefore not be ruled out even for the most constrained genes. Interestingly furthermore, a small fraction of genes were associated with two different modes of inheritance and with several OMIM phenotypes, indicating that even if a gene is associated with a phenotype and a mode of inheritance, the existence of another phenotype with a different mode of inheritance cannot be excluded either.

Compared with a random group of genes, highly constrained genes were significantly more likely to be associated with a Mendelian disease. Although it cannot be ruled out that this difference simply reflects the fact that constrained gene are more readily suspected and investigated, the data show that on average the constrained genes were not associated with diseases earlier than those in the randomly selected group, suggesting on the contrary that this result is not due to selection bias.

Genes with autosomal dominant inheritance were found to have more CCRs in the 99th percentile and lower mean GEVIR scores than autosomal recessive genes did, with the scores of mixed inheritance genes roughly half way between those of dominant and recessive genes. This suggests that exon specific metrics may be better indicators of the mode of Mendelian inheritance. However, the ranges of the scores considered here overlapped between the three modes of Mendelian inheritance. The only significant difference between autosomal dominant and autosomal recessive genes identified by the analysis of gene ontology terms was that autosomal dominant genes were more likely to be associated with DNA binding.

A possible limitation of this study is the use of pLI instead of the more recently proposed loss-of-function observed/expected upper bound fraction (LOEUF). However, since all genes with a pLI = 1 also have a LOEUF < 0.24,which is less than the proposed value for constrained gene (< 0.35) (*9*), these results probably hold for genes with low LOEUF scores.

The emergence of genes associated with two different modes of inheritance is intriguing. Whether continued sequencing efforts will lead to all genes being associated with two modes of inheritance or whether this will remain a property of a small subset is unclear.

In conclusion, this study shows that even the most highly constrained genes are not necessarily autosomal dominant. Gene-specific constraint scores are useful indicators of the mode of inheritance, whose precision will likely improve as genomic databases continue to expand.

Acknowledgements

Pr. Alexandre Belot for useful discussion which lead to this work. We thank Paul Guerry (GreenGrow Scientific) for editing the article.

Funding: None.

Conflict of Interest: The authors have no conflicts of interest to disclose.

References

1. Bennett CA, Petrovski S, Oliver KL, Berkovic SF. ExACtly zero or once: A clinically helpful guide to assessing genetic variants in mild epilepsies. Neurol Genet. 2017; 3:e163.
2. Lek M, Karczewski KJ, Minikel EV, *et al*. Analysis of protein-coding genetic variation in 60,706 humans. Nature. 2016; 536:285-291.
3. Ziegler A, Colin E, Goudenège D, Bonneau D. A snapshot of some pLI score pitfalls. Hum Mutat. 2019; 40:839-841.
4. Karczewski KJ, Francioli LC, Tiao G, *et al*. The mutational constraint spectrum quantified from variation in 141,456 humans. Nature. 2020; 581:434-443.
5. Abramovs N, Brass A, Tassabehji M. GeVIR is a continuous gene-level metric that uses variant distribution patterns to prioritize disease candidate genes. Nat Genet. 2020; 52:35-39.
6. Havrilla JM, Pedersen BS, Layer RM, Quinlan AR. A map of constrained coding regions in the human genome. Nat Genet. 2019; 51:88-95.
7. Cassa CA, Weghorn D, Balick DJ, Jordan DM, Nusinow D, Samocha KE, O'Donnell-Luria A, MacArthur DG, Daly MJ, Beier DR, Sunyaev SR. Estimating the selective effects of heterozygous protein-truncating variants from human exome data. Nat Genet. 2017; 49:806-810.
8. Mi H, Ebert D, Muruganujan A, Mills C, Albou LP, Mushayamaha T, Thomas PD. PANTHER version 16: a revised family classification, tree-based classification tool, enhancer regions and extensive API. Nucleic Acids Res. 2021; 49:D394-D403.
9. Francioli L. gnomAD v2.1. *https://macarthurlab.org/2018/10/17/gnomad-v2-1/* (accessed February 25, 2022).

Received January 25, 2022; Revised February 25, 2022; Accepted February 27, 2022.

**Address correspondence to:*
Alexandre Fabre, Service de Pédiatrie Multidisciplinaire, Hôpital de la Timone Enfant, 264 Rue Saint Pierre, Marseille 13005, France.
E-mail: Alexandre.fabre@ap-hm.fr

Communication

DOI: 10.5582/irdr.2022.01034

The definition of rare disease in China and its prospects

Yanqin Lu*, Jinxiang Han*

Key Laboratory for Biotech-Drugs of National Health Commission, Key Laboratory for Rare & Uncommon Diseases of Shandong Province, Biomedical Sciences College, Shandong First Medical University & Shandong Academy of Medical Sciences, Ji'nan, Shandong, China.

SUMMARY The latest definition of rare disease in China was released on September 11, 2021 at the third multidisciplinary expert seminar on the definition of rare diseases/orphan drugs in China. A rare disease is defined as a condition satisfying at least one of the following three criteria: an incidence among newborns of less than 1/10,000, a prevalence of less than 1/10,000, and an affected population of less than 140,000. Before this new definition, rare diseases were defined by different agencies with different parameters in China. The 2021 definition is a milestone, it could further spur the development of rare diseases beyond *China's First List of Rare Disease* in May 2018. This definition also provides a reference for the total number of rare diseases in China.

Keywords Rare disease, definition, China, incidence, prevalence, *China's First List of Rare Disease*

The latest definition of rare diseases in China was released on September 11, 2021, as suggested at the third multidisciplinary expert seminar on the definition of rare diseases/orphan drugs in China. A rare disease is defined as a condition with an incidence of less than 1/10,000 among newborns, a prevalence of less than 1/10,000, or an affected population of less than 140,000 (*1*). The definition refers to the number of patients with a given rare disease since it is difficulty to determining the incidence and prevalence of some rare diseases and emerging diseases is difficult. The number 140,000 was calculated based on the China's total population of 1.4 billion multiplied by a prevalence of 1/10,000 (*1*).

A number of years before the new definition was issued, the National Health Commission, the Ministry of Science and Technology, the Ministry of Industry and Information Technology, the National Medical Products Administration, and the National Administration of Traditional Chinese Medicine issued *China's First List of Rare Disease* in May 2018. This marks China as the world's first country to use a list to classify rare diseases (*2*).

In 2010, the Medical Genetics Branch of Chinese Medical Association suggested that a rare disease be defined as one with a prevalence of less than 1 in 500,000 or a neonatal incidence of less than 1 in 10,000. From the point of view of orphan drugs, 300,000 - 500,000 patients was suggested as the threshold for a rare disease (*3*). In 1980s, rare diseases were termed rare and uncommon diseases by Chinese scholars Gui Lin and Chenglin Wang. Wang suggested that the term rare and uncommon disease is a relative concept. From the perspective of dialectics, rare is related to uncommon, and uncommon is related to common diseases (*4*). Rare and uncommon diseases were recorded as a medical record index as early as in 1990 in China (*5*).

According to the definition of rare diseases that was updated in 2021, 12 rare diseases should be removed from the first list of rare diseases, including cardiac ion channelopathies, Charcot-Marie-Tooth Disease, congenital scoliosis, coronary artery ectasia, familial Mediterranean fever, Marfan syndrome, myotonic dystrophy, non-syndromic deafness, Noonan syndrome, primary hereditary dystonia, progressive muscular dystrophy, and retinitis pigmentosa (*1*). As the registration of patients with rare diseases and the epidemiological study of those diseases advance, the population of patients with hemophilia and idiopathic pulmonary arterial hypertension has grown larger than most of the patients with rare diseases on the list (*6-8*). Hence, revision of the *China's First List of Rare Disease* should be considered in accordance with the new 2021 definition of rare diseases and epidemiological data. The national rare disease list and the definition of rare diseases will co-exist and complement each other for some time in China due to a lack of epidemiological data for most rare diseases.

The incidence of rare diseases in newborns is used as a criterion in China but not in other countries. Approximately 80% of rare diseases are genetic diseases caused by specific pathogenic genes. Data from newborns is useful in tallying the number of patients

with rare diseases and helps with clinical diagnosis and treatment in a disease's early stage. Since some rare diseases occur in children (*e.g*., pediatric lupus nephritis and children's interstitial lung disease), others occur in both children and adulthood (*e.g*., central hypoventilation syndrome), and others occur only in adulthood (*e.g*., Huntington-chorea and Gaucher-disease), there will be some discrepancies in incidence/prevalence between a disease's actual rate and its rate according to the definition.

The Chinese population has aged and the birthrate has declined, so the definition of rare diseases should be a dynamic concept. Some influencing factors, environmental factors, and models should be considered when tallying rare diseases. Modeling is one of the main criteria for evaluation of rare diseases, and especially for those lacking a nationwide registry and epidemiological data.

There is no standard definition of rare diseases, it is affected by many factors, such as medical status, the level of social security, social and economic development, and human cognition of disease. The criteria for defining rare diseases differ in various countries or regions, including the total population affected, prevalence, and the severity of the disease (*9-11*). The definition of rare diseases is a key factor to determining the number of rare diseases. The terminology used to define rare diseases is another essential aspect of rare diseases figures that China should take into account. Whether rare infectious diseases, trauma, cancer, or other conditions that are caused by environmental factors, such as PM2.5 pollutants, should be included or excluded as rare diseases will definitely affect the total number of rare diseases. For example, hepatitis E infection would be classified as a rare disease due to its low prevalence (*12*), but hepatitis B, C, and D would not under current definition of rare diseases in China. The definition of rare diseases will help China to expand research on rare diseases, raise the level of medical technology, and meet the healthcare needs of society as a whole. The new 2021 definition of rare diseases represents just the tip of the rare disease iceberg.

Funding: This study was supported by Grants-in-Aid from the Project to Promote Academics of Shandong First Medical University (no. 2019LJ001).

Conflict of Interest: The authors have no conflicts of interest to disclose.

References

1. Joint Meeting of the Chairpersons of Rare Disease Societies. A report on the definition of rare diseases in China (2021). Shanghai, 2021. (in Chinese)
2. He J, Kang Q, Hu J, Song P, Jin C. China has officially released its first national list of rare diseases. Intract & Rare Dis Res. 2018; 7:145-147.
3. Cui Y, Han J. A proposed definition of rare diseases for China: From the perspective of return on investment in new orphan drugs. Orphanet J Rare Dis. 2015; 10:28.
4. Wang C, Lin G. Some problems with rare and uncommon diseases - A study of aricles over ten years. Chin J Rare and Uncommon Dis 1994; 1:12-15. (in Chinese)
5. Lin G, Wang C. Record index for rare and uncommon diseases. China Expectation Press, 1990. (in Chinese)
6. Guo J, Liu P, Chen L, Lv H, Li J, Yu W, Xu K, Zhu Y, Wu Z, Tian Z, Jin Y, Yang R, Gu W, Zhang S. National Rare Diseases Registry System (NRDRS): China's first nation-wide rare diseases demographic analyses. Orphanet J Rare Dis. 2021; 16:515.
7. Shi XM LH, Wang L, Wang ZX, Dong CY, Wang YF, Yao C, Zhan SY, Ding J, Li Y. Study on the current situation of China's First List of Rare Diseases based on 15 million hospitalizations. Natl Med J China. 2018;98:3274-3278.
8. Cai X, Genchev GZ, He P, Lu H, Yu G. Demographics, in-hospital analysis, and prevalence of 33 rare diseases with effective treatment in Shanghai. Orphanet J Rare Dis. 2021; 16:262.
9. Stolk P, Willemen MJ, Leufkens HG. Rare essentials: Drugs for rare diseases as essential medicines. Bull WHO. 2006; 84:745-751.
10. Taruscio D, Capozzoli F, Frank C. Rare diseases and orphan drugs. Ann dell'Istituto Super di Sanita. 2011; 47:83-93.
11. Rinaldi A. Adopting an orphan. EMBO reports. 2005; 6:507-510.
12. Zhou Y, Zhuang H. Recent advances in the epidemiological research on hepatitis E in China. Chin J Epidem. 2010; 31:1414-1416. (in Chinese)

Received February 17, 2022; Revised February 24, 2022; Accepted February 25, 2022.

**Address correspondence to:*
Yanqin Lu and Jinxiang Han, Shandong First Medical University & Shandong Academy of Medical Sciences, Ji'nan 250117, Shandong, China.
E-mail: yqlu@sdfmu.edu.cn, jxhan@sdfmu.edu.cn

Released online in J-STAGE as advance publication February 27, 2022.

Communication

DOI: 10.5582/irdr.2020.01008

The cardiovascular outcomes of finerenone in patients with chronic kidney disease and type 2 diabetes: A meta-analysis of randomized clinical trials

Basel Abdelazeem[1,2,*], Merihan A. Elbadawy[3], Ahmed K. Awad[3], Babikir Kheiri[4], Arvind Kunadi[1]

[1] Department of Internal Medicine, McLaren Health Care, Flint, Michigan, USA;
[2] Michigan State University, East Lansing, Michigan, USA;
[3] Faculty of Medicine, Ain-Shams University, Cairo, Egypt;
[4] Knight Cardiovascular Institute, Oregon Health & Science University, Portland, Oregon, USA.

SUMMARY Recently, a few randomized control trials (RCTs) suggested that finerenone has been shown to reduce cardiovascular events in patients with CKD and DM-2. We aimed to analyze the cardiovascular benefits of using finerenone in patients with CKD and DM-2. Electronic databases were systematically searched to identify only RCTs comparing finerenone versus placebo. Pooled risk ratios (RR) and their 95% confidence intervals (CI) were calculated using random-effects models. Three RCTs were included, with a total of 13,847 patients. Compared with the placebo group, the use of finerenone was associated with significantly lower rates of cardiovascular events (RR: 0.88; 95% CI: 0.80, 0.96; $p < 0.01$), which was mainly driven by lower hospitalizations for heart failure (RR: 0.79; 95% CI: 0.66, 0.94; $p = 0.01$). However, there were no significant differences between groups in terms of cardiovascular death (RR: 0.88; 95% CI: 0.76, 1.02; $p = 0.09$), non-fatal myocardial infarction (RR: 0.91; 95% CI: 0.74, 1.12; $p = 0.38$), non-fatal stroke (RR: 0.99; 95% CI: 0.80, 1.22; $p = 0.90$).

Keywords finerenone, chronic kidney disease, type 2 diabetes, mineralocorticoid, meta-analysis

Patients with chronic kidney disease (CKD) and diabetes mellitus type 2 (DM-2) have increased cardiovascular morbidity and mortality due to enhanced and over-activation of mineralocorticoid receptors, leading to widespread inflammation and fibrosis affecting the heart, kidneys, and peripheral vessels (*1*). Aldosterone is a mineralocorticoid hormone, which increases proteinuria and affects cardiomyocytes, endothelial cells, and vascular smooth muscle cells by causing chronic inflammation that leads to fibrosis and remodeling of the heart and kidneys. Thus, the use of aldosterone antagonists might reverse these pathophysiological remodeling. Finerenone (BAY 94–8862) is a novel third-generation nonsteroidal selective mineralocorticoid receptor antagonist that has been shown to reduce cardiovascular events in patients with CKD and DM-2 (*2-4*). However, data from randomized controlled trials (RCTs) are limited. Therefore, we aim to conduct a meta-analysis of solely RCTs to evaluate the effects of finerenone on cardiovascular outcomes in patients with CKD and DM-2.

Our Systematic review was carried out in accordance with the Preferred Reporting Items for Systematic Reviews and Meta-Analyses (PRISMA) statement. We searched PubMed, EMBASE, Scopus, Web of Science, Cochrane Central, and Google Scholar for RCTs comparing finerenone versus placebo among patients with CKD and DM-2. We performed our search from inception to January 7th, 2022. Our eligibility criteria included; type of study: RCTs; type of subject: patients with CKD and DM-2; type of intervention: studies that evaluated the effect of finerenone compared to placebo; the primary outcome was cardiovascular events defined as death from cardiovascular causes, non-fatal myocardial infarction, non-fatal stroke, or hospitalization for heart failure; secondary outcomes included the individual primary outcome composite. We calculated risk ratios (RRs) with their 95% confidence intervals (CIs) using the random-effects model. All analyses were performed using RevMan manager v5.3 software.

We identified three RCTs (*2-4*) with 13,847 total patients (finerenone = 7,246 *vs*. placebo = 6,601) with a median follow up was 1.6 years. The mean age was 64.7 ± 8.7 years and 70.3% were male. The

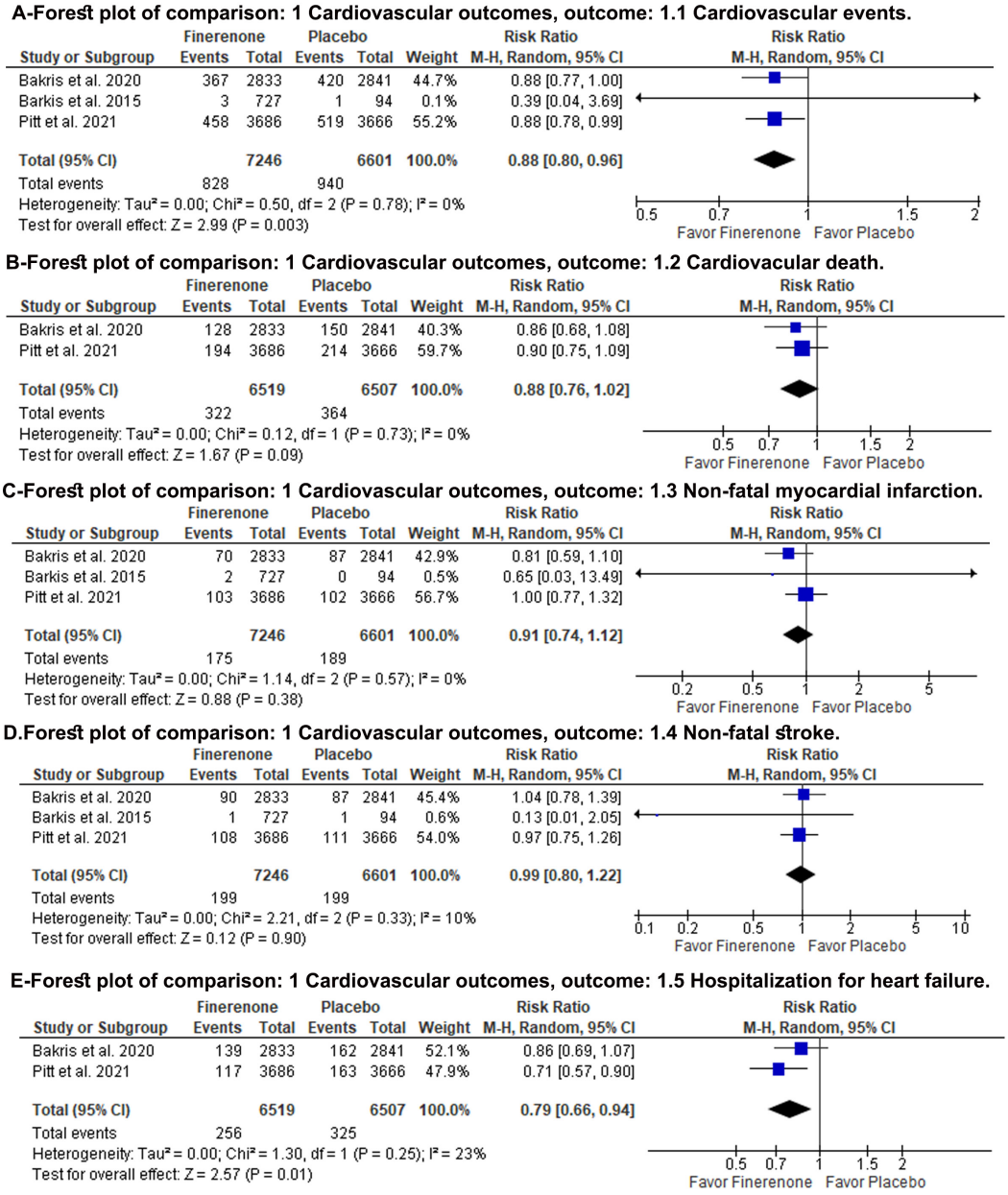

Figure 1. Forest plot comparing the clinical outcomes among patients who received finerenone. (A) Cardiovascular events; **(B)** Cardiovascular death; **(C)** Non-fatal myocardial infarction; **(D)** Non-fatal stroke; **(E)** Hospitalization for heart failure. df: degrees of freedom; I2: I-squared; M-H: Mantel-Haenszel variance; CI: confidence interval.

mean hemoglobin A1c was 7.6% ± 1.24 with mean estimated glomerular filtration rate (eGFR) of 54.9 ±15.5mL/min/1.73m2. Compared to the placebo group, finerenone was associated with significantly lower rates of cardiovascular events (RR: 0.88; 95% CI: 0.80,0.96; $p < 0.01$) (Figure 1). Finerenone was associated with significantly lower heart failure hospitalizations (RR: 0.79; 95% CI: 0.66, 0.94; $p = 0.01$) compared to placebo. However, there were no significant differences between groups in terms of cardiovascular death (RR: 0.88; 95% CI: 0.76, 1.02; $p = 0.09$), non-fatal myocardial infarction (MI) (RR: 0.91; 95% CI: 0.74, 1.12; $p = 0.38$), non-fatal stroke (RR: 0.99; 95% CI: 0.80, 1.22; $p = 0.90$) (Figure 1).

This meta-analysis showed that finerenone was associated with a statistically significant reduction in cardiovascular events, mainly driven by lower hospitalization for heart failure compared to placebo. However, there were no significant differences in terms of cardiovascular death, non-fatal MI, or non-fatal stroke.

In patients with DM-2 and CKD with albuminuria > 30 mg/g and eGFR > 30 mL/min/1.73 m^2, current guidelines recommend sodium-glucose cotransporter-2 inhibitors (SGLT2i) added to angiotensin-converting enzyme inhibitors (ACEi) or angiotensin receptor blockers (ARB) to reduce the risk of end-stage renal disease (ESRD) and cardiovascular mortality (*5*). However, despite the use of ACEi (or ARB) and

SGLT2i, the risk of progression to ESRD is still high (*6*). Currently, there is growing evidence that the overactivation of mineralocorticoid receptors contributes to the progression of CKD. Therefore, first-generation aldosterone antagonists -which competitively inhibit aldosterone-dependent sodium-potassium exchange channels in the distal convoluted tubule (such as spironolactone and eplerenone) have been used in patients CKD and DM-2 to reduce mortality and hospitalization despite having side effects, such as hyperkalemia (*7*). Finerenone is a novel medication that demonstrated a lower incidence of hyperkalemia (*8*) and a significant reduction in albuminuria compared to spironolactone (*2*). In our study, we found that finerenone reduced overall cardiovascular events and hospitalization for heart failure but not cardiovascular death, non-fatal MI, or non-fatal stroke. This is likely due to the low sample size and events rates of the included RCTs for these clinical outcomes.

The RALES trial evaluated the effect of spironolactone versus placebo on morbidity and mortality for patients with severe heart failure (*9*). The patients included in our study were similar to the patients in the RALES trial (9) regarding age, sex, and race. However, the RALES trial focused on patients with heart failure (New York Heart Association class IV) with a left ventricular ejection fraction of no more than 35 percent (*9*). Meanwhile, our article focused on patients with type 2 diabetes and CKD. Therefore, more RCTs are needed to compare the spironolactone to finerenone.

The main limitations to our meta-analysis are the low number of included RCTs in our analysis, low events rate, and had relatively short follow-up duration. Therefore, more RCTs are still needed to shed more light on the growing interest in finerenone.

In conclusion, among patients with CKD and DM-2, finerenone is associated with lower risks of cardiovascular events and heart failure hospitalizations compared with placebo. Further large clinical trials and long-term follow-up with a focus on cost-effectiveness are needed.

Funding: None

Conflict of Interest: The authors have no conflicts of interest to disclose.

References

1. Gilbert KC, Brown NJ. Aldosterone and inflammation. Curr Opin Endocrinol Diabetes Obes. 2010; 17:199-204.
2. Bakris GL, Agarwal R, Chan JC, *et al*. Effect of finerenone on albuminuria in patients with diabetic nephropathy: A randomized clinical trial. JAMA. 2015; 314:884-894.
3. Bakris GL, Agarwal R, Anker SD, Pitt B, Ruilope LM, Rossing P, Kolkhof P, Nowack C, Schloemer P, Joseph A, Filippatos G; FIDELIO-DKD Investigators. Effect of finerenone on chronic kidney disease outcomes in type 2 diabetes. N Engl J Med. 2020; 383:2219-2229.
4. Pitt B, Filippatos G, Agarwal R, Anker SD, Bakris GL, Rossing P, Joseph A, Kolkhof P, Nowack C, Schloemer P, Ruilope LM; FIGARO-DKD Investigators. Cardiovascular events with finerenone in kidney disease and type 2 diabetes. N Engl J Med. 2021; 385:2252-2263.
5. American Diabetes Association. Microvascular complications and foot care:standards of medical care in diabetes – 2020.Diabetes Care. 2020; 43(Suppl 1):S135-S151.
6. Perkovic V, Jardine MJ, Neal B, *et al*. Canagliflozin and renal outcomes in type 2 diabetes and nephropathy. N Engl J Med. 2019; 380:2295-2306.
7. Agarwal R, Kolkhof P, Bakris G, Bauersachs J, Haller H, Wada T, Zannad F. Steroidal and non-steroidal mineralocorticoid receptor antagonists in cardiorenal medicine. Eur Heart J. 2021; 42:152-161.
8. Pitt B, Kober L, Ponikowski P, Gheorghiade M, Filippatos G, Krum H, Nowack C, Kolkhof P, Kim SY, Zannad F. Safety and tolerability of the novel non-steroidal mineralocorticoid receptor antagonist BAY 94-8862 in patients with chronic heart failure and mild or moderate chronic kidney disease: a randomized, double-blind trial. Eur Heart J. 2013; 34:2453-2463.
9. Pitt B, Zannad F, Remme WJ, Cody R, Castaigne A, Perez A, Palensky J, Wittes J. The effect of spironolactone on morbidity and mortality in patients with severe heart failure. Randomized Aldactone Evaluation Study Investigators. N Engl J Med. 1999; 341:709-717.

Received January 23, 2021; Revised February 6, 2022; Accepted February February 9, 2022.

**Address correspondence to:*
Basel Abdelazeem, Department of Internal Medicine, McLaren Health Care, 401 S Ballenger Hwy, Flint, MI 48532, USA.
E-mail: Baselelramly@gmail.com

Released online in J-STAGE as advance publication February 12, 2022.

Letter

DOI: 10.5582/irdr.2021.01132

Fabry disease – a genetically conditioned extremely rare disease with a very unusual course

Mirosław Śnit, Marcela Przyłudzka*, Władysław Grzeszczak

Department of Internal Medicine, Diabetology and Nephrology, Medical University of Silesia, Katowice, Poland.

SUMMARY Fabry disease (FD) is a rare lysosomal storage disease. FD is caused by the presence of a deleterious mutation in the GLA gene encoding the enzyme alpha galactosidase A (αGAL A) on the X chromosome. The accumulation of Gb3 and lyso-GL-3 in nerve fiber cells, endothelium, vascular muscle cells, mesangial cells, podocytes, renal tubular epithelial cells and cardiomyocytes is the most important pathogenetic factor. The rate of disease progression depends on residual conserved enzymatic activity. In this article we present an example of a 25-year-old patient with FD with an initial asymptomatic course. The first manifestation of FD developed in the third decade of life. These include high blood pressure, urinary changes and grade V renal failure, requiring renal replacement therapy. The diagnosis was made very late, when renal failure and cerebro-cardiac complications occurred, including stroke and dangerous cardiac tamponade.

Keywords fabry disease, renal failure, cardiovascular complications

Fabry disease (FD) was first described in 1898 by two independent physicians: surgeon William Anderson and dermatologist Johannes Fabry. These authors demonstrated the association of skin lesions ("angiokeratoma corporis diffusum") with the risk of developing renal failure (*1,2*).

To date, more than 50 genetic lysosomal storage disorders (LSDs) have been identified, of which FD [OMIM number: 301500] is probably the most common. FD is caused by the presence of a deleterious mutation in the GLA gene [Xq22.1] encoding the enzyme alphagalactosidase A (αGAL A) on the X chromosome (*3,4*). FD is described as an ultra-rare disease, with a frequency of 1/40,000 in men and 1/117,000 in the female population (*5-7*). The rate of development of the disorder depends on the preserved residual enzymatic activity, *i.e*. the lower the enzyme activity, the earlier the manifestation of the disease and the faster its progression.

A 25-year-old Caucasian male, previously untreated, was admitted to the nephrology department for high blood pressure (BP > 200/120 mm Hg) and macroscopic hematuria. The patient's general condition was moderate, with no signs of pulmonary stasis or peripheral edema. Physical examination revealed mild redness of the throat, nasal mucus leakage, as well as caries, excessive body fat (BMI = 32 kg/m^2), and lower extremity varicose veins. No skin lesions were found. Laboratory tests performed showed mild anemia, prolonged activated partial thromboplastin time (APTT), very significantly elevated creatinine levels, as well as hematuria and proteinuria [5.4 g/L] (Table 1). Aminotransferase, gamma glutamyl transpeptidase (GGTP), alkaline phosphatase and bilirubin activities were normal. Ultrasound imaging of the urinary tract showed no significant abnormalities. The radiologist performing the examination also noted that the spleen was slightly enlarged (to 12.6 cm). Urine culture showed no bacterial growth. A cystoscopy was performed in which the source of bleeding was not visible and the bladder mucosa was smooth. Following treatment (etamsylate, tranexamic acid), hematuria resolved. During hospitalization, the patient required intensive hypotensive treatment due to repeated high blood pressure values (> 180/100 mmHg). In the following days, progressive weakness was observed, nausea appeared, and laboratory tests showed a further increase in creatinine levels and increased proteinuria to 24 g/L, increased metabolic acidosis and hyperkalemia. The patient was treated with renal replacement hemodialysis. There was no improvement in renal function during hospitalization, but there was a significant reduction in proteinuria and normalization of APTT.

Six months later the patient was hospitalized twice for dyspnea. The dyspnea was already present at rest, but clearly worsened after exertion. The electrocardiogram (ECG) was normal. Echocardiography shows that left

Table 1. Basic results of laboratory tests performed on the patient on admission to the nephrology department

White blood cells	Observed value	Normal value
Red blood cells	8.28 [10*3/uL]	4–10 [10*3/uL]
Hemoglobin	3.85 [10*6/uL]	4.2–5.4 [10*6/uL]
Platelets	11.5 g/L	14–18 g/L
Prothrombin time	147 [10*3/uL]	150–450 [10*3/uL]
Partial thromboplastin time	12.8 sec	11–16b sec
Creatinine	45.5 sec	28–40 sec
Natrium	868 µmol/L	< 130 µmol/L
Kalium	142 mmol/L	135–145 mmol/L
Phosphate	4.86 mmol/L	3.5–5.1 mmol/L
Calcium	1.7 mmol/L	< 1.6 mmol/L
Bicarbonate	2.35 mmol/L	2.25–2.55 mmol/L
Protein	19.2 mmol/L	22–26 mmol/L
Uric acid	55 g/dL	> 60 g/dL
C-reactive protein	669 umol/L	< 420 µmol/L
Antinuclear antibodies	0.79 mg/L	0-5 mg/L
Antineutrophil cytoplasmic antibodies	Negative	Negative
Urine - general examination	Negative reaction: acidic specific gravity: 1015 glucose: not detected protein: 5.4 g/L urobilinogen: normal bilirubin: negative ketone bodies: negative sediment: fresh and leached erythrocytes, very numerous ; leukocytes 2-5	Negative reaction: acidic specific gravity: > 1023 glucose: absent protein: absent urobilinogen: normal bilirubin: negative ketone bodies: negative precipitate: leukocytes < 5 erythrocytes 1-2

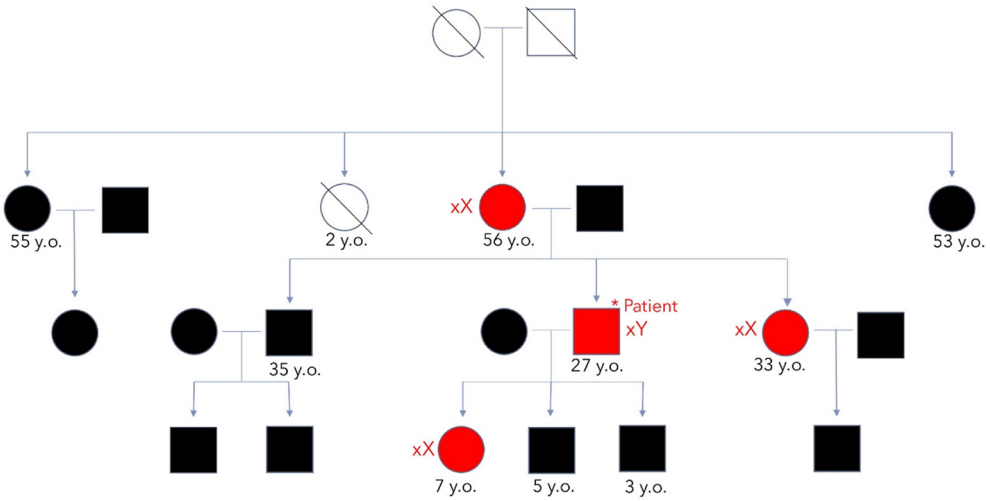

Figure 1. Inheritance of the c.109G> C mutation occurring in Fabry disease on the example of the patient's family. Red color - the presence of a mutation. Black color - no mutation. White - unaudited family members (deceased).

ventricular systolic fraction (LVEF) is normal and left ventricular diastolic fraction (LVDF) is abnormal. Cardiac echocardiography shows myocardial dilatation and thickening with a small amount of fluid in the pericardial sac (up to 3 mm).

A few months later, the patient was diagnosed with a dangerous cardiac tamponade manifested by unconsciousness and weakness in the course of hypotension. The pericardium was decanted, yielding 710 mL of bloody fluid. Subsequent histological examination of the pericardial fluid showed signs of acute chronic pericarditis secondary to uremia. A cardiac MRI was performed, which showed no pathology other than myocardial hypertrophy.

After several weeks, the patient was urgently admitted to the neurology department due to speech disorders and right hemiparesis. Central nervous system bleeding was ruled out, but cerebrovascular abnormalities were noted.

Taking into account the general clinical picture and the result of the consultation, FD was suspected. Blood was drawn from the patient (dry blood spot) to determine alpha-galactosidase activity. The test showed: alpha-galactosidase activity < 0.1 µmol/L/h; normal > 2.8 µmol/L/h, lyso-Gl-3 globotriaosylphingosine

concentration = 57.1 ng/mL; normal < 3.5 ng/mL. Genetic testing revealed the presence of the c.109G> C mutation (p.Ala37Pro). This finally confirmed the diagnosis of FD. In this situation, the patient started treatment with agalsidase alfa. Genetic testing in the patient's family confirmed the presence of the mutation in the patient's mother, sister, and daughter. The inheritance of the c.109G> C mutation found in FD in the patient's family is shown in Figure 1.

The first symptoms of the classic form of FD appear already in childhood. The most common symptoms observed at this time are: peripheral limb pain [acroparesthesia], angiokeratoma type skin lesions, hearing disorders and eye diseases such as cataract and keratopathy and others. In our patient, such symptoms were not present in childhood. In our patient, the first manifestation of the disease was renal failure with hypertension, proteinuria and hematuria. The cerebro-cardiovascular complications that we observed in the patient included stroke, the presence of left ventricular diastolic dysfunction and cardiac tamponade. Only one case of cardiac tamponade in a patient with FD was described (*8*). In conclusions, the patient presented with a very atypical course of FD - initial asymptomatic course. The diagnosis was made very late, when organ complications occurred.

Funding: None.

Conflict of interest: The authors have no conflicts of interest to disclose.

References

1. Fabry J. "Ein Beitrag zur Kenntniss der Purpura haemorrhagica nodularis (Purpura papulosa haemorrhagica Hebrae)". Archiv für Dermatologie und Syphilis. 1898; 43:187-200. doi:10.1007/bf01986897. ISSN 0340-3696. S2CID 33956139. (in German)
2. Anderson W. A Case of "Angeio-Keratoma". Br J Dermatol. 1898; 10:113-117.
3. Chimenti C, Scopelliti F, Vulpis E, Tafani M, Villanova L, Verardo R, De Paulis R, Russo MA, Frustaci A. Increased oxidative stress contributes to cardiomyocyte dysfunction and death in patients with Fabry disease cardiomyopathy. Hum Pathol. 2015; 46:1760-1768.
4. Rozenfeld PA, de Los Angeles Bolla M, Quieto P, Pisani A, Feriozzi S, Neuman P, Bondar C. Pathogenesis of Fabry nephropathy: The pathways leading to fibrosis. Mol Genet Metab. 2020; 129:132-141.
5. McGovern MM, Desnick RJ. Lysosomal storage diseases. Cecil Textbook of Medicine. In: Goldman L, editor. 21st ed. St. Louis: W.B. Saunders Company; 2000. pp.1104-1107.
6. Jahan S, Sarathchandran S, Akhter S, Goldblatt J, Stark S, Crawford D, Mallett A, Thomas M. Prevalence of Fabry disease in dialysis patients: Western Australia Fabry disease screening study - the FoRWARD study. Orphanet J Rare Dis. 2020; 15:10.
7. Rozenfeld P, Feriozzi S. Contribution of inflammatory pathways to Fabry disease pathogenesis. Mol Genet Metab. 2017; 122:19-27.
8. Burton JO, Dormer JP, Binns HE, Pickering WP. Sometimes when you hear hoof beats, it could be a zebra: consider the diagnosis of Fabry disease. BMC Nephrol. 2012; 13:73.

Received October 23, 2021; Revised February 18, 2022; Accepted February 27, 2022.

**Address correspondence to:*
Marcela Przyłudzka, Department of Internal Medicine, Diabetology and Nephrology, Medical University of Silesia, Katowice 40-055, Poland.
E-mail: przyludzkamarcela@gmail.com

Letter

DOI: 10.5582/irdr.2021.01142

Lemierre's syndrome complicated by cerebral venous sinus thrombosis: A life threatening and rare disease successfully treated with empiric antimicrobial therapy and conservative approach

Maurizio Giorelli[1,*], Sergio Altomare[1], Maria Stella Aniello[1], Ruggiero Leone[1], Daniele Liuzzi[1], Immacolata Plasmati[1], Michele Sardaro[1], Maria Superbo[1], Giuseppe Mennea[2], Nicola Fioretto[3], Giuseppe Guglielmi[3], Rosario Balzano[3], Tommaso Scarabino[4], Giuseppe Cuccorese[5], Francesca Cialdella[6], Giuseppe Campobasso[6], Michele Barbara[6]

[1] Operative Unit of Neurology, "Dimiccoli" General Hospital, Barletta, Italy;
[2] Operative Unit of Internal Medicine, "Bonomo" General Hospital, Andria, Italy;
[3] Operative Unit of Radiology, "Dimiccoli" General Hospital, Barletta, Italy;
[4] Operative Unit of Radiology, "Bonomo" General Hospital, Andria, Italy;
[5] Operative Unit of Internal Medicine, "Dimiccoli" General Hospital, Barletta, Italy;
[6] Operative Unit of Otorhinolaryngology, "Dimiccoli" General Hospital, Barletta, Italy.

SUMMARY Lemierre's syndrome (LS) is a "forgotten" condition characterized by septic thrombophlebitis of the jugular vein that follows an otolaryngological infection. Fusobacterium necrophorum is the aetiological agent responsible for the syndrome in adolescents and young adults whereas in older people even common bacteria are involved. Complications arise from spreading of septic emboli distally, *i.e.* to the brain, lungs, bones and internal organs everywhere in the body. We report a middle-aged woman who presented with headache and bilateral sixth cranial nerve palsy following a sphenoidal sinusitis and left mastoiditis. Imaging revealed thrombotic involvement of the left internal jugular vein as well as of several cerebral venous sinuses thrombosis (CVT). Currently, precise management protocols of LS with CVT complication do not exist although a combination of macrolides and second or third-generation cephalosporins, as well as anti-coagulants represent the mainstream of therapeutics. Surgical drainage is associated to remove septic foci but is burdened by severe complications and side effects. Complete recovery was achieved following pharmacological treatment in our patient. This report adds further evidence that LS complicated by CVT may be effectively treated adopting a conservative approach thus avoiding surgical drainage and severe complications.

Keywords jugular vein thrombosis, cerebral venous circulation, sinusitis, otomastoiditis

Lemierre's syndrome (LS) is a rare and potentially life-threatening condition that follows oropharyngeal infection. It usually occurs in adolescents and young adults and is mostly associated with infection of upper airways (*1-3*). Infection triggers a septic thrombophlebitis of the jugular vein, which can spread to cerebral sinuses, lungs, liver, spleen, joints, and heart (*3*). In the pre-antibiotic era, LS had a case-mortality rate ranging from 32% to 90% (*4*) decreased currently to 17% despite best medical practice (*1,2*).

A 68-year-old woman with a 15-days history of fever, frontal headache and vomiting presented to ED. She reported intermittent fever, binocular diplopia in the left direction of gaze and xerostomia. CT brain/neck angiography revealed occlusion of the left internal jugular vein at its origin and its main secondary branches. Thrombosis of the sigmoid cerebral sinus was also apparent (Figure 1). Based on these findings, the patient was admitted to the Neurological unit. Neurological examination revealed only left VI cranial nerve palsy while physical examination showed herpes labialis and a non-painful, tense-elastic, swelling at the left retromandibular level.

Laboratory tests revealed increased d-dimers (2,501 ng/mL), leukocytes (14,890 WBC/μL, 89% neutrophils), and C-reactive protein (CPR) (31.3 mg/dL). Serology

for common viruses and bacteria was negative as well as blood cultures, onconeural paraneoplastic antibodies, anti-gangliosides, tumor markers and anti-phospholipids.

In suspect of Lemierre's syndrome, empirical antibiotic therapy was started. Therapy included Enoxaparin 6,000 IU b.i.d s.c., Ceftriaxone 2 g b.i.d i.v., Linezolid 600 mg b.i.d., and Acyclovir 5 mg/kg/die t.i.d. Starting from the fifth day from admission, the patient was afebrile and gradually we observed normalization of WBC counts (6.09×10^3 cells/μL) and reduction of CRP (5.61 mg/dL).

At the ninth day, head and neck MRI revealed a solid mass (2.7 × 1.7 cm) in the context of the left parotid gland, thrombosis of the left transverse sinus, the left sigmoid sinus, the origin of the left internal jugular internal vein and the deep facial venous plexus of the same side. Partial thrombosis was even detected in the right transverse sinus. The sphenoidal sinus was obliterated by fluid material and showed parietal thickening. Some left mastoidal cells resulted in obliteration by fluid material similarly. MRI revealed also inflammatory involvement of the interstitial tissue surrounding the left jugular vein with spreading towards the upper airways (Figure 2). Subsequently, by fine needle aspiration, cytological examination of the parotidal mass was performed, revealing the presence of adenomatous cells.

Head and neck MRI performed 10 days later revealed partial thrombosis of the origin of the left internal jugular vein with inflammatory involvement of surrounding soft tissues, sphenoidal sinusitis and mastoiditis. Thrombosis of cerebral sinuses and jugular branches were no more appreciable. Based on the clinical amelioration (significant decrease of frontal headache and diplopia) and the consistent imaging improvement, surgical drainage of sphenoidal sinus was not performed and the patient was discharged after 21 days with indication to switch to Ciprofloxacin 500 mg/die for the next 10 days and to start anticoagulation with warfarin. Informed consent was obtained from the patient and the study checked for ethics.

LS and septic CVT can associate because both share identical etiological and physiopathological mechanisms (*1,2,5-7*). Sometimes, CVT may represent intracranial extension of jugular vein thrombosis. Signs

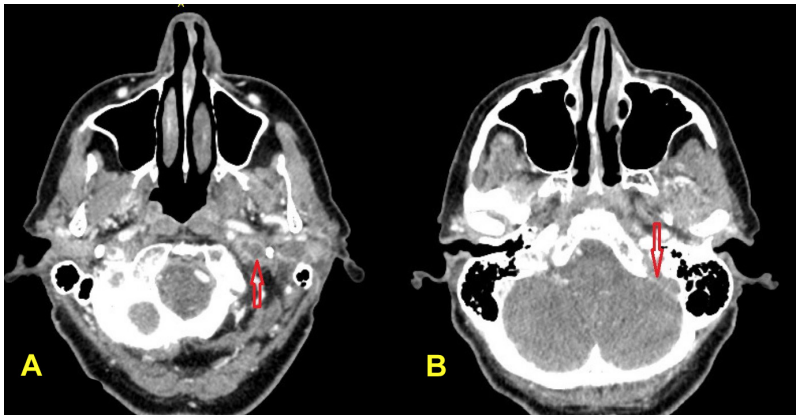

Figure 1. Initial CT scan of the head enhanced with contrast medium. Thrombosis of the jugular left vein **(A)** and filing defect of the left sigmoid sinus **(B)**.

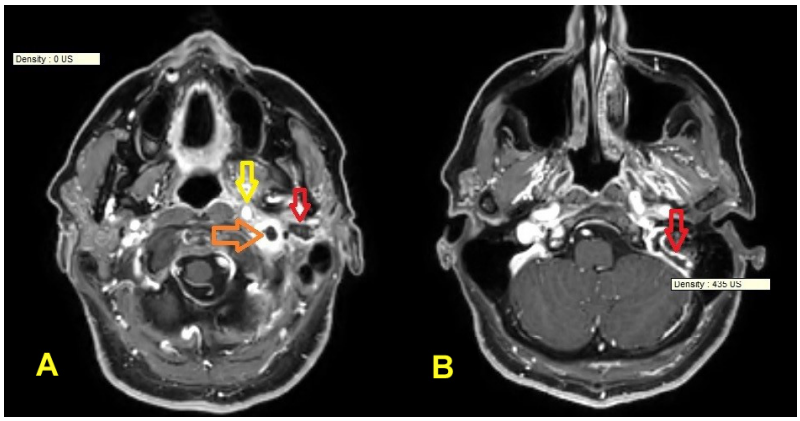

Figure 2. T1 W sequence with gadolinium of transverse head section at the level of pharynx. (A) Filling defect indicating thrombosis at the origin of the left internal jugular vein with hyperintense signal of the surrounding tissue suggestive of inflammatory imbibition (orange arrow). Pseudo-abscess mass diagnosed as parotid adenoma following needle- aspiration (red arrow). Inflammatory solid tissue imprinting the left wall of pharynx (yellow arrow), **(B)** Filing defect indicating thrombosis of the left sigmoid sinus (red arrow).

and symptoms of intracranial hypertension such as headache, decreased visual acuity, papilledema and bilateral sixth cranial nerve palsy may be indicative of a CVT condition (*8*).

In the literature, case reports describing LS complicated with CVT are few (*5,9,10*). Therapeutic protocol include treatment with antibiotics combined with local surgical drainage and removal of the infected site, with poor outcome in half of the cases and side effects spanning from mild hearing impairment (specially in children) to iatrogenic facial palsy (*10*).

Neck MRI in our patient initially suggested the presence of an abscess in the context of parotid gland, so making possible a surgical drainage. However, this was a confounding detection. In fact appropriate needle-aspiration clarified the adenomatous origin of the mass. Inflammatory imbibition of the surrounding tissues of the internal jugular vein as well as the presence of left mastoiditis and sphenoidal sinusitis were nevertheless clearly evident and could be the causative triggers of septic thrombophlebitis. Currently, precise management protocols of LS with CVT complication do not exist. Choice of antibiotics still follows empiric criteria principally based on expert knowledge (*3*) and were immediately started in our patient as well as subcutaneous enoxaparin b.i.d. Enoxaparin was chosen as it was considered the most manageable anticoagulation therapy while waiting for a drainage decision. When discharged, the patient was advised to bridge enoxaparin to warfarin. A clinical follow-up three months later showed that she had completely recovered. As in previous reports (*5*), this is another evidence suggesting that surgical drainage is not a necessary step in all cases of LS complicated with CVT and that a conservative approach may avoid fearsome complications.

Funding: None.

Conflict of Interest: The authors have no conflicts of interest to disclose.

References

1. Lemierre A. On certain septicaemias due to anaerobic organisms. Lancet 1936; 227:701-703.
2. Hagelskjaer Kristensen L, Prag J. Lemierre's syndrome and other disseminated Fusobacterium necrophorum infections in Denmark: a prospective epidemiological and clinical survey. Eur J Clin Microbiol Infect Dis. 2008; 27:779-789.
3. Johannesen KM, Bodtger U. Lemierre's syndrome: current perspectives on diagnosis and management. Infect Drug Resist. 2016; 9:221-227.
4. Hagelskjaer Kristensen L, Prag J. Human necrobacillosis, with emphasis on Lemierre's syndrome. Clin Infect Dis. 2000; 31:524-532.
5. Baltasar-Corral J, Martín-Rojas RM, Parra-Virto A, Galeano-Valle F, Del-Valle-Diéguez M, Del-Toro-Cervera J, Demelo-Rodríguez P. Torcular herophili and lateral sinus thrombosis: An atypical presentation of Lemièrre's syndrome. Intractable Rare Dis Res. 2019; 8:206-209.
6. Wang L, Duan J, Bian T, Meng R, Wu L, Zhang Z, Zhang X, Wang C, Ji X. Inflammation is correlated with severity and outcome of cerebral venous thrombosis. J Neuroinflammation. 2018; 15:329.
7. Fleet J, Birns J, Bhalla A. Cerebral venous thrombosis in adults. J Neurol Disord Stroke. 2014; 2: 1033.
8. Ferro JM, Canhao P, Aguiar de Sousa D. Cerebral venous thrombosis. Presse Med. 2016; 45:e429-e450.
9. Villamar MF, Lee JD. Cerebral venous sinus thrombosis secondary to otomastoiditis. Postgrad Med J. 2017; 93:569.
10. Bales CB, Sobol S, Wetmore R, Elden LM. Lateral sinus thrombosis as a complication of otitis media: 10-year experience at the children's hospital of Philadelphia. Pediatrics. 2009; 123:709-713.

Received November 16, 2021; Revised January 23, 2022; Accepted February 6, 2022.

**Address correspondence to:*
Maurizio Giorelli, Operative Unit of Neurology, "Dimiccoli" General Hospital, Viale Ippocrate 11, Barletta 76121, Italy.
E-mail: maurizio.giorelli@aslbat.it

Released online in J-STAGE as advance publication February 10, 2022.

Letter

DOI: 10.5582/irdr.2021.01148

Posterior reversible encephalopathy syndrome due to arterial hypertension may mark the onset of the symptomatic phase in Huntington's disease

Maurizio Giorelli*

Operative Unit of Neurology, "Dimiccoli" General Hospital, Barletta, Italy.

SUMMARY Autonomic dysregulation of cardiovascular functions marks early Huntington's disease (HD). Blood-brain barrier (BBB) is dysfunctional in HD. A 37-year-old female carrying 41 CAG triplets in the huntingtin gene acutely presented with a multifaceted syndrome attributable to posterior reversible encephalopathy syndrome (PRES). Syndrome was associated with arterial hypertension (AHT). The syndrome fully recovered both by imaging and clinical signs after normalization of arterial pressure during hospitalization. Immediately after hospital discharge, the patient developed a complex psychiatric syndrome and choreic movements that represented conversion to the symptomatic phase of HD. A one-year later follow up clearly showed the patient had developed the symptomatic stage of HD by presenting both psychiatric symptoms and choreic movements. Onset of AHT may represent an early premonitory signal of HD becoming manifested. Induction of PRES might be associated with BBB impairment in HD.

Keywords Huntington's disease, arterial hypertension, autonomic dysfunction, posterior reversible encephalopathy syndrome, blood-brain barrier

1. Introduction

Huntington's disease (HD) is a hereditary neurodegenerative disorder caused by the abnormal expansion of a trinucleotide (CAG) repeat in the *huntingtin* gene of chromosome 4 (*1*). A triad of symptoms consisting of either an extrapiramidal movement disorder as well as cognitive and behavioral impairment characterizes HD (*2*).

People with the same number of triplet repeat expansion may indeed start to develop symptoms at different ages, clearly showing that both genetic and epigenetic factors are involved in disease onset and symptoms appearance (*2*). Arterial hypertension (AHT) has been found to delay development of motor symptoms in a large cohort of HD patients harboring a range of 40-50 CAG triplets and collected from the Registry project of the European Huntington's Disease Network (*3*).

A 37-year-old female presented to the ED reporting episodes of visual blurring and ideative slowing, severe headache not responsive to common anti-inflammatory drugs, and disturbance of speech. At first evaluation she presented with mixed aphasia, hesitations, difficulty on starting speech, and phonemic parafasias. Motor deficits and extrapyramidal signs (including chorea) were both absent. Her arterial blood pressure (BP) was 190/100 mmHg and required aggressive intravenous anti-hypertensive therapy (urapidil) to reach full normalization. The patient reported to have both the father and the paternal uncle affected by HD and to have herself uncovered to have 41 CAG triplets on one of the two huntingtin (HTT) alleles while performing genetic testing two years earlier. She had not suffered from any symptom nor had her neurological examination been found abnormal in regular checkups performed by a movement disorder specialist up to the date of evaluation. She had only suffered from rare episodes of "empty head" and her BP was frequently found elevated in the few months earlier (180/100 as average).

At acceptance, a cranial tomography (CT) was performed with the help of contrast medium. The exam showed the presence of several focal areas of hypodensity at the subcortical level of both parieto-occipital regions. A diagnosis of posterior reversible encephalopathy syndrome (PRES) was made on the basis of clinical-radiological findings. Two days after admittance to hospital, magnetic resonance imaging (MRI) of the brain revealed areas of altered signal consistent with cerebral edema on both sides of parieto-occipital regions as well in the left frontal lobe in both FLAIR and DWI sequences (Figure 1). Constant

measurement of BP revealed persistently normal values (130/80 mm Hg as average) after administering Ramipril 5 mg/qd and amlodipine 5 mg/qd per os. Normalization of pressure parameters lead to disappearance of all symptoms including headache and disturbance of speech. A second MRI conducted 10 days later revealed great volumetric reduction of the already reported areas of altered signal (Figure 2). Pathological conditions known to be triggers to PRES were excluded by deep investigation during hospitalization. The patient was finally dismissed with advice to continue the prescribed anti-hypertensive therapy.

At a first follow up, two months later, the patient complained of episodes of confusion and misperceptions consisting of vision of animals. In addition, subtle and inconstant choreic movements had appeared in the distal segments of her limbs. A clinical evaluation performed one year later showed the patient had entered the full symptomatic phase of HD, characterized by both psychiatric and motor (choreic) phenomena. A written informed consent was obtained from the patient for publication of this case report.

Effect of AHT on risk, time of symptoms onset and speed of progression is still debated when discussing pathogenesis of any neurodegenerative disease. AHT has been associated with delayed onset of HD in one study, especially when anti-hypertensive medications were used *(3)*.

At variance with the latter study, the case in the present study developed onset of all HD-related symptoms after presenting with PRES due to AHT. Several reports have recently demonstrated the presence of early autonomic dysfunction in both premanifest HD mutation carriers as well as in early symptomatic HD patients (*4-6*) and might be the trigger of AHT in the patient described herein. The pathogenesis of PRES is not fully understood but evidence suggests that systemic mean arterial pressure (MAP) exceeding the brain's autoregulatory capability may lead to focal dilation in cerebral blood vessels, resulting in vasodilation and vasoconstriction (*7*). This can result in the extravasation of fluid and in vasogenic edema.

Brain vessels characterized for impairment of continence and increase in blood-brain barrier permeability due to abnormalities in tight junctions and increase in endothelial transcytosis in HD (*8,9*). Rapid surges in BP as is seen in untreated AHT at the onset, and endothelial dysfunction of cerebral vessels due to HTT deposition may, at least in part, explain PRES pathogenesis in the case reported herein.

Aggressive and continuous measurement of blood pressure is a key medical behavior as its detection and treatment induction may delay turning to symptomatic phase in HD carriers. Suggesting a protective role of anti-hypertensive drugs is intriguing and should be strongly and deeply verified further with prospective studies.

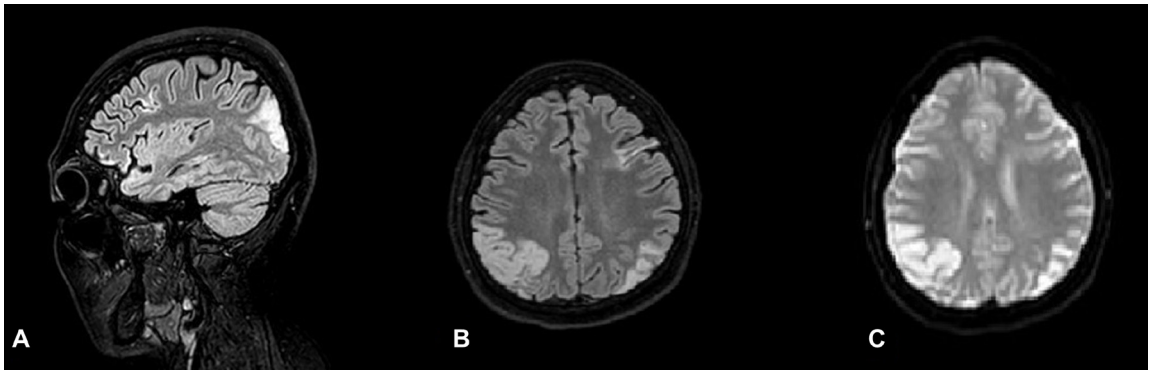

Figure 1. Magnetic Resonance Imaging of subject's brain showing bilateral parieto-occipital hyperintensities in FLAIR (A, B) as well in DWI (C) sequences compatible with oedema due to PRES.

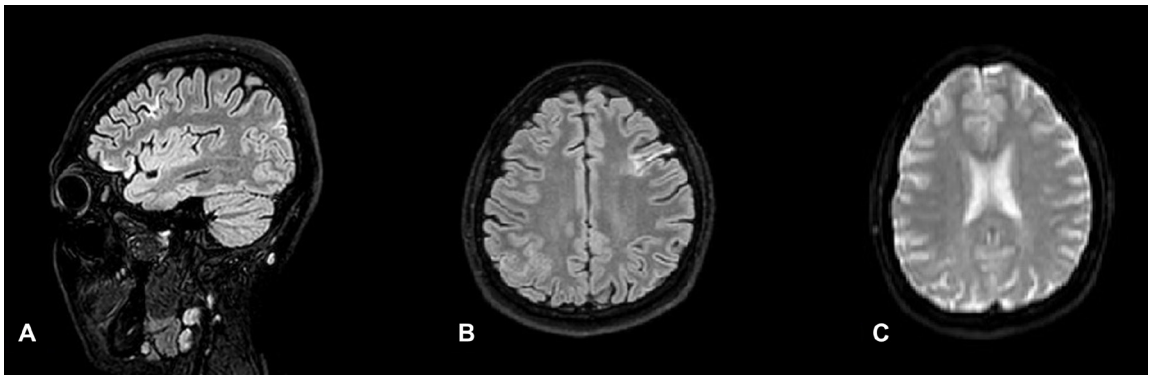

Figure 2. Magnetic Resonance Imaging showed almost complete resolution of brain hyperintensities 10 days later as shown both by FLAIR (A, B) and DWI (C) sequences.

Funding: None.

Conflict of Interest: The author has no conflict of interest to disclose.

References

1. Wexler NS, Lorimer J, Porter J, *et al*. Venezuelan kindreds reveal that genetic and environmental factors modulate Huntington's disease age of onset. Proc Natl Acad Sci U S A. 2004; 101:3498-3503.
2. Genetic Modifiers of Huntington's Disease (GeM-HD) Consortium. Identification of genetic factors that modify clinical onset of Huntington's disease. Cell. 2015; 162:516-526.
3. Valcárcel-Ocete L, Fullaondo A, Alkorta-Aranburu G, García-Barcina M, Roos RAC, Hjermind LE, Saft C, Frontali M, Reilmann R, Rickards H; REGISTRY investigators of the European Huntington's Disease Network (EHDN), Zubiaga AM, Aguirre A. Does arterial hypertension influence the onset of Huntington's disease? PLoS One. 2018; 13:e0197975.
4. Bellosta Diago E, Pérez Pérez J, Santos Lasaosa S, Viloria Alebesque A, Martínez Horta S, Kulisevsky J, López Del Val J. Circadian rhythm and autonomic dysfunction in presymptomatic and early Huntington's disease. Parkinsonism Relat Disord. 2017; 44:95-100.
5. Kobal J, Meglic B, Mesec A, Peterlin B. Early sympathetic hyperactivity in Huntington's disease. Eur J Neurol. 2004; 11:842-848.
6. Kobal J, Melik Z, Cankar K, Bajrovic FF, Meglic B, Peterlin B, Zaletel M. Autonomic dysfunction in presymptomatic and early symptomatic Huntington's disease. Acta Neurol Scand. 2010; 121:392-399.
7. Fittro K, Dizon R. Understanding posterior reversible encephalopathy syndrome. JAAPA. 2018; 31:31-34.
8. Drouin-Ouellet J, Sawiak SJ, Cisbani G, *et al*. Cerebrovascular and blood-brain barrier impairments in Huntington's disease: Potential implications for its pathophysiology. Ann Neurol. 2015; 78:160-177.
9. Sweeney MD, Sagare AP, Zlokovic BV. Blood-brain barrier breakdown in Alzheimer disease and other neurodegenerative disorders. Nat Rev Neurol. 2018; 14:133-150.

Received November 28, 2021; Revised January 23, 2022; Accepted February 2, 2022.

**Address correspondence to:*
Maurizio Giorelli, Operative Unit of Neurology, "Dimiccoli" General Hospital, Viale Ippocrate 11, Barletta 76121, Italy.
E-mail: Maurizio.giorelli@aslbat.it

Released online in J-STAGE as advance publication February 10, 2022.

Letter

DOI: 10.5582/irdr.2022.01019

Diffuse astrocytoma with mosaic *IDH1*-R132H-mutant immunophenotype and low subclonal allele frequency

Katherine M. Morgan[1], Shabbar Danish[2], Zhenggang Xiong[1,3,*]

[1] Department of Pathology and Laboratory Medicine, Robert Wood Johnson Medical School, Rutgers University, New Brunswick, New Jersey, USA;
[2] Department of Neurosurgery, Robert Wood Johnson Medical School, Rutgers University, New Brunswick, New Jersey, USA;
[3] Department of Pathology and Laboratory Medicine, University of Cincinnati College of Medicine, Cincinnati, Ohio, USA.

SUMMARY Molecular alterations found in gliomas are now considered entity-defining features. The World Health Organization (WHO) classification system currently classifies the vast majority of gliomas utilizing an integrated genotype-phenotype approach. We present a case of diffuse astrocytoma with a mosaic isocitrate dehydrogenase (IDH)1-R132H-mutant immunophenotype and low subclonal allele frequency. A 35-year-old patient with a history of *IDH1*-R132H mutated diffuse astrocytoma in 20014 presented to the hospital again in 2019. MRI examination showed a non-enhancing abnormal signal in the periphery of her previous surgical cavity. Histopathological examination revealed that the tumor was hypercellular and without high grade histopathological features. The neoplastic cells were immunohistologically positive for GFAP, Olig2, and ATRX. However, only some scattered tumor cells were positive for *IDH1*-R132H. Cytogenetic studies revealed a lack of chromosomal 1p/19q co-deletion. Further next-generation sequencing (NGS) demonstrated a low-level *IDH1*-R132H mutation and allele frequency. Based on these findings, the diagnosis of diffuse astrocytoma with mosaic *IDH1*-R132H-mutant immunophenotype and low subclonal allele frequency (WHO grade II) was generated. This case indicates that gliomas may have heterogeneous molecular profile and the intra-tumoral molecular heterogeneity highlights the need to further characterize the molecular profile for glioma classification and clinical management.

Keywords diffuse glioma, isocitrate dehydrogenase, *IDH1*, mosaic, intratumoral heterogeneity

Gliomas are the most common primary brain tumor in adults and, despite intensive treatment with surgery and chemoradiation, almost all gliomas relapse (*1,2*). With increasing evidence that molecular markers, such as isocitrate dehydrogenase (*IDH*) 1/2, are more informative than histologic subtype for prediction of tumor response to treatment and prognosis, an integrated genotype-phenotype approach was adopted for the latest World Health Organization (WHO) Classification (*3*). Nowadays, the pathological examination of glial tumors involves immunohistochemical (IHC), cytogenetic, and molecular studies. As a result, rare gliomas with intra-tumoral molecular heterogeneity were identified (*4-6*). We describe a case of recurrent diffuse astrocytoma (WHO grade II) with a mosaic *IDH1* R132H-mutant IHC staining pattern and low subclonal allele frequency to discuss the underlying causes and implications of molecular heterogeneity of gliomas.

A 35-year-old patient presented in March 2014 to the emergency room complaining of long-standing frontal headaches and new onset left-sided paresthesia which became generalized. A magnetic resonance imaging (MRI) examination at that time revealed a non-enhancing T2 signal and FLAIR abnormality within the left superior frontal lobe with no mass effect (Figure 1A). In June 2014, the patient underwent a craniotomy with resection of the tumor. In September 2019, the patient presented to the emergency room after multiple episodes of complex partial seizures. A MRI examination showed a non-enhancing abnormal signal in the periphery of her previous surgical cavity in the left frontal lobe (Figure 1B), consistent with recurrence of a low-grade tumor. The patient underwent a revision craniotomy with total resection of the recurrent tumor. The patient subsequently received radiotherapy and temozolomide with a brain MRI in March 2021 demonstrating no evidence of recurrent enhancement (data not shown). Informed consent was obtained from the patient and the study checked for ethics.

A needle biopsy of the initial tumor performed at an outside institution in 2014 revealed a WHO grade II fibrillary astrocytoma with *IDH1* mutation, and the

total resection specimen from June 2014 confirmed the diagnosis (data not shown). The total resection of the recurrent left frontal tumor in 2020 revealed that the tumor had increased cellularity of infiltrative atypical cells with moderate nuclear pleomorphism and inconspicuous to wispy eosinophilic cytoplasm. There was no necrosis, vascular endothelial hyperplasia, or mitoses identified. The neoplastic cells were diffusely, immunohistologically positive for GFAP, Olig2, and ATRX (Figure 2A-2D). Of note, only scattered tumor cells among other neoplastic cells were immunohistologically positive for the *IDH1*-R132H (Figure 2E and 2F). Ki67 labeling index was approximately 1% in the specimen (data not shown). Fluorescence in situ hybridization (FISH) studies indicated a lack of chromosomal 1p/19q co-deletion. A next generation sequencing (NGS) was performed on microdissected tumor tissue and demonstrated a low-level *IDH1*-R132H mutation (c.395G>A) with an allele frequency of 1.0%. Based on the above findings and the patient's clinical history, the diagnosis of recurrent/residual diffuse astrocytoma with mosaic *IDH1*-R132H-mutant immunophenotype and low subclonal allele frequency was rendered.

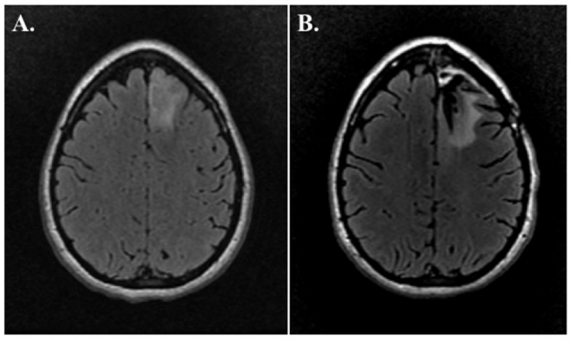

Figure 1. Radiologic images of initial and recurrent tumor. MRI-brain with contrast performed in 2014 **(A)** and 2019 **(B)** revealed a nonenhancing abnormal signal in the left frontal lobe, suggestive of the initial primary glioma and later recurrence, respectively (A, B, Axial FLAIR).

IDH mutation is closely associated with gliomas. *IDH1* encodes a protein located in the cytoplasm and peroxisomes that catalyzes the oxidative decarboxylation of isocitrate to α-ketoglutarate. The most common *IDH1* mutation found in approximately 90% of diffusely infiltrating gliomas is R132H, a missense mutation (c.395G>A) leading to a single amino acid substitution of arginine by histidine at codon 132 in exon 4 of the enzymatic active site (*6-7*). Mutant *IDH1* favors production of 2-hydroxyglutarate, an oncometabolite with multiple downstream effects found to promote tumorigenesis (*2,8*). *IDH2*, localized to the mitochondria, may be mutated at an analogous residue with R172K (c.515G>A) being the most common missense substitution. Oncogenic *IDH* mutations are believed to alter DNA and histone methylation and inhibit normal differentiation processes in gliomas (*2*).

Gliomas are a diverse group of brain tumors (*3,9*). They are among the most difficult cancers to treat, owing to their intra- and inter-tumoral heterogeneity and invasive nature, as well as the inherent challenge of central nervous system (CNS) pharmacokinetics and blood-brain barrier therapy penetration. First-line treatment is limited to a combination of maximally-allowed surgical resection, radiotherapy, and/or chemotherapy with few, if any, effective targeted therapies (*1,9-10*).

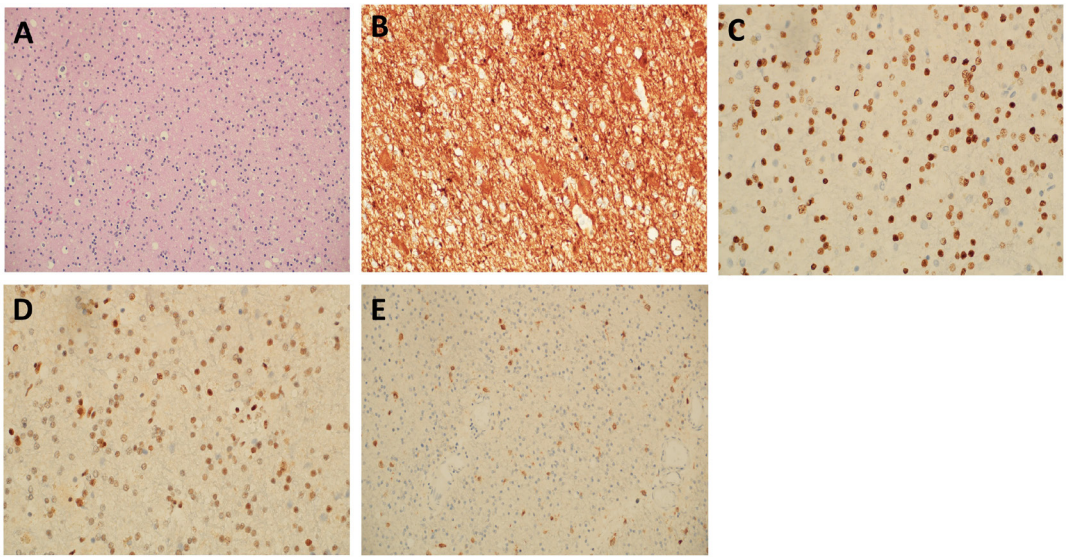

Figure 2. Microscopic findings of tumor recurrence. (A) Hypercellularity with nuclear atypia; no necrosis, vascular endothelial hyperplasia, or mitoses was identified (H&E, A: 100×). **(B, C, D)** The immunophenotype was positive for GFAP (B: 400×) and Olig2 (C: 200×) with retention of ATRX nuclear staining (D: 200×). **(E)** Mosaic staining was noted for the mutant IDH1-R132H epitope with nuclear and cytoplasmic positivity in a subset of scattered tumor cells (100×).

In general, cancer is associated with progressive genomic instability, and the interaction of acquired somatic mutations with environmental selection pressures drives tumor evolution and emergence of genetically distinct subclones (*10*). In particular, it has been found that gliomas undergo significant cellular and molecular evolution during disease progression. Resultant intratumoral heterogeneity such as in our case ultimately confounds diagnosis, creates challenges for the design of effective therapeutics, and acts as a determinant of resistance and recurrence (*1*). These warrant the need for a comprehensive molecular workup and classification of gliomas.

Funding: None.

Conflict of interest: The authors have no conflicts of interest to disclose.

References

1. Aldape K, Amin SB, Ashley DM, *et al*. Glioma through the looking GLASS: molecular evolution of diffuse gliomas and the glioma longitudinal analysis consortium. Neuro Oncol. 2018; 20:873-884.
2. Cohen AL, Holmen SL, Colman H. *IDH1* and *IDH2* mutations in gliomas. Curr Neurol Neurosci Rep. 2013; 13:345.
3. Louis DN, Perry A, Reifenberger G, von Deimling A, Figarella-Branger D, Cavenee WK, Ohgaki H, Wiestler OD, Kleihues P, Ellison DW. The 2016 World Health Organization Classification of Tumors of the Central Nervous System: a summary. Acta Neuropathol. 2016; 131:803-820.
4. Purkait S, Miller CA, Kumar A, Sharma V, Pathak P, Jha P, Sharma MC, Suri V, Suri A, Sharma BS, Fulton RS, Kale SS, Dahiya S, Sarkar C. ATRX in diffuse gliomas with its mosaic/heterogeneous expression in a subset. Brain Pathol. 2017; 27:138-145.
5. Lopez GY, Oberheim Bush NA, Phillips JJ, Bouffard JP, Moshel YA, Jaeckle K, Kleinschmidt-DeMasters BK, Rosenblum MK, Perry A, Solomon DA. Diffuse midline gliomas with subclonal H3F3A K27M mutation and mosaic H3.3 K27M mutant protein expression. Acta Neuropathol. 2017; 134:961-963.
6. Cai J, Zhu P, Zhang C, Li Q, Wang Z, Li G, Wang G, Yang P, Li J, Han B, Jiang C, Sun Y, Jiang T. Detection of ATRX and *IDH1*-R132H immunohistochemistry in the progression of 211 paired gliomas. Oncotarget. 2016; 7:16384-16395.
7. Pisapia DJ. The updated World Health Organization Glioma Classification: cellular and molecular origins of adult infiltrating gliomas. Arch Pathol Lab Med. 2017; 141:1633-1645.
8. Bruce-Brand C, Govender D. Gene of the month: *IDH1*. J Clin Pathol. 2020; 73:611-615.
9. Brat DJ, Verhaak RG, Aldape KD, *et al*. Comprehensive, integrative genomic analysis of diffuse lower-grade gliomas. N Engl J Med. 2015; 372:2481-2498.
10. Nicholson JG, Fine HA. Diffuse glioma heterogeneity and its therapeutic implications. Cancer Discov. 2021; 11:575-590.

Received February 6, 2022; Revised February 18, 2022; Accepted February 21, 2022.

**Address correspondence to:*
Zhenggang Xiong, Department of Pathology and Laboratory Medicine, University of Cincinnati College of Medicine, LMB, Suite 110, 234 Goodman Street, Cincinnati, OH 45219, USA.
E-mail: xiongzg@ucmail.uc.edu

Released online in J-STAGE as advance publication February 25, 2022.

IRDR
Intractable & Rare Diseases Research

Guide for Authors

1. Scope of Articles

Intractable & Rare Diseases Research (Print ISSN 2186-3644, Online ISSN 2186-361X) is an international peer-reviewed journal. Intractable & Rare Diseases Research devotes to publishing the latest and most significant research in intractable and rare diseases. Articles cover all aspects of intractable and rare diseases research such as molecular biology, genetics, clinical diagnosis, prevention and treatment, epidemiology, health economics, health management, medical care system, and social science in order to encourage cooperation and exchange among scientists and clinical researchers.

2. Submission Types

Original Articles should be well-documented, novel, and significant to the field as a whole. An Original Article should be arranged into the following sections: Title page, Abstract, Introduction, Materials and Methods, Results, Discussion, Acknowledgments, and References. Original articles should not exceed 5,000 words in length (excluding references) and should be limited to a maximum of 50 references. Articles may contain a maximum of 10 figures and/or tables. Supplementary Data are permitted but should be limited to information that is not essential to the general understanding of the research presented in the main text, such as unaltered blots and source data as well as other file types.

Brief Reports definitively documenting either experimental results or informative clinical observations will be considered for publication in this category. Brief Reports are not intended for publication of incomplete or preliminary findings. Brief Reports should not exceed 3,000 words in length (excluding references) and should be limited to a maximum of 4 figures and/or tables and 30 references. A Brief Report contains the same sections as an Original Article, but the Results and Discussion sections should be combined.

Reviews should present a full and up-to-date account of recent developments within an area of research. Normally, reviews should not exceed 8,000 words in length (excluding references) and should be limited to a maximum of a maximum of 10 figures and/or tables and 100 references. Mini reviews are also accepted, which should not exceed 4,000 words in length (excluding references) and should be limited to a maximum of 5 figures and/or tables and 50 references.

Policy Forum articles discuss research and policy issues in areas related to life science such as public health, the medical care system, and social science and may address governmental issues at district, national, and international levels of discourse. Policy Forum articles should not exceed 3,000 words in length (excluding references) and should be limited to a maximum of 5 figures and/or tables and 30 references.

Communications are short, timely pieces that spotlight new research findings or policy issues of interest to the field of global health and medical practice that are of immediate importance. Depending on their content, Communications will be published as "Comments" or "Correspondence". Communications should not exceed 1,500 words in length (excluding references) and should be limited to a maximum of 2 figures and/or tables and 20 references.

Editorials are short, invited opinion pieces that discuss an issue of immediate importance to the fields of global health, medical practice, and basic science oriented for clinical application. Editorials should not exceed 1,000 words in length (excluding references) and should be limited to a maximum of 10 references. Editorials may contain one figure or table.

News articles should report the latest events in health sciences and medical research from around the world. News should not exceed 500 words in length.

Letters should present considered opinions in response to articles published in *Intractable & Rare Diseases Research* in the last 6 months or issues of general interest. Summaries of research results and sharing of experiences in clinical practice and basic research (findings based on case reports, clinical pictures, *etc.*) can also be published as Letters. Letters should not exceed 800 words in length and may contain a maximum of 10 references. Letters may contain one figure or table.

3. Editorial Policies

For publishing and ethical standards, *Intractable & Rare Diseases Research* follows the Recommendations for the Conduct, Reporting, Editing, and Publication of Scholarly Work in Medical Journals (*http://www.icmje.org/recommendations*) issued by the International Committee of Medical Journal Editors (ICMJE), and the Principles of Transparency and Best Practice in Scholarly Publishing (*https://doaj.org/bestpractice*) jointly issued by the Committee on Publication Ethics (COPE), the Directory of Open Access Journals (DOAJ), the Open Access Scholarly Publishers Association (OASPA), and the World Association of Medical Editors (WAME).

Intractable & Rare Diseases Research will perform an especially prompt review to encourage innovative work. All original research will be subjected to a rigorous standard of peer review and will be edited by experienced copy editors to the highest standards.

Ethics: *Intractable & Rare Diseases Research* requires that authors of reports of investigations in humans or animals indicate that those studies were formally approved by a relevant ethics committee or review board. For research involving human experiments, a statement that the participants gave informed consent before taking part (or a statement that it was not required and why) should be indicated. Authors should also state that the study conformed to the provisions of the Declaration of Helsinki (as revised in 2013). When reporting experiments on animals, authors should indicate whether the institutional and national guide for the care and use of laboratory animals was followed.

Conflict of Interest: All authors are required to disclose any actual or potential conflict of interest including financial interests or relationships with other people or organizations that might raise questions of bias in the work reported. If no

conflict of interest exists for each author, please state "There is no conflict of interest to disclose".

Submission Declaration: When a manuscript is considered for submission to *Intractable & Rare Diseases Research*, the authors should confirm that 1) no part of this manuscript is currently under consideration for publication elsewhere; 2) this manuscript does not contain the same information in whole or in part as manuscripts that have been published, accepted, or are under review elsewhere, except in the form of an abstract, a letter to the editor, or part of a published lecture or academic thesis; 3) authorization for publication has been obtained from the authors' employer or institution; and 4) all contributing authors have agreed to submit this manuscript.

Cover Letter: The manuscript must be accompanied by a cover letter prepared by the corresponding author on behalf of all authors. The letter should indicate the basic findings of the work and their significance. The letter should also include a statement affirming that all authors concur with the submission and that the material submitted for publication has not been published previously or is not under consideration for publication elsewhere. The cover letter should be submitted in PDF format. For example of Cover Letter, please visit: Download Centre (*https://www.irdrjournal.com/downcentre*).

Copyright: When a manuscript is accepted for publication in *Intractable & Rare Diseases Research*, the transfer of copyright is necessary. A JOURNAL PUBLISHING AGREEMENT (JPA) form will be e-mailed to the authors by the Editorial Office and must be returned by the authors as a scan. Only forms with a hand-written signature are accepted. This copyright will ensure the widest possible dissemination of information. Please note that your manuscript will not proceed to the next step in publication until the JPA Form is received. In addition, if excerpts from other copyrighted works are included, the author(s) must obtain written permission from the copyright owners and credit the source(s) in the article.

Peer Review: *Intractable & Rare Diseases Research* uses single-blind peer review, which means that reviewers know the names of the authors, but the authors do not know who reviewed their manuscript. The external peer review is performed for research articles by at least two reviewers, and sometimes the opinions of more reviewers are sought. Peer reviewers are selected based on their expertise and ability to provide high quality, constructive, and fair reviews. For research manuscripts, the editors may, in addition, seek the opinion of a statistical reviewer. Consideration for publication is based on the article's originality, novelty, and scientific soundness, and the appropriateness of its analysis.

Suggested Reviewers: A list of up to 3 reviewers who are qualified to assess the scientific merit of the study is welcomed. Reviewer information including names, affiliations, addresses, and e-mail should be provided at the same time the manuscript is submitted online. Please do not suggest reviewers with known conflicts of interest, including participants or anyone with a stake in the proposed research; anyone from the same institution; former students, advisors, or research collaborators (within the last three years); or close personal contacts. Please note that the Editor-in-Chief may accept one or more of the proposed reviewers or may request a review by other qualified persons.

Language Editing: Manuscripts prepared by authors whose native language is not English should have their work proofread by a native English speaker before submission. If not, this might delay the publication of your manuscript in *Intractable & Rare Diseases Research*.

The Editing Support Organization can provide English proofreading, Japanese-English translation, and Chinese-English translation services to authors who want to publish in *Intractable & Rare Diseases Research* and need assistance before submitting a manuscript. Authors can visit this organization directly at *http://www.iacmhr.com/iac-eso/support.php?lang=en*. IAC-ESO was established to facilitate manuscript preparation by researchers whose native language is not English and to help edit works intended for international academic journals.

4. Manuscript Preparation

Manuscripts are suggested to be prepared in accordance with the "Recommendations for the Conduct, Reporting, Editing, and Publication of Scholarly Work in Medical Journals", as presented at *http://www.ICMJE.org*.

Manuscripts should be written in clear, grammatically correct English and submitted as a Microsoft Word file in a single-column format. Manuscripts must be paginated and typed in 12-point Times New Roman font with 24-point line spacing. Please do not embed figures in the text. Abbreviations should be used as little as possible and should be explained at first mention unless the term is a well-known abbreviation (*e.g.* DNA). Single words should not be abbreviated.

Title page: The title page must include 1) the title of the paper (Please note the title should be short, informative, and contain the major key words); 2) full name(s) and affiliation(s) of the author(s), 3) abbreviated names of the author(s), 4) full name, mailing address, telephone/fax numbers, and e-mail address of the corresponding author; and 5) conflicts of interest (if you have an actual or potential conflict of interest to disclose, it must be included as a footnote on the title page of the manuscript; if no conflict of interest exists for each author, please state "There is no conflict of interest to disclose"). Please visit Download Centre and refer to the title page of the manuscript sample.

Abstract: The abstract should briefly state the purpose of the study, methods, main findings, and conclusions. For articles that are Original Articles, Brief Reports, Reviews, or Policy Forum articles, a one-paragraph abstract consisting of no more than 250 words must be included in the manuscript. For Communications, Editorials, News, or Letters, a brief summary of main content in 150 words or fewer should be included in the manuscript. Abbreviations must be kept to a minimum and non-standard abbreviations explained in brackets at first mention. References should be avoided in the abstract. Three to six key words or phrases that do not occur in the title should be included in the Abstract page.

Introduction: The introduction should be a concise statement of the basis for the study and its scientific context.

Materials and Methods: The description should be brief but with sufficient detail to enable others to reproduce the experiments. Procedures that have been published

previously should not be described in detail but appropriate references should simply be cited. Only new and significant modifications of previously published procedures require complete description. Names of products and manufacturers with their locations (city and state/country) should be given and sources of animals and cell lines should always be indicated. All clinical investigations must have been conducted in accordance with Declaration of Helsinki principles. All human and animal studies must have been approved by the appropriate institutional review board(s) and a specific declaration of approval must be made within this section.

Results: The description of the experimental results should be succinct but in sufficient detail to allow the experiments to be analyzed and interpreted by an independent reader. If necessary, subheadings may be used for an orderly presentation. All figures and tables must be referred to in the text.

Discussion: The data should be interpreted concisely without repeating material already presented in the Results section. Speculation is permissible, but it must be well-founded, and discussion of the wider implications of the findings is encouraged. Conclusions derived from the study should be included in this section.

Acknowledgments: All funding sources should be credited in the Acknowledgments section. In addition, people who contributed to the work but who do not meet the criteria for authors should be listed along with their contributions.

References: References should be numbered in the order in which they appear in the text. Citing of unpublished results, personal communications, conference abstracts, and theses in the reference list is not recommended but these sources may be mentioned in the text. In the reference list, cite the names of all authors when there are fifteen or fewer authors; if there are sixteen or more authors, list the first three followed by *et al*. Names of journals should be abbreviated in the style used in PubMed. Authors are responsible for the accuracy of the references. The EndNote Style of *Intractable & Rare Diseases Research* could be downloaded at **EndNote** (*https://www.irdrjournal.com/examples/Intractable_Rare_Diseases_Research.ens*).

Examples are given below:

Example 1 (Sample journal reference):

Inagaki Y, Tang W, Zhang L, Du GH, Xu WF, Kokudo N. Novel aminopeptidase N (APN/CD13) inhibitor 24F can suppress invasion of hepatocellular carcinoma cells as well as angiogenesis. Biosci Trends. 2010; 4:56-60.

Example 2 (Sample journal reference with more than 15 authors):

Darby S, Hill D, Auvinen A, *et al*. Radon in homes and risk of lung cancer: Collaborative analysis of individual data from 13 European case-control studies. BMJ. 2005; 330:223.

Example 3 (Sample book reference):
Shalev AY. Post-traumatic stress disorder: Diagnosis, history and life course. In: Post-traumatic Stress Disorder, Diagnosis, Management and Treatment (Nutt DJ, Davidson JR, Zohar J, eds.). Martin Dunitz, London, UK, 2000; pp. 1-15.

Example 4 (Sample web page reference):

World Health Organization. The World Health Report 2008 – primary health care: Now more than ever. *http://www.who.int/whr/2008/whr08_en.pdf* (accessed September 23, 2010).

Tables: All tables should be prepared in Microsoft Word or Excel and should be arranged at the end of the manuscript after the References section. Please note that tables should not in image format. All tables should have a concise title and should be numbered consecutively with Arabic numerals. If necessary, additional information should be given below the table.

Figure Legend: The figure legend should be typed on a separate page of the main manuscript and should include a short title and explanation. The legend should be concise but comprehensive and should be understood without referring to the text. Symbols used in figures must be explained. Any individually labeled figure parts or panels (A, B, *etc*.) should be specifically described by part name within the legend.

Figure Preparation: All figures should be clear and cited in numerical order in the text. Figures must fit a one- or two-column format on the journal page: 8.3 cm (3.3 in.) wide for a single column, 17.3 cm (6.8 in.) wide for a double column; maximum height: 24.0 cm (9.5 in.). Please make sure that the symbols and numbers appeared in the figures should be clear. Please make sure that artwork files are in an acceptable format (TIFF or JPEG) at minimum resolution (600 dpi for illustrations, graphs, and annotated artwork, and 300 dpi for micrographs and photographs). Please provide all figures as separate files. Please note that low-resolution images are one of the leading causes of article resubmission and schedule delays.

Units and Symbols: Units and symbols conforming to the International System of Units (SI) should be used for physicochemical quantities. Solidus notation (*e.g*. mg/kg, mg/mL, mol/mm^2/min) should be used. Please refer to the SI Guide *www.bipm.org/en/si/* for standard units.

Supplemental data: Supplemental data might be useful for supporting and enhancing your scientific research and *Intractable & Rare Diseases Research* accepts the submission of these materials which will be only published online alongside the electronic version of your article. Supplemental files (figures, tables, and other text materials) should be prepared according to the above guidelines, numbered in Arabic numerals (*e.g*., Figure S1, Figure S2, and Table S1, Table S2) and referred to in the text. All figures and tables should have titles and legends. All figure legends, tables and supplemental text materials should be placed at the end of the paper. Please note all of these supplemental data should be provided at the time of initial submission and note that the editors reserve the right to limit the size and length of Supplemental Data.

5. Submission Checklist

The Submission Checklist will be useful during the final checking of a manuscript prior to sending it to *Intractable & Rare Diseases Research* for review. Please visit Download

Centre and download the Submission Checklist file.

6. Online Submission

Manuscripts should be submitted to *Intractable & Rare Diseases Research* online at *https://www.irdrjournal.com*. The manuscript file should be smaller than 5 MB in size. If for any reason you are unable to submit a file online, please contact the Editorial Office by e-mail at *office@irdrjournal.com*

7. Accepted Manuscripts

Proofs: Galley proofs in PDF format will be sent to the corresponding author *via* e-mail. Corrections must be returned to the editor (*office@irdrjournal.com*) within 3 working days.

Offprints: Authors will be provided with electronic offprints of their article. Paper offprints can be ordered at prices quoted on the order form that accompanies the proofs.

Page Charge: No page charges will be levied to authors for the publication of their article except for reprints.

Misconduct: *Intractable & Rare Diseases Research* takes seriously all allegations of potential misconduct and adhere to the ICMJE Guideline (*http://www.icmje.org/recommendations*) and COPE Guideline (*http://publicationethics.org/files/Code_of_conduct_for_journal_editors.pdf*). In cases of suspected research or publication misconduct, it may be necessary for the Editor or Publisher to contact and share submission details with third parties including authors' institutions and ethics committees. The corrections, retractions, or editorial expressions of concern will be performed in line with above guidelines.

(As of February 2022)

Intractable & Rare Diseases Research
Editorial and Head Office
Pearl City Koishikawa 603,
2-4-5 Kasuga, Bunkyo-ku,
Tokyo 112-0003, Japan.
E-mail: office@irdrjournal.com